THERMAL DIFFUSION AND LEVITATION MELTING

THERMAL DIFFUSION
IN KINETIC AND EQUILIBRIUM MEASUREMENTS
BY LEVITATION TECHNIQUE

By

MALCOLM SUNDERLAND, B.Sc., M.Eng.

A Thesis

Submitted to the School of Graduate Studies

in Partial Fulfilment of the Requirements

for the Degree

Doctor of Philosophy

McMaster University

May, 1972

DOCTOR OF PHILOSOPHY (1972)
(Chemical Engineering)

McMaster University
Hamilton, Ontario

TITLE: Thermal Diffusion in Kinetic and Equilibrium Measurements by Levitation Technique.

AUTHOR: Malcolm Sunderland, B.Sc. (University of Salford)
M.Eng. (McMaster University)

SUPERVISORS: Professors A. E. Hamielec and W-K. Lu

NUMBER OF PAGES: xv,147.

SCOPE AND CONTENTS:

An experimental investigation of thermal diffusion was carried out using a levitated iron sample and a binary gas mixture of hydrogen and hydrogen sulphide. The iron was liquid and the moving gas stream was at room temperature. A range of drop temperatures, gas flow rates and compositions was studied.

The fluxes due to thermal diffusion were found to be significant in this particular system. Interpretation of the rate data for the sulphurisation and desulphurisation of the iron showed a pronounced effect of thermal diffusion upon rate and equilibrium measurements.

An overall rate expression which accounts for thermal diffusion and normal mass transfer in the gas phase has been developed. It is in agreement with experiment. Equilibrium data in the literature have been corrected for thermal diffusion error by means of this expression. These corrected equilibria are in agreement with measurements made by crucible techniques.

ACKNOWLEDGMENTS

I am indebted to Dr. A. McLean for his suggestion of this particular research project. A special debt is felt for his enthusiastic introduction of the general field of iron- and steelmaking to the author.

I would like to record the deep gratitude which I feel to Dr. A. E. Hamielec and Dr. W-K. Lu. Both supervisors provided extensive advice which assisted my progress considerably. The guidance was continuous and always available. In addition, I appreciate particularly the freedom which they so readily permitted, to explore many fringe areas which were subsidiary to the main project.

TABLE OF CONTENTS

CHAPTER 1. INTRODUCTION 1

CHAPTER 2. REVIEW OF THE TOPIC 5

2.1 Previous Applications of the Levitation Technique 5

2.2 Advantages of Levitation Melting 10

2.3 Disadvantages of Levitation Melting 13

2.4 Design of Coil 14

2.5 Thermal Diffusion 19

2.5.1 Origin and Derivation 19
2.5.2 In Metallurgical Studies 24
2.5.3 In Process Engineering 26

2.6 Kinetic Studies 28

2.6.1 Interpretation and Mechanism 28
2.6.2 Mass Transfer Coefficients 29

2.7 Thermodynamics of Fe-H_2-H_2S 34

2.8 Enhanced Vaporisation of Sulphur 38

CHAPTER 3. EXPERIMENTAL CONSIDERATIONS 40

3.1 Apparatus and Materials 40

3.1.1 Reaction Chamber 41
3.1.2 Levitation Coil and Supply 42
3.1.3 The Iron Specimen 44
3.1.4 The Gases 45

3.2 Measurement of Temperature 46

3.2.1 The Pyrometer 46
3.2.2 Calibration of the Pyrometer 47
3.2.3 Use of the Pyrometer 48

3.3 Procedure 49

3.3.1 Specimen Preparation 49
3.3.2 Obtaining Rate Curves 50
3.3.3 Gas Sampling and Analysis 51
3.3.4 Analysis of Sulphur in Iron 52
3.3.5 Sulphur Profiles 53

CHAPTER 4. EXPERIMENTAL RESULTS 55

4.1 Sulphurisation in H_2-H_2S Mixtures 55

4.1.1 Drop Temperatures at 1600°C 56
4.1.2 Other Drop Temperatures 56

4.2 Desulphurisation 57

4.2.1 Desulphurisation by Pure Hydrogen 57
4.2.2 Desulphurisation by Inert Gas 58

4.3 Sulphur Profiles 58

CHAPTER 5. DISCUSSION OF RESULTS: KINETIC ASPECTS 61

5.1 Interpretation of Transport Process 61

5.1.1 Transport Control 61
5.1.2 Thermal Diffusion Flux 74

5.2 Proof of Flux Equation 78

5.2.1 Methods of Solution 79
5.2.2 Solutions at 1600°C 82
5.2.3 Desulphurisation in Hydrogen 85
5.2.4 Solutions at Other Temperatures 86

5.3 Calculation of Mass Transfer Coefficients, kg 88

5.4 Calculation of Thermal Diffusion Constants, b 92

5.5 Desulphurisation by Inert Gases 96

CHAPTER 6. DISCUSSION OF RESULTS: THERMODYNAMIC ASPECTS 99

6.1 Introduction 99

6.2 Evaluation of K from Rate Curves 100

6.3 Evaluation of K from "Spot" Measurements 102

6.4 Comparison of K with Other Measurements 103

CHAPTER 7. INTERPRETATION OF EXISTING DATA 105

7.1 Introduction 105

7.2 Equilibria under H_2-H_2O Gas 106

7.3 Equilibria under CO-CO_2 Gas 108

CHAPTER 8. DISCUSSION OF ERRORS 111

8.1 Sulphur Content of Levitated Drops 111

8.2 Error in Coefficients, kg and b 113

CHAPTER 9. SUMMARY AND CONCLUSIONS 115

REFERENCES 117

APPENDIX 1 123

APPENDIX 2 125

APPENDIX 3 131

APPENDIX 4 133

APPENDIX 5 135

APPENDIX 6 139

APPENDIX 7 146

TABLES

FIGURES

LIST OF TABLES

TABLE

1. Oxygen Removal from Levitated Drops.

2-28. Experimental Results of Sulphurisation of Levitated Iron Drops by Various H_2-H_2S Gas Mixtures:

2-16: Drop Temperature of 1600°C

17-22: Drop Temperature of 1500°C

23-27: Drop Temperature of 1750°C

28 : Drop Temperature of 1675°C.

29-31. Desulphurisation with Pure Hydrogen of Levitated Drops at 1600°C:

29: Flow rate of 900 cm^3 per min.

30: Flow rate of 2680 cm^3 per min.

31: Flow rate of 5070 cm^3 per min.

32-34. Desulphurisation with Inert Gases of Levitated Drops at 1600°C:

32: Pure Helium

33: Helium-Hydrogen Mixtures

34: Nitrogen-Hydrogen Mixtures

35. Synopsis of Experimental Results in Tables 2 to 28.

36. Comparison of Measured Sherwood Numbers with Values Calculated by Correlations on Three Different Bases.

37. Values of Thermal Diffusion Factor for Binary Gas Mixture of Hydrogen-Hydrogen Sulphide Found by Experiment at Drop Temperatures of 1500 and 1600°C.

38. Values of the Equilibrium Constant Found from Six Independent Experimental Rate Curves at 1675 and 1750°C.

39. Correction of Equilibria for Iron Drops Levitated in Hydrogen-Water Vapour Gas Mixtures.

LIST OF ILLUSTRATIONS

FIGURE

1. Schematic Illustration of the Overall Apparatus.

2. Diagram of the Levitation Tube and Charging Arrangement.

3. Cross-Section of a Typical Levitation Coil and the Former on which it was Wound.

4. Apparatus for Calibration of Pyrometer on a Liquid Iron Melt.

5. Calibration Curve for Pyrometer Against Thermocouple.

6. Cross-Section of Device for Taking Samples of the Gas Mixtures for Analysis.

7. Sulphur Content of Supercooled Drops for Rapid Quenching.

8. Initial Rates of Sulphurisation of Drops Levitated in Various H_2-H_2S Gas Ratios.

9. Weight Percent Sulphur in Levitated Drops Against Time (Table 8). Comparison with Chipman's Value.

10. Weight Percent Sulphur in Levitated Drops against Time (Table 3).

11. Weight Percent Sulphur in Levitated Drops against Time (Table 12).

12. Weight Percent Sulphur in Levitated Drops against Time (Table 14).

13. Desulphurisation of Iron Drops with Pure Hydrogen Flowing at 2680 cm^3 per min.

14. Desulphurisation of Iron Drops with Pure Hydrogen Flowing at 900 cm^3 per min.

15. Desulphurisation of Iron Drops with Pure Hydrogen Flowing at 5070 cm^3 per min.

16. Weight Percent Sulphur in Levitated Drops against Time (Table 18).

17. Weight Percent Sulphur in Levitated Drops against Time (Table 19).

18. Weight Percent Sulphur in Levitated Drops against Time (Table 21).

19. Desulphurisation of Iron Drops with Pure Helium.

20. Equilibrium Constants at 1750 and 1675^{o}C Found by Experimental Rate Curves at Different H_2-H_2S Gas Flow Rates.

21. Equilibrium Constants by Rate Curves and "Spot" Measurements in H_2-H_2S Gas Mixtures.

22. Comparison of Equilibrium Constants Found in the Present Study with those of Other Workers Over the Temperature Range 1500 to 1750°C in H_2-H_2S Gas Mixtures.

23. Correction of Larche's Measurements of the Equilibrium Constant for Hydrogen-Water Vapour Mixtures over Liquid Iron.

24. Correction of Larche's Measurements of the Equilibrium Constant for CO-CO_2 Mixtures over Liquid Iron.

25. Comparison of Experimental Data for Sulphurisation at 1600°C and Flow Rate of 2680 cm^3 per min. (Table 3) with Various Solutions of the Flux Equation. Values of kg and b were Perturbed and the Resulting Solutions Compared with Experimental Points by a Least Squares Criterion.

26. General Curve for Attainment of Steady State for Sulphur Transfer into a Stagnant Drop of Iron, where All Resistance to Transfer is in the Drop Alone (Appendix I).

NOMENCLATURE

The following symbols occur frequently in the text. Additional symbols occur in isolated instances, in which case their specialised use is defined clearly at that time.

A	Surface area of the drop.
a	Radius of the drop.
a_s	Activity of sulphur.
b	Collective constant defined by equation (5.23). Appears as B on some tables.
$\bar{B}$	Magnetic field strength vector.
C	Total molar concentration of the gas.
C_p	Specific heat.
D_{A-B}	Molecular diffusion coefficient for the binary mixture of A and B.
D_T	Thermal diffusion coefficient.
E	Collective constant defined by equation (7.2).
e_s	Interaction parameter for sulphur.
f_s	Activity coefficient for sulphur.
g	Acceleration due to gravity.
h	Heat transfer coefficient.
$\bar{J}$	Any flux vector.
K	Equilibrium constant.
K'	$\log K' = \log f_s + \log K$.
K_s	Equilibrium constant for $Fe\text{-}S\text{-}S_2$.

k	Thermal conductivity.
k_g	Gas phase mass transfer coefficient.
k_L	Liquid phase mass transfer coefficient.
k_T	Thermal diffusion ratio.
$k_{1,\ldots 8}$	Rate constants for various transfer mechanisms.
L	Phenomenological coefficient (scalar).
Nu	$\frac{h.2a}{k}$
Pr	$\frac{Cp.\mu}{k}$
PH_2S	Partial pressure of hydrogen sulphide.
PH_2	Partial pressure of hydrogen.
P_T	Total pressure.
Q	Heat flux from the surface of the drop (radiation excluded).
R	Universal gas constant.
Re	$\frac{\rho.2a.V}{\mu}$
r	Radial dimension from the centre of the drop.
Sc	$\frac{\mu}{\rho.D_{A-B}}$
Sh	$\frac{kg.2a}{D_{A-B}}$
T	Absolute temperature.
t	Time of any operation.
V	Velocity of the gas.
wt	Weight of the drop.
$\bar{X}$	Driving force vector
x	Mole fraction in a mixture of gases
α	Thermal diffusion factor.
θ	Fraction of the total number of active sites at the interface.

η Chemical potential.

ρ Density.

ρ_d Density of the liquid drop.

μ Viscosity.

ω Radian frequency of the magnetic field.

∇ Vector del operator.

%S Concentration of sulphur in iron on a weight percentage basis.

Subscript o refers to the Fe-H_2O-H_2 system in Chapter 7

Subscript ∞ refers to the bulk state (of gas or liquid).

Subscript i refers to the gas-liquid interface.

Subscript f refers to some average condition in the gas between state ∞ and state i. This is a concept rather than a physical location.

CHAPTER I

INTRODUCTION

The history of steelmaking shows that the manufacture of steel for many years, has been by processes which have involved the interaction of metal and slag. In recent years, the introduction of oxygen steelmaking, of inert gas purging and of vacuum degassing, has emphasised the importance of gas-metal interactions in industrial practice. The new technology is far from fully understood. Information remains to be gathered in the area where metal refining is achieved primarily by gases. Much of the information must be derived from experimental study.

The levitation technique, in which a specimen of metal may be both melted and supported without direct physical means by an electromagnetic field, is ideally suited to gas-metal studies. It offers certain advantages over the tedious crucible and furnace techniques. It has been used widely for the preparation of alloys and for limited thermodynamic measurements. However, cursory inspection of the technique indicates that it lends considerable scope for examination of the kinetic aspects of any interaction between liquid metal and gas. One of the aims of the study reported here, was to demonstrate and estimate the value of the levitation technique as an experimental tool for use in kinetic and equilibrium studies.

The use of gases in metallurgical experiments is usually handicapped by the difficulty of accounting for the phenomenon of thermal diffusion. If steep temperature gradients exist in a gaseous mixture, as they often do in apparatuses which contain liquid metal, then pronounced segregation of the

components of the mixture may occur. The segregation, if not accounted for, may lead to erroneous conclusions from the experiment. The severity of the temperature gradients which may be generated around a levitated drop is likely to create significant thermal segregation. The thermal diffusion flux is dynamic in nature and occurs at all instances of time, including both the kinetic and the steady state regimes of any experiment. If equilibrium data are to be obtained from the steady state studies, thermal diffusion must first be isolated and quantified. The second aim of the present study was to examine the usefulness of the levitation experiment for measuring gas-metal equilibria, which may or may not require compensation for the errors created by thermal diffusion. No comprehensive investigation has ever been made of thermal diffusion in the levitation apparatus. No precedent was available for the choice of system with which to perform the investigation.

The iron-hydrogen-hydrogen sulphide system was selected. The components of the gaseous mixture are widely dissimilar, and consequently the thermal diffusion effect is large. A limited, but accurate, amount of thermodynamic data are available for the dissolution of sulphur in liquid iron. The gases are common and as such the physical properties are well known or may be predicted theoretically. Other reasons for this choice will become apparent in the main body of this report.

Many liquid metal kinetic and thermodynamic studies of the past have terminated at the presentation of the laboratory readings. Interpretation has been lacking, or has been based upon premises which have not been completely verified. The usual reason for this has been the complexity of the mechanisms under study, or the random nature of the experimental characteristics. For example, any mechanism proposed to describe the net transfer of a species,

first must be proved to be the correct mechanism before attempts are made to find the numerical values of the parameters contained within that mechanism. The transfer rates investigated by the present study were governed by conditions in the gas phase alone. This mechanism was clearly demonstrated. Transfer coefficients were measured and incorporated into a quantitative explanation of the transfer rates which included the fluxes due to thermal diffusion.

Established methods are available for the prediction of transfer coefficients which apply for spherical geometries. Their derivation invokes the assumption of constant physical properties in the gas surrounding the sphere. The non-isothermal gas which is necessary around a levitated drop of iron far from satisfies this assumption. A comparison of the measured coefficients with the predicted coefficients may be expected to show some disagreement. Our present knowledge is insufficient to permit an estimate of the error in the predictions. The error is compounded by the presence of natural convection forces which arise as a consequence of the differences in gas density. The dangers of heavy reliance upon the predictions of the empirical correlations are great and can no longer be ignored.

The essence of this thesis represents a chemical engineering approach to a long established area of metallurgical study. It stands on the boundary between the chemical engineer and the metallurgical engineer. The reader may be from the field of transport phenomena, or may be a metallurgical thermodynamicist. The language of each must be used, and must be combined so that it is clear to both. There is a great need for the boundary to be bridged; the chemical engineer is introduced to the very real problems and practical demands which face the chemical pyrometallurgist in the laboratory; the metallurgical

engineer may have much to learn from the chemical engineering techniques by which a deeper insight into his experiments may be obtained.

CHAPTER 2

REVIEW OF THE TOPIC

2.1 Previous Applications of the Levitation Technique

As an experimental device, the levitation technique has found use towards many goals. It has been used for a wide range of purposes which may be categorised as follows:

(a) Preparation of metal alloys

(b) Casting

(c) Purification of metals

(d) Measurement of certain physical properties

(e) Vaporisation

(f) Measurement of the thermodynamic properties of gas-metal and of slag-metal interaction

(g) Measurement of gas-metal reaction rates

The above purposes, in the order shown above, are enlarged upon below.

The levitation technique was first suggested in 1923[1], but the first significant application was not until 1952[2].

Polonis and Parr[3] in their study of phase transformation phenomena, prepared 5 gram samples of iron-titanium alloys. A plug of iron was inserted into a hole drilled in a titanium specimen which was then levitated and melted in an argon atmosphere. Iron-sulphur alloys were prepared by Sunderland[4], by

allowing 1 gram drops of iron to fall from a levitated coil into a copper mould containing a small quantity of sulphur or iron sulphide. Samples of very pure aluminum nitride were prepared by Cooper et al[5], by levitating drops of aluminum in an atmosphere of nitrogen.

Comenetz and Salatka[6] made castings of various shapes of various pure metals by levitating 10 gram samples. By the reduction of the electromagnetic field they were able to create an "electromagnetic funnel". While part of the large specimen was subjected to a lifting force, the remainder was coaxed to pour through the neck of the "funnel" into the mould. Extremely large castings were achieved by Bunshah and Juntz[7] when they levitated 60 - 120 grams of aluminum in air, and of beryllium in vacuo. The melts were cast in rods of 1 - 1.5 inches diameter, completely free from contamination.

Begley et al[8] levitated various specimens in vacuo and evaporated impurities from the liquid metal. Purification of 15 grams of niobium was facilitated in less than 2 minutes, with a drastic reduction in the oxygen content of the drop.

The density of liquid nickel has been measured[9] by photographic measurement of the volume of a levitated drop of known weight. Full advantage was taken of the flexibility in temperature and the measurements were made over a range of 1149 to 1866°C. Such a wide range would have been impossible in a crucible, particularly in view of the fact that 300°C of the range was below the normal melting point of pure nickel. El-Mehairy and Ward[10] made measurements of the density of molten copper over the temperature range 1097 to 1827°C by an identical technique. A novel technique was suggested by Hulsey[11] for measurement of surface tension and density of liquid metals. Experimental measurement of surface tension has always presented problems to

the metallurgist, mainly stemming from liquid purity, surface contamination and containment. Levitation overcomes these problems. The method suggested involves a force balance along the central vertical axis of the drop. Exploitation of this approach has not been reported in the literature. Murarka et al[12] measured the surface tension of iron and nickel, by taking high speed photographs in order to determine the frequency of oscillation of the surface. The frequency is very accurately related to surface tension, but the relationship may be applied only for a spherical specimen.

Vaporisation studies were performed by Ward and Smith[13] which included the evaporation of liquid iron into a vacuum. From this, the vapour pressure of iron was calculated in the temperature range 1687 to 1840°C. Similar measurements were made by Svyazhin et al[14], with the exception that the drop was surrounded by a carrier gas. Turkdogan et al[15] studied the rates of vaporisation from drops of iron, copper, nickel, cobalt, manganese, in streams of gas which had a certain oxygen potential. The rates of iron vaporisation were found to be greatly accelerated due to iron oxide fume formation. Robertson et al[16] successfully levitated and melted a variety of sulphides of metals, despite their general classification as electrical non-conductors. Vaporisation rates, partially of elemental sulphur, were measured but mainly on a qualitative basis.

The equilibria between liquid metal and slag have been studied by Distin et al[17] for the liquid phase of iron and the slag phase of iron oxide. The temperature range was 1785 to 1960°C. Experimental limitations prevented the range being extended at the lower end. A more thorough trial with different designs of levitation coil may have enabled lower drop temperatures to be established. The matter is discussed more fully in Section 2.4. While Distin took

full advantage of the assets (see Section 2.2) of levitation melting, the slag-metal studies were handicapped by the problem of determining the phase compositions. A novel means was used for separately taking samples of slag and iron from the suspended drop at high temperatures. An alternative means was by Caryll and Ward[18] who, at steady state, switched off the power and allowed the specimen to fall between the faces of an anvil and a moving piston. The specimen was crushed so rapidly, that the compositions of the two solid phases at room temperature were truly representative of the liquid phase before quenching. In this way they measured the distribution of manganese between a metal and a slag. It is interesting to note that in both studies the steady state conditions were attained in periods of time which were measured in seconds. It is apparent that, although the slag is a non-conductor and is subject to no motion by magnetic forces, the vigorous internal motion of the metal phase is transferred to the slag by viscous forces. Such motion, which is absent from crucible melts, leads to rapid equilibrium between the phases.

Various studies have been made of the equilibria between gases and liquid metals. Kershaw[19] measured the equilibrium very successfully between iron-vanadium alloys in contact with hydrogen-water vapour mixtures. The same gas mixture was used by Shiraishi[20] who measured the oxygen content of levitated drops of iron-chromium alloys. Larche[21] continued the study of this alloy more thoroughly, and compared the oxygen contents of the liquid when they were created both by hydrogen-water vapour mixtures, and by carbon monoxide-carbon dioxide mixtures. Toop and Richardson[22] reported equilibrium values for the partition of oxygen between CO-CO_2 mixtures and copper, or nickel.

The ternary of iron-chromium-sulphur has been examined[23] using gases of H_2-H_2S. The solubility of nitrogen has been measured[24] in liquids of iron, iron-carbon and iron-aluminum. The above gas-metal studies were certainly more easily and more efficiently facilitated by the levitation technique than by conventional methods. The studies clearly demonstrated the experimental potential of the technique. However, in all the investigations, the gases were at room temperature while the drops were at temperatures in excess of 1000°C. The results are clouded by the element of doubt that stems from thermal diffusion, which is not explained by the authors. This matter is fully introduced in Section 2.5.

The period of time required for the attainment of equilibrium has received some attention in the past. The rates of decarburisation of iron drops were studied by Baker et al[25,26] using either oxygen or carbon dioxide as oxidant, with diluents of carbon monoxide or helium. Although the decarburisation process may appear to be easily understood at first glance, it is in fact a very complicated process. The levitated drop provided an excellent means for visual observation, which yielded informative, qualitative evidence about the decarburisation mechanisms. The kinetics of oxidation of various binary and ternary alloys of iron[27], and of pure iron[28], have been studied. The wide range of gaseous combinations which could be employed in a levitation apparatus was clearly demonstrated by Distin[29,30]. The transfer rates of various species to an iron drop were measured from a wide variety of gases, including oxygen, ethylene, and methane.

The rates of mass transfer to drops of iron, falling freely under gravity have received attention in recent years. Various transfer mechanisms have been studied[31,32,33] for drops falling through various gases which were in columns of different heights. Baker[31] initiated his experiments by a wire melting technique which created a stream of discrete drops at the top of the column of gas. This method suffers from an inability to predict and control accurately the size of the drops; the temperature is limited to that of the melting point of the wire. The shortcomings may be overcome by adoption of the levitation technique. Falling iron drop studies[32,33] have demonstrated that the levitation coil serves as an excellent device for preparation of iron drops, in well controlled conditions, prior to passage through a column of reactive gas.

2.2 Advantages of Levitation Melting

The previous section has outlined the many services for which the levitation technique has been utilised. These uses have taken advantage of one or more of the assets of the method. For the benefit of the chemical engineering reader, these advantages -- particularly where pertinent to gas-metal studies such as Fe-H_2-H_2S -- are outlined below.

Speed. The time involved in heating and melting the metal is extremely short. Many specimens may be levitated during the course of a laboratory day. In contrast to this, any experimental system which involves delicate refractory materials with their low thermal shock resistance, may take as

much as a day merely to heat up from room temperature.

Non-contamination. There is no physical contact between the specimen and material of support or containment. The metal, once purified, (which may be performed within the coil) will remain pure without fear of contamination and dissolution during the course of an experiment. The problems created by the dissolution of refractory crucibles are obviated.

Aggressive materials. A corollary of the freedom of contamination is that studies may be performed which involve corrosive slags and aggressive gases (e.g., H_2S).

Liquid stirring. The liquid metal is probably homogeneous at all times, due to the electromagnetic stirring from the coil. This is often desired in certain mass transfer experiments. Uniform temperatures throughout the metal are always desired. The problems of sampling are simplified since the whole specimen is taken for analysis. When suction samples are taken from a crucible melt, particularly when immersed in a resistance-wound furnace, there is always the question of how representative is the sample.

Temperature range. A major advantage of the levitation technique is the wide range of temperatures which may be employed. The absence of materials of support, and the absence of a thermocouple sheath in the metal, remove any external limit on the upper temperature. Very high temperatures may be achieved, which are limited only by the severity of vaporisation or fume formation from the specimen itself. The high purity of the melt means the absence of any sites for any heterogeneous nucleation process, including solidification. The temperature range for liquid phase study may be extended well below the normal melting point. Gomersall et al[34] demonstrated that nickel and iron could be supercooled as much as 400°C below the melting

point, in an atmosphere of hydrogen, with complete liquid phase stability. The narrowness of the range of temperature over which equilibria are already known is a hindrance to the thermodynamicist at the moment.

Geometry. The simple geometry of the system provides other desirable features, as well as that of simplicity of experimental method. Although the specimen is spherical, the surface area is large for the volumes of metal used. The geometry may be accurately reproduced in further experiments, whereas the complex geometry of crucible and furnace apparatuses often defies reproduction in another laboratory. Not only is reproduction difficult but the results cannot be interpreted fully or extrapolated. Many examples[35,36,37] of these types of experiment abound in the metallurgical literature, where a gas is blown down a tube onto the surface of a melt in a crucible within a vertical furnace chamber. Rates of mass transfer from gas to liquid are measured. Often, no record is made of such important parameters as: diameter of the gas-bearing tube; its height above the melt surface; surface area of the melt; depth of the melt; diameter of the furnace. Even where some of these parameters are recorded -- such as Peters et al[37] who desulphurised crucible melts of iron by blowing with mixtures of hydrogen, helium and argon -- the experimental results cannot be extrapolated beyond the framework of the apparatus in which they were collected. In contrast to this, since the levitation apparatus may be described mathematically, there is some scope for the extension of the data collected from it.

Chemical engineering. The chemical engineer has for many years studied the mechanisms of heat and mass transfer to and from spheres. In some cases a deliberate effort has been made to achieve severe, non-isothermal conditions in the continuous phase. In some cases the studies have been handicapped by

the necessity to provide a physical means of support for the sphere. The inherent advantages of levitation are immediately relevant to the aforementioned two points. The chemical engineer may well find it profitable to consider the levitated sphere as a technique with which to perform certain non-isothermal studies in the field of transport phenomena.

2.3 Disadvantages of Levitation Melting

There are four major limitations in the use of levitation melting. The first one is the obvious fact that specimens must be limited to electrical conductors. Although this limitation is quite rigid, it is not frequently encountered in the metallurgical field, with the exception of slag studies. However, the work of Robertson et al[16] with metal sulphides demonstrated that even many non-metallic materials may be levitated.

The second disadvantage is that for a given system where all conditions are fixed with the exception of the power to the coil, the range of temperature is limited[17]. The most serious failing of the technique is that studies in the past have been invalidated by errors caused by thermal diffusion in the continuous phase. These two disadvantages, particularly the latter, are a major concern of this thesis. They are clarified in more detail in Sections 2.4 and 2.5.

The fourth disadvantage, of more significance to the chemical engineer than to the metallurgist, is the wide variation of physical properties of the gas phase in the non-isothermal film around the drop.

2.4 Design of Coil

The fundamental explanation of the phenomena, whereby interacting electromagnetic fields are arranged so as to overcome gravitational force and to support an object, is complex. Detailed understanding of the theory is often not essential for practical use of the technique. As a consequence, the levitation apparatus has often been used qualitatively by the metallurgist with little reference to the theory behind it. Only recently have users of the tool concerned themselves[16] with the theoretical basis.

The factors which affect levitability are as follows:

a) Coil current and characteristics, including frequency and power;

b) Coil geometry;

c) Size and density of specimen;

d) Electrical properties of specimen, such as conductivity and permeability;

e) Permeability of the surrounding media.

When a study is to be undertaken many of the above factors are fixed prior to commencement of the laboratory work. The coil current, characteristics and total power available, are usually dictated by the particular generator which is available. High frequency generators are expensive, and usually limited in number at any particular research establishment. The properties of the specimen and continuous medium are those of the system under examination. A small degree of latitude in the size of the specimen is possible but usually the size must remain constant from specimen to specimen. Below a certain size levitation is impossible. The upper radius is determined by

the maximum power output of the generator; by the surface tension of the specimen if sphericity is to be maintained; and by the maximum temperature requirements. The factors which may be controlled are thus, by elimination, the geometry of the coil, and the power output from the generator between zero and maximum. If the only consideration is that the specimen be levitated, then the limitations would be minor. In addition, however, often the specimen must be melted and its temperature must be accurately controlled. The situation is greatly compounded. The self-same electromagnetic forces which provide lift, also give rise to eddy currents in the specimen, which in turn generate heat. The amount of heat is determined by the strength of the field, but the power requirements must be fixed initially by the gravitational forces on the specimen.

An introductory treatment of the theory of levitation is given by Rony[38]. More practical explanations are given by Hulsey[39] and Robertson[16] Rony gives the basic equations for the lifting force and power input to a sphere in a sinusoidally alternating magnetic field:

$$\frac{\text{Force vector}}{\text{wt}} = -\frac{3}{2\rho_d \cdot \mu_o} G(y).(\bar{B}.\nabla)\bar{B} \qquad (2.1)$$

$$\text{Power} = \frac{3\pi a}{\sigma_d \cdot \mu_o^2} H(y).(\bar{B}.\bar{B}) \qquad (2.2)$$

where ρ_d is the density of the metal sphere;

μ_o is the permeability of free space;

∇ is the vector del operator;

$\bar{B}$ is the magnetic field strength vector;

a is the radius of the sphere;

σ_d is the electrical conductivity of the metal.

The symbols μ and σ are used according to conventional electrical engineering practice to denote permeability and conductivity in equations (2.1), (2.2) and (2.3) only. In the remainder of this thesis the symbols will have meanings which are common to chemical engineering. The functions G(y) and H(y), are functions of the skin depth (field penetration into the liquid).

$$y = a. (1/2 . \omega . \mu_d . \sigma_d)^{1/2} \qquad (2.3)$$

where μ_d is the permeability of the metal;

ω is the radian frequency of the magnetic field.

The solutions to the functions G(y) and H(y) are given in complete detail by Rony, in both algebraic and graphical form. The solutions are independent of coil geometry and the strength of the magnetic field.

The salient points which stem from equations (2.1), (2.2) and (2.3) are listed. The only control characteristic during an experiment is the strengt of the magnetic field. The control may be effected by the adjustment of the power output from the generator, or by the coil geometry. The magnetic field, simultaneously, performs two duties. Alterations in the field strength in order to adjust the power for heating requirements, also change the strength of the lifting force. However, the dependence of the (I^2R) losses is different from the dependence of the lifting forces. Some degree of uncoupling does exist between the power input to the sphere and the lift of the sphere. The slight uncoupling has never been exploited by previous workers.

While the theoretical description by Rony is correct it is extremely fundamental. Most of the levitation coils which have actually been used, have been designed from practical experience. A qualitative description of levitation theory, with more practical value, has been given by Rostron[40]. However, most workers have taken as their starting point the design of Harris and Jenkins[41] whose names have subsequently come to be used to describe this particular design. Their coil consisted of seven turns of silver tubing, the lower two of which were co-planar. The next three turns above formed a 45^{o} cone, widening from the inner bottom turn. The final two turns were reversed in direction, directly above the cone, and of the same diameter as the lowest turns. The design gave a magnetic null point which was completely enclosed by two opposing magnetic fields. This configuration gave stability to the specimen and reduced irregular motion and bodily oscillations.

A variation on the design of Harris was tried by Begley et al[8] who replaced the upper, reverse turns with a water-cooled disc. This in turn was modified by Lewis et al[42] who claimed a marked increase in specimen stability. By making the disc movable relative to the coil compensation could be made for lack of symmetry in the winding of the coil.

Further description of the various designs is unnecessary here. An excellent review of the many different coils, and their many uses, is given by Peifer[43]. More details about the forces of levitation are given by Fromm and Jehn[44] and Hatch and Smith[45].

Most workers in the past have manufactured coils of the Harris and Jenkins design, and put them to trial for their particular purpose. Often, coils which have identical appearances give widely varying levitation performances. The workers have then chosen the one particular coil which produced

the best levitation behaviour for their specific purposes, and used that one throughout their experiments. As Booth and Charles[46] point out, this choice is made on levitability only, and whatever heating effect is produced is merely tolerated. The temperature of the drop is controlled by varying the rate of heat removal. Choice of gas composition and gas flow rate gives adequate temperature control. For most experiments this approach is satisfactor However, for two cases of gas-metal interaction this approach becomes invalid.

For kinetic studies, the rates of mass transfer may be dependent upon the gas flow rate, and thus the gas flow rate must be predetermined and cannot be adjusted during the course of experiments for considerations of temperature. This has been a major obstacle in the use of levitation for kinetic studies. The obstacle must be overcome if future kinetic experiments are contemplated, and temperature control must be achieved solely by adjustment of the power input to the specimen.

The second case is that of the measurement of equilibria between liquid metal and soluble gas. In many such measurements thermal diffusion (see 2.5) may influence the steady state composition of the metal. The degree of thermal diffusion, and hence the extent of its influence, may be a function of gas flow rate. Thermodynamic studies[19,21,22] in the past may have contained errors, which were not only due to the presence of thermal diffusion in the gas phase, but were also due to changes in the magnitude of the thermal diffusion. Thus, temperature control of the drop by changing the gas flow rate is a practice which is open to question.

2.5 Thermal Diffusion

Previously (Section 2.2) the advantages of levitation melting were discussed in some detail. While the disadvantages are few in number, their importance is probably paramount and cannot be disregarded. One of the disadvantages alone has been considered insurmountable. The seriousness of the latter, that of thermal diffusion in the gas phase, stems from the fact that it is inherent in the technique. So far only fleeting mention of this subject has been made. Section 2.5 will attempt to provide further explanation.

2.5.1 Origin and Derivation

Qualitative description of the phenomenon is simple. Suppose a fluid is a mixture of more than one species and is subjected to a difference in temperature throughout its body. In the absence of any other external forces, for a mixture which is originally homogeneous, the non-uniform temperature leads to a state of non-uniform composition. A migration of molecules takes place. For simplicity, if the mixture were binary one component would tend to move to the hot region, while the other would collect in the cold region. Usually (but exceptions are known) the gas with the lighter/smaller molecule collects in the hot zone while the heavier/larger molecules migrate to the cold zone.

The phenomenon is not to be confused with natural (free) convection which stems from differences in density which may or may not be a result of temperature differences.

The consequent gradient of composition is in the same direction as

the original temperature gradient. Of course, the concentration differences give rise to ordinary molecular diffusion which tends to reduce the newly created concentration profiles. The thermal diffusion and molecular diffusion are in opposition. If the temperature gradient is time independent, a steady state is eventually attained, in which the composition is non-uniform and the transport by molecular diffusion is equal and opposite to transport by thermal diffusion.

Thermal diffusion has been well known for many years but the origin of the discovery is interesting. Enskog first predicted it in 1911, as a result of his theoretical work on the mathematical description of the thermodynamics of gases, which is fully reviewed by Chapman and Cowling[47]. Enskog's theory predicted the existence of thermal diffusion in gas mixtures although the phenomenon had not been observed at that time. Subsequently, the effect was isolated in the laboratory in 1917[48]. The classical manner of its discovery illustrates the fact that the causes which give rise to thermal diffusion cannot be described by a physical or a molecular picture. Of all the many works in the literature, only Present[49] attempts to draw a visual explanation of the molecular interactions. We must accept that the explanation of thermal diffusion derives from the mathematical theory of gas phase behaviour.

Many of the early studies of thermal diffusion were classical and theoretical, carried out by mathematicians or theoretical physicists. The explanations are many[50,51,52] but all are very similar, varying mainly in the degree of complexity. Frankel[52] points out that thermal diffusion is not amenable to elementary derivation. However, Gillespie[53] does

attempt to sum up his earlier approximate theory[51] into one final equation which represents the first engineering equation. While there is still scope for discussion among the theoretical physicists at the present time, an engineering explanation is available, as shown below.

Many irreversible processes occur in nature and may be described by the familiar phenomenological laws, e.g., Ohm's law relates electrical current and potential gradient; Fourier's law relates heat flow and temperature gradient. However, when two or more phenomena occur simultaneously, they interact and create cross effects with which we are less familiar. The driving forces may be temperature gradient, gradient of chemical potential, potential gradient, velocity gradient, etc. These give rise to flow of heat, mass, electrical current, momentum, etc. In general, any force can give rise to any flow. Considerations of irreversible thermodynamics for a multicomponent mixture give the general phenomenological equation:

$$\bar{J}_i = \sum_{m=1}^{n} L_{im} \bar{X}_m \qquad (2.4)$$

where vector $\bar{J}_i$ is any (i=1---n) flow or flux,

vector $\bar{X}_m$ is any (m=1---n) force,

L_{im} are the phenomenological coefficients of the nature of a conductance, or reciprocal of resistance,

L is a scalar quantity.

The flux and force are linearly proportional.

The forces at the moment have not been rigidly defined. Onsager's analysis defines them in such a way, that the sum of the products of each flow and its appropriate force is equal to the product of the absolute temperature and the rate of creation of entropy per unit volume of the system.

An essential consequence of this is a symmetry of the system, usually referred to as Onsager's reciprocal relationship:

$$L_{im} = L_{mi} \tag{2.5}$$

Electrical conductivity and molecular diffusivity are examples of coefficients L_{ii}. Coefficients L_{im}, where $m \neq i$, pertain to the mutual interference phenomena.

Consider the case of a binary mixture in which mechanical, electrical, and gravitational forces are absent. If subscript 1 refers to energy, and subscript 2 refers to the mass of one component of the mixture, equation (2.4) simplifies to:

$$J_1 = L_{11} X_1 + L_{12} X_2 \tag{2.6}$$

$$J_2 = L_{21} X_1 + L_{22} X_2 \tag{2.7}$$

The term $L_{11} X_1$ represents the transfer of energy by ordinary conduction. The term $L_{12} X_2$ represents the transfer of energy due to a gradient of chemical potential within the mixture, (Dufour effect). The term $L_{22} X_2$ represents ordinary molecular diffusion of one component. The term $L_{21} X_1$ represents the flux of mass due to a thermal driving force (Soret effect).

Excellent explanations of equations (2.4) to (2.7) are given in the books by DeGroot[54] and by Denbigh[55]. Of interest to us, without going into depth, is the fact that Onsager's analysis precisely defines the

forces, and hence:

$$X_1 = - \text{ grad. } \ln T = \frac{- \text{ grad. } T}{T} \tag{2.8}$$

$$X_2 = - T. \text{ grad. } \frac{\eta_2}{T} \tag{2.9}$$

where T is the absolute temperature,

η_2 is the chemical potential of species 2.

When the chemical potential is rewritten in terms of concentration, the familiar form of Fick's law for molecular diffusion results:

$$\text{Molecular diffusion flux} = D_{AB} \cdot C \cdot \text{grad. } x_2 \tag{2.10}$$

where D_{AB} is the molecular diffusion coefficient,

C is the total molar concentration,

x_2 is the mole fraction in the mixture.

When defining a coefficient for thermal diffusion, the analogy with Fick's law is made:

$$\text{Thermal diffusion flux} = D_T \cdot C. \text{ grad. } \ln T \tag{2.11}$$

where D_T is the thermal diffusion coefficient, or Soret coefficient.

Traditionally, studies of thermal diffusion have been made in the two bulb apparatus, which is free from convective forces. One bulb is hot and the other bulb is cold. The bulbs are connected by a horizontal, narrow tube. The apparatus is filled with the gaseous mixture. The system is

allowed to reach steady state, in which the thermal diffusion flux balances the molecular diffusion flux. Samples are taken of the gases in each bulb and analysed. The resulting measurements, for obvious reasons, are often expressed as a ratio:

$$k_T = \frac{D_T}{D_{AB}} \tag{2.12}$$

where k_T is the thermal diffusion ratio.

Irreversible thermodynamics gives us the form of the flux equation; we must look elsewhere for evaluation of the coefficients. The kinetic theory of gases provides methods for evaluation of both coefficients. This is discussed later.

2.5.2 In Metallurgical Studies

The interaction coefficients (Soret and Dufour) are small compared to the main effects, and as a consequence the interaction effects are relatively small in chemical engineering systems. However, the chemical engineer does not encounter the temperature differences frequently encountered by the metallurgical engineer. The high temperatures present in many metallurgical systems which also comprise room temperature gases, give rise to significant thermal diffusion despite the small coefficients.

In general, there are three types of apparatus available for studies of gas-liquid, and gas-solid, metal equilibria: levitation, induction furnace, and resistance furnace. The order in which the three apparatuses are stated represents the order of increasing experimental complexity and time but the order of decreasing thermal segregation.

In the levitation and induction apparatus the heat is generated within the metal itself. The gas is usually at room temperature and its flow rate and temperature may be essential to the control of the metal temperature. Very little heating of the bulk gas takes place, but the molecules adjacent to, and thus in equilibrium with, the metal attain the metal temperature. The hot gas may be deficient in the larger molecules due to thermal diffusion. The gas composition in equilibrium with the metal is different from that found by room temperature analysis of the inlet gas. Four ways have been suggested to nullify this difficulty.

The first and obvious way was suggested by Dastur and Chipman[56] who preheated mixtures of hydrogen and water vapour. This method cannot be used for levitation where the gas must dissipate heat. The practical aspects of heating and containing the gas, particularly if corrosive, are formidable.

The second alternative is based on the rule of thumb (which may well be false) i.e., that increasing the gas flow rate reduces the thermal diffusion error ultimately to a negligible amount. This unwritten law has some experimental justification[57,58,59]. However, it is contrary to the fact that increases in gas flow rate, increase the heat transfer and therefore increase the gas phase, surface temperature gradient, which is the driving force for thermal diffusion.

The complete solution is to use a resistance furnace, where the source of heat is the whole refractory furnace tube. A slow moving gas is heated by the furnace tube and contacts the crucible and melt at the melt temperature. Kontopoulos[60] who studied the equilibria of hydrogen-water vapour mixtures with iron and iron-vanadium alloys, obtained many inexplicable results after

much work with an induction furnace. The same experiments were then performed in a resistance furnace with complete success. Unfortunately, the cumbersome resistance furnace with its delicate refractories seriously reduces the speed, flexibility, and temperature range.

A fourth alternative to overcome thermal diffusion errors has been suggested by Dondelinger[23] for limited use in ternary solutions. He argues that if a binary equilibrium (e.g., iron and sulphur under hydrogen-hydrogen sulphide gas) is measured, it may be in error due to thermal segregation. However, the experiments may be repeated for a ternary solution (e.g., iron-sulphur-chromium) under identical conditions, and hence identical errors. While the equilibrium constant is again in error, it is possible to extract a valid interaction coefficient (e.g., chromium-sulphur coefficient) from the false equilibria. Although the ternary interaction parameter is of little value without activity coefficients for the binary solution, the argument has potential.

2.5.3 In Process Engineering

In general the Soret and Dufour effects are relatively small (although Delancey and Chiang[61] suggest that the Dufour effect in certain liquid systems may sometimes be significant). In most conventional heat or mass transfer apparatus, thermal diffusion is overshadowed. Industrial technology has found difficulty in exploiting the phenomenon for commercial gain. Consequently, the early theoretical and fundamental studies of the subject have not led to a large amount of technological application, nor to the accompanying information necessary for process design. The only text which does not involve a highly mathematical description of gases but takes an engineering approach is that of Grew and Ibbs[62].

The diffusion phenomenon, although weak, has been utilised in one specialised separation of mixtures and a process of industrial dimensions has been developed. In cases where the more conventional, physical and chemical methods of separating gas mixtures are inoperable, thermal diffusion may offer a solution. One such case is the separation of mixtures of isotopes. The process is carried out in a Clusius-Dickel column[49,62]. The separation is achieved by a novel counter-current arrangement which creates increasing segregation of the components as the gas moves through the column. In principle, the closed column may be equated to two flat vertical walls facing each other. One wall is hot, the other is cold. The gas occupies the space between the walls. Thermal diffusion occurs in the horizontal plane along the temperature gradient. Simultaneously, natural convection creates circulation as the gas mixture adjacent to the hot wall bodily rises and the gas mixture adjacent to the cold wall bodily descends. The interaction of the two motions may be carefully controlled so that a wide degree of separation may be achieved. The gases are taken off at the top and bottom of the column. Unfortunately, the process is slow, must be carefully controlled to prevent any external source of gas turbulence, and the column may have to be extremely large. A full scale plant was built in 1944 at Oak Ridge, Tennessee[63] for separation of uranium isotopes. The plant was successful in operation and ceased to operate only when superseded by the gaseous diffusion process.

2.6 Kinetic Studies

Very few kinetic studies have been performed with levitated drops. Some[22,25-30] have been mentioned already. The number is few because of experimental difficulties and because of difficulty in explaining the experimental data quantitatively. Appreciating the latter problem Robertson and Jenkins[64] restricted themselves to a qualitative, yet revealing, study of decarburisation and desiliconisation of iron drops by oxygen-bearing gases, which was made by use of high speed photography. Further desiliconisation rate measurements were made by Sano and Matsushita[65] by contacting iron-silicon drops with oxygen or carbon dioxide. Even for this apparently simple system, interpretation of the rate data becomes difficult because of the nature of the reaction product. The product may be gaseous SiO, or silica which collects on the drop surface, or a mixture of both.

If the system is complex interpretation is probably impossible. If the system is simple then some attempt at interpretation may be possible. The attempt probably involves chemical engineering techniques with which the metallurgical engineer may not be completely familiar.

2.6.1 Interpretation and Mechanism

Mass transfer to and from a room temperature gas which involves a chemical reaction, from and to a liquid metal, levitated or in a crucible, is a complicated process. Fortunately, the overall mechanism is sequential and usually one single stage controls the overall rate of the process. It is customary to suggest a preliminary model based upon this stage. However,

for such a model to be valid, the proposed controlling step must first be proved, conclusively, to be the step which is in fact controlling. Only then should the parameters of the model be examined. Too frequently in metallurgical studies, the isolation and proof of the controlling step is neglected or based upon indirect evidence.

Earlier levitation studies[25-30,33,65] have suggested that the rates of transfer are controlled by the gas phase conditions. If a similar mechanism applies to sulphur transfer, a more comprehensive interpretation will be attempted here.

2.6.2 Mass Transfer Coefficients

Gas phase controlled mass transfer is analogous to the evaporation of pure spheres into an inert atmosphere. Such vaporisation has been well studied by chemical engineers, as has the process of heat transfer to and from spheres. The product of these studies has been the suggestion of many correlations, similar but not identical, for calculating heat and mass transfer coefficients. The correlations are empirical, or semi-empirical, and their variation from system to system is evidence in itself that the correlations do not fully describe the events. There are qualifications and limitations to their use. The metallurgical engineer has not always appreciated these limiting considerations.

Some of the earliest work in the field of evaporation from spheres was performed by Ranz and Marshall[66,67] whose names are now often used to describe the correlations. The correlations apply to a single sphere in an infinite medium of which the physical properties remain constant. Heat

removal is by pure conduction and forced convection (radiation is neglected). Evaporation is by molecular diffusion and forced convection. Natural convection is not considered and no chemical reaction occurs. Ranz and Marshall find that the rates may be well described, in terms of dimensionless groups, by:

$$Nu = 2.0 + 0.6\ Re^{1/2} \cdot Pr^{1/3} \qquad (2.13)$$

$$Sh = 2.0 + 0.6\ Re^{1/2} \cdot Sc^{1/3} \qquad (2.14)$$

where the Nusselt number, $Nu = \frac{h.2a}{k}$;

the Sherwood number, $Sh = \frac{kg.2a}{D_{AB}}$;

the Reynolds number, $Re = \frac{\rho.2a.V}{\mu}$;

the Prandtl number, $Pr = \frac{Cp.\mu}{k}$;

the Schmidt number, $Sc = \frac{\mu}{\rho.D_{AB}}$;

h is the heat transfer coefficient,

k is the thermal conductivity of the fluid;

kg is the mass transfer coefficient in the fluid;

ρ is the density of the fluid;

V is the approach velocity of the continuous fluid;

μ is the viscosity of the fluid;

Cp is the specific heat of the fluid.

In equation (2.13) for heat transfer, and equation (2.14) for mass transfer, the constant 2.0 represents the flux by pure conduction or by molecular diffusion. The value is determined from theoretical considerations of a sphere in a stagnant medium of constant physical properties (see later). The second term represents the flux due to forced convection caused by the externally imposed motion of the fluid past the sphere. The exponents of the Re, Pr and Sc are predicted by laminar boundary layer theory. Some later workers have rigidly borne in mind the theoretical considerations when attempting to correlate their experimental measurements to Nu - Re - Pr or Sh - Re - Sc type relationships. Other workers have empirically chosen the constants and exponents which gave the best fit to their measurements. In the latter, the particular experimental conditions, specifically the range of Re, are the only ones for which the correlations truly apply.

Any fluid motion past the sphere gives rise to convection transfer. In addition to an imposed velocity of the continuous phase, motion may be caused by density differences, resulting in natural or free convection. The driving force for such motion is the density difference itself, regardless of whether the difference is caused by temperature differences or by concentration differences. If the sphere's presence creates a density decrease, e.g., a hot sphere and a cold inlet gas - and the fluid is flowing vertically upwards, then natural convection aids forced convection transfer. Conversely, if the flow direction is reversed for the same hot sphere, the two convective forces interact in opposition.

Natural convection, with and without forced convection around spheres, has been widely studied. Various correlations have been suggested

for predicting heat and mass transfer coefficients. Steinberger and Treybal[68] have reviewed many earlier measurements and used them to suggest a correlation. This equation is typical of those in the literature and applies for the product [Gr.Sc] less than 10^8. It is written here for mass transfer.

$$Sh = 2.0 + 0.347\ (Re.Sc^{1/2})^{0.62} + 0.569(Gr.Sc)^{1/4} \qquad (2.15)$$

where the Grashof number, $Gr = \dfrac{g.(2a)^3.(\rho_\infty - \rho_i).\rho_f}{\mu_f^2}$

in which g is the local acceleration due to gravity. The subscripts ∞ and i apply, respectively, to the state of the continuous phase in the bulk, and at the interface between fluid and sphere. The subscript f is introduced as a concept for the evaluation of physical properties. It refers to a condition (not a physical location) which lies between ∞ and i. By definition, natural convection is accompanied by changing density which of course is accompanied by changing of all physical properties. The problem of choosing a single value for each property arises. Customary practice is to evaluate a mean, which is given at an arithmetic mean film temperature, T_f.

$$T_f = \frac{T_\infty + T_i}{2} \qquad (2.16)$$

There is no theoretical basis for this choice of T_f. When used in the correlations, it has been found reliable for narrow ranges of temperature. Neither its use, nor the empirical correlations themselves, have been proved for the magnitude of the changes in physical properties which is generated

by temperature differences of 1600°C. There is strong reason to suspect the accuracy of mass transfer coefficients which are predicted for a levitated drop of liquid iron surrounded by a room temperature gas.

Equation (2.15) epitomises the concept that the three fluxes (molecular diffusion, forced convection, and natural convection) which constitute the gross transfer, are independent and that they may be collected together by simple addition. Modern thought is that the flow behaviour is not so simple. Simultaneous forced and natural convection may interact with each other so that each may be mutually influenced by the other[69]. This trend is a consequence of the drift away from the empirical correlations towards fundamental studies. The inability of the correlations to explain and predict accurately for non-isothermal systems is being overcome by numerical attempts to solve the equations of continuity, energy and momentum, which correctly and more fundamentally describe fluid flow around a sphere.

The non-isothermal conditions, close proximity of the reaction tube wall, and the slight distortion in the sphericity of the drop in a levitation apparatus, are conditions far removed from those in which the correlations were devised. For a levitation apparatus, the best way to evaluate mass transfer coefficients is to measure them experimentally in the levitation apparatus itself.

It is not the object of this study to specifically measure mass transfer coefficients with the aim of suggesting a non-isothermal correlation for their prediction. However, their significance in levitation studies will be more clearly shown. Further review is omitted here. The reader is

recommended to the excellent, and very readable, review of non-isothermal heat and mass transfer from spheres given by Narasimhan[69].

2.7 Thermodynamics of Fe-H_2-H_2S

Historically the steelmaker has been interested in the thermodynamics of sulphur partitioned across a liquid steel-slag interface. The introduction of oxygen steelmaking furnaces, gas bubbling in the ladle, and vacuum degassing, has created an increasing interest in the thermodynamics of sulphur between liquid steel and gas phases. However, there is a surprising lack of accurate thermodynamic data for the dissolution of sulphur in iron and its alloys from sulphur-bearing gases.

The equilibria for the reaction

$$H_2(gas) + \underline{S}\ (dissolved\ in\ liquid\ iron) = H_2S\ (gas)$$

were studied as early as 1937[70]. Ten years later White and Skelly[71] carried out measurements, followed by Morris and Williams[72] in 1949. These early works were limited and also, when calculating the equilibrium constant K, did not allow for the solution's deviation from Henry's law.

Sherman et al[73] studied the dissolution of sulphur in iron over the temperature range 1530 to 1730°C. Cordier and Chipman[74] subsequently used the same apparatus and technique for melts of iron and iron-nickel alloys at 1600°C. Both methods used induction melting, which gave stirring of the melt, and also permitted high melt temperatures yet not so high

refractory tube temperatures. Attempts were made to minimise thermal diffusion errors by some degree of gas preheating. However, errors were probably still caused by thermal segregation and additionally probably occurred in the temperature measurement which was by a disappearing-filament, optical pyrometer focussed on the melt surface. Deviation from Henry's law was observed and values for an activity coefficient were determined.

A mention of customary, metallurgical practice may be relevant here for the benefit of the chemical engineer. Studies of gas-metal equilibria usually follow a certain pattern which is shown for purposes of example, for the Fe-H_2-H_2S equilibrium. The equilibrium constant may be defined:

$$K = \frac{PH_2S}{PH_2.a_s} = \frac{PH_2S}{PH_2.(\%S).f_s} \qquad (2.17)$$

The gas composition is given by ratio of the partial pressures, PH_2S and PH_2. The activity of sulphur in the iron, a_s, is given by the product of the weight percentage of sulphur (%S), and the activity coefficient f_s. If a solution obeys Henry's law (or Raoult's), the activity coefficient is constant, independent of composition. Most metallic solutions exhibit deviation from Henry's law and the coefficient is a function of composition. Thermodynamic data are usually only known (if at all) sufficiently accurately to allow a first order dependence upon solute content to be stated. A second term is defined:

$$K' = \frac{PH_2S}{PH_2.(\%S)} \qquad (2.18)$$

Therefore

$$\log K' = \log f_s + \log K \qquad (2.19)$$

Measurements are made of the gas ratio and the sulphur in the iron at equilibrium. A plot of log K' against (%S) is made. At infinite dilution of the solvent, f_s is unity and log K' = log K, enabling K to be read off from the ordinate. The data are caused to fit a straight line, so that:

$$\log f_s = e_s^s (\%S) \qquad (2.20)$$

where the constant, e_s^s is the sulphur self-interaction parameter, (first order) and is the slope of the straight line. The whole procedure may be repeated at various melt temperatures to yield K and the interaction parameter as a function of temperature.

The procedure above has been followed by most workers, including Adachi and Morita[75] who studied the equilibria over 1550 to 1750°C, with sulphur concentrations as high as 5%. A carbon tube resistance furnace and H_2-H_2S gas bubbling were used in order to eliminate thermal diffusion and accelerate the attainment of equilibrium. The temperature was measured by a disappearing-filament pyrometer sighted on the melt surface. Unfortunately, the turbulent surface and changing emissivity of the melt with sulphur content, probably created errors. The crucibles were alumina which, at the higher temperatures, were a source of contamination when agitated by the bubbling of the sulphurous gases. Corrosion of the crucibles, although not mentioned, must have been severe particularly when dealing with the melts of high sulphur content.

Further Japanese studies have been performed[76] with an induction furnace. The gases were preheated, but were not bubbled into the melt. Attempts to minimise temperature errors were made by using an immersed thermocouple in addition to an optical pyrometer. Measurements were made at 1500, 1600 and 1700°C. While the data at the lowest temperature appear to be excellent, considerable scatter is present at the higher temperatures.

Much improved data were obtained by Fuwa et al[77] using a similar apparatus without a thermocouple immersed in the melt. Experimental inconvenience was minimised by using only three close temperatures; 1600, 1665 and 1700°C.

However, speculation about the binary Fe-S, and ternaries Fe-X-S, continued until the broad systematic study of Chipman and Ban-ya. Their study occupies three publications of which Part I[78] concerns the binary equilibrium. A multi-crucible resistance wound furnace was used, of such a design that thermal diffusion error was reduced, probably to a negligible amount. Errors due to optical pyrometry were obviated by use of a thermocouple; moreover contamination by the sheath was obviated by avoiding immersion in the melt. The melts were very small (3 grams) and were quenched as a whole unit in order to reduce the errors which may arise from suction sampling from a large melt. Temperatures in excess of 1600°C were not employed. Hence, contamination by the refractories should have been negligible. At temperatures of 1600°C and above, H_2S exhibits a small degree of dissociation into H_2, HS, S and S_2. Very accurate free energies of formation of the products of dissociation were employed by Chipman and Ban-ya, in a very precise manner in order to correct, if necessary, the room temperature gas analysis for dissociation at the high temperatures. Despite the absence of

measurements above 1600°C, this study is excellent and their values are becoming the accepted ones in the field. The equilibrium constant at 1500, 1550 and 1600°C by Chipman and Ban-ya has been used as the standard throughout this thesis.

Two general points emerge from the review of past equilibria studies. Disagreement between workers is greater at higher temperatures. This is compatible with the increasing experimental difficulties of contamination and refractory wear that occurs at higher temperatures. The second point is that our present knowledge is insufficient to allow any dependence of the interaction parameter upon temperature to be stated.

2.8 Enhanced Vaporisation of Sulphur

It is a well known metallurgical fact that when molten metals are contacted by unreactive gases at room temperature, the rates of vaporisation of the metal are considerably greater than those predicted by the use of conventional mass transfer correlations. The reason is simple. As the metallic vapour leaves the hot surface and moves towards the bulk of the gas, it encounters a continuously decreasing temperature. Condensation of the vapour occurs to create a steepened concentration profile of the vapour in the gaseous environment. The net effect is very similar to, but not to be confused with, the accelerated iron vaporisation caused by the formation of iron-oxide fume[15]. In the latter case, the iron vapour concentration gradient is steepened by chemical reaction close to the surface due to the presence of oxygen in the gas. The former phenomenon may be anticipated to

occur when elemental sulphur (melting point 445°C) vaporises from a levitated iron drop into an inert gas at room temperature.

Thoughts on future methods of steelmaking include gas bubbling or purging of the bath to remove many impurities, including sulphur. The choice of gas for efficient sulphur removal would be important; the choice may be clearly demonstrated, on a qualitative basis to the steelmaker, by use of a levitated drop. The rates of removal of sulphur from the iron drop into an inert atmosphere, and into a reactive gas, under similar conditions, may be compared.

Toop and Richardson[22] observed that the rates of vaporisation of levitated drops of copper, nickel and silver were unusually high in H_2-N_2 mixtures. Further examination of copper drops at 1400, 1500 and 1600°C in streams of pure nitrogen by Glen and Richardson[79] confirmed the enhanced rates of vaporisation. Drops of iron are known to vaporise at similarly high rates. The subject has been discussed briefly by Turkdogan[80] and by Szekely and Hills[81,82]. However, a theoretical prediction of the degree of enhancement of vaporisation rates is at present not possible.

Any study of the rates of sulphur transfer between an iron drop and a reactive gas would be complemented by the inclusion of similar measurements in an unreactive gas. If an apparatus were successfully developed for sulphurisation and desulphurisation studies in reactive gases, a small additional effort to conduct a limited number of exploratory, vaporisation measurements in an inert gas, would not be excessively time consuming. The small effort may lead to a disproportionately large contribution to our knowledge.

CHAPTER 3

EXPERIMENTAL CONSIDERATIONS

The levitation technique lends itself to two basic types of cell for contacting gas and liquid drop. The levitated drop may be inside a vertical tube, which itself passes inside the coil. Alternatively, the coil, drop, and any other ancillary equipment, may be contained within a large chamber[12]. While the latter has advantages, little may be defined about the characteristics of the gas motion, even when a small bore injection tube is introduced to "blow" onto the drop. Only when a long vertical tube is used, which contains nothing but a single drop within its walls, may a meaningful gas flow rate be quoted. The second type of cell was chosen for this study's experiments which are described in detail in this Chapter.

3.1 Apparatus and Materials

A schematic view of the general apparatus is shown in Figure 1, which requires little explanation. The scheme shown is that for sulphurisation experiments which represented the major portion of the total experiments performed. For other experiments the pattern could be easily changed, allowing a switch, or an addition, of flowmeters. Glass stopcocks were used for on/off control or change of gases. Needle valves were used for control of flow rate. Wherever possible, glass ware was used. Flexible polyethylene tubing which may have an affinity for H_2S was avoided.

In the early stages of this study additional, classical purifiers were included in the gas train. It was found that their omission had not the slightest effect on the final results. Even the chamber of powdered magnesium perchlorate drying agent was omitted in some experiments.

The flowmeters were of high quality and the stainless steel floats were always steady. Concern that the corrosive nature of H_2S would affect the reliability of the flowmeters did not materialise, although the same was not true of the needle valves. The flowmeters were calibrated against a wet-test gas meter at frequent intervals.

The temperature of the gases at inlet was shown on the mercury in glass thermometer. No arrangement was made for varying the gas pressure at the drop. The level of liquid in the waste gas bubbler was constant, and the final discharge was at ambient pressure.

3.1.1 Reaction Chamber

The gas train allowed the gases to enter the reaction chamber under controlled conditions. The glass chamber is shown in Figure 2 in cross section. The gas entered a 50 mm O.D. pyrex chamber, and rose vertically past the drop. The bottom was sealed with an aluminum disc, fitted with an "O" ring which gave a gas tight seal yet allowed the disc to be completely rotated. The disc carried the quartz charging rod and copper mould, either of which could be aligned directly below the specimen by rotation of the disc. The charger and mould were inserted through Swagelok connections with Teflon seals which were again gas tight but yet allowed both rods to be raised and lowered. In certain experiments (Section 3.2.3) an aluminum base, which carried an optical prism as well as the two rods, was used

enabling the specimen to be viewed from below as well as from above, as shown.

The specimen was contained in a 15 mm O.D. Vycor reaction tube, about 27 cm long, placed eccentrically above the lower chamber. By use of ground glass unions, the tube could be easily replaced if damaged by contact with liquid specimens. Although replacement was frequent in order to maintain a clean tube at all times, the Vycor was found to have considerable resistance to limited contact with molten iron. The ground glass unions were also necessary to permit installation of the coil.

The choice of direction of gas flow was somewhat arbitrary. However, upward motion ensured that the copper mould and seals were swept clean and free from fume deposition. Such a choice merely transferred the problem to the upper section. In order to prevent any chance of error in temperature measurement due to deposition on the window, the narrow section was adopted. The narrowing of the tube did not restrict the sighting of the specimen, but trapped a stagnant pocket of gas which prevented condensation of fume or deposition of impurities on the prism.

3.1.2 Levitation Coil and Supply

The power supply was from a Toccotron high frequency generator, rated with an output of 10 KW at 200 amps and 450 kHz. The coil was connected to the generator through a water-cooled, 7.5:1 stepdown transformer.

The water-cooled coil itself was of 1/8 inch O.D. copper tubing sheathed in fibre glass insulation. After the coil had been wound, it was dipped in a weak solution of epoxy resin (cold mount) which added robustness and mechanical strength to the coil during frequent handling and coupling

to the generator. Many different types of coil were used, but basically the design was that of Harris and Jenkins[41], shown in Figure 3. Also shown is the brass former around which the copper tube was wound. The former had to be split and removed to allow the two upper reverse turns to be wound.

As mentioned earlier, previous levitation studies have involved the use of a coil which was chosen for its lift characteristics alone. In the present study, the gas flow rate was constant, thus compelling the power input control to be used for lift and temperature of the specimen. For a given generator, given specimen material and size, and given gas, the flexibili remaining for the operator was in the power input and in the coil geometry. For a given coil a temperature range of 75°C was typical; one extreme was the maximum power output of the generator, and the other extreme was the minimum power to support the specimen. Consequently, many coils were manufactured and each one chosen according to the experimental conditions desired.

The basic coil consisted of seven turns. Five of the turns were in a conical section, in which the lowest two turns were co-planar. The remaining two turns were above the cone, but wound in the reverse direction. A reduction of the number of lower turns, to 4 or to 3, weakened the induced field which reduced the heat generation within the sample and yet had only a small effect upon lift. Alternatively coils with 6 or more lower turns had differing characteristics. A coil with only one reverse turn had a smaller gradient of the magnetic field generated by the conical section. A similar reduction of the gradient could be obtained by widening the space between the two upper turns and the conical section, even after the coil had been coupled to the generator. Changing the gradient of the field, but not the field itself, permitted some degree of uncoupling of the forces of lift

and the forces of heat generation.

Despite the manufacture of many coils, the ranges of drop temperature and of gas flow rate were still narrow. Despite a theoretical understanding of the coil parameters which dictated heat generation and lift, a trial and error approach was often required in making the final choice. It was often possible to wind what appeared to be identical coils, but find the behaviour of a specimen in each of them to be different. The difference was often one of drop stability which was most pronounced in the lateral plane. The cause of the instability was usually a slight asymmetry in the coil, which may have stemmed from winding, or from the input/output leads, or from the loop necessary to reverse the direction of winding. A coil which produced an unstable specimen was discarded.

3.1.3 The Iron Specimen

The iron used to commence all experiments was Armco magnetic ingot iron, supplied in 1/4 inch, cold drawn rods with the manufacturer's analysis shown below:

C - 0.032%	P - 0.007%
Mn - 0.042%	S - 0.019%

Si is quoted as zero

O_2 is not quoted, but our analysis showed that it was approximately 0.06%.

Weight of specimen was of the order of 1 gram; the choice was a compromise between too light to levitate and too large for the reaction tube.

Samples were cut to a weight tolerance of $\pm$ 2%, when making a batch for each experiment. For most experiments, the average weight was slightly less than a gram, although occasionally it was in excess or well below a gram.

3.1.4 The Gases

The hydrogen sulphide had the typical gas analysis shown below:

Hydrogen sulphide	-	99.70 molar percent
Carbon disulphide	-	0.09 molar percent
Carbon dioxide	-	0.13 molar percent
Methyl mercaptan	-	0.02 molar percent
Carbonyl sulphide	-	0.01 molar percent
Sulphur dioxide	-	0.05 molar percent

The hydrogen used in the H_2-H_2S mixtures, and for desulphurisation, was of a minimum purity (on a helium-free basis) of 99.999%. A typical analysis of the high purity gas is shown below:

Oxygen	-	1 p.p.m.
Carbon dioxide and monoxide	-	1 p.p.m.
Hydrocarbons	-	0.8 p.p.m.
Moisture	-	5 p.p.m.
Helium	-	50 p.p.m.

The preparation for experiments often involved the use of argon, helium, nitrogen or hydrogen for purging, melting, testing, etc. High purity was not essential for these auxiliary purposes and commercial grade gases were used.

The H_2-H_2S mixtures were purchased and supplied already prepared in gas cylinders. Despite rigid specification in ordering, and despite the manufacturer's quoted analysis, the H_2-H_2S ratios could not be predicted prior to experiments. As a consequence some control of the experiments was lost. Gas mixtures were delivered well before their time of use and allowed to stand in the laboratory to permit complete mixing. If stainless steel cylinders were not employed, H_2S was slowly absorbed by the walls of the cylinder over prolonged periods of time. For this reason, gas analysis was always performed on the day of use.

3.2 Measurement of Temperature

3.2.1 The Pyrometer

The temperature of the specimen was measured by means of a Milletron, two-colour optical pyrometer with a remote direct reading indicator. The instrument collects the radiation from the hot surface and selects two wavelengths, approximately green and red. The intensities of the two wavebands are compared as a ratio. The theory invoked is that emissivity and waveband are mutually independent, and thus the ratio depends solely on temperature. The measurement of temperature in this way needs to make no allowance for changing emissivity, any absorption effects, or size of the radiating source, providing that both the selected wavelengths are equally attenuated by the intervening media. This principle in the operation causes the two-colour pyrometer to be vastly superior to other forms of optical pyrometry.

3.2.2 Calibration of the Pyrometer

Despite confidence in the two-colour pyrometer, calibration of the instrument was, of course, necessary. Calibration was performed regularly on a routine basis, and at any other times when the slightest element of doubt arose. The calibration apparatus is shown in Figure 4. Approximately 50 grams of Armco iron was melted in a small crucible of recrystallised alumina. This sat inside another crucible of graphite which acted as a susceptor in which the heat was generated by the induction coil. Further alumina insulation was used to protect the quartz tube from intense radiation from the graphite. The furnace atmosphere was hydrogen which maintained a clean metal surface on which to focus the pyrometer. The thermocouple sheath was alumina. The thermocouple itself was platinum - 5% rhodium/ platinum - 20% rhodium, which could tolerate intermittent immersion in the melt as high as 1750°C. The lower limit of the calibration was fixed by the melting point of iron (1540°C). The assumption was made that the calibration curve could be extrapolated below this point if necessary. In this way the need to use carbon-saturated melts was obviated.

Simultaneous readings of pyrometer and thermocouple were made, at each step, of both an increasing temperature pattern and a decreasing temperature pattern. Finally, the melt was allowed to freeze which gave an additional check on both pyrometer and thermocouple. A typical calibration curve is shown in Figure 5.

Early attempts at calibration were made with the graphite susceptor absent. Occasionally, spurious and erratic thermocouple readings were obtained. The suspected cause was some kind of electrical interaction

between the inductive field, the thermocouple and/or the melt. The problem disappeared when the graphite was included and the potentiometer was grounded.

3.2.3 Use of the Pyrometer

As Figure 2 clearly shows, the drop temperature was measured by viewing the pyrometer from above. At temperatures below 1700°C, this arrangement was extremely satisfactory. Above 1700°C fume could occasionally be seen above the drop which, while not depositing on the optical window, could have interfered with the light path. In these cases, the temperature was measured from below by installation of an optical prism in the aluminum base. This arrangement was also quite satisfactory, although the pyrometer had to be resighted each time the aluminum base was rotated or removed. The identity of both arrangements was checked at a temperature below 1700°C by sighting on a drop from above and then from below while all conditions were kept constant. Both arrangements recorded the same temperature which, incidently, demonstrated the severity of the internal liquid motion as well as the flexibility in sighting the pyrometer.

Before each experiment the pyrometer was checked against the melting point of pure iron in a manner described below. If the check was not in agreement with the calibration curve, a new calibration was performed.

A specimen of iron was levitated, melted, purified and then held in hydrogen. The temperature was carefully reduced until the liquid drop was supercooled to 20 - 30°C below the normal melting point. With all conditions steady, solidification from this unstable state was nucleated by

some perturbation of the system. By observing the motion of the instrument needle as it climbed to the melting point and then fell again, the freezing process was demonstrated and the melting point was easily read off the scale. This procedure became common practice throughout this study, and is recommended to other levitation workers.

Errors in temperature measurement were difficult to evaluate due to the arbitrary nature of temperature scales. Earlier workers[19,21,24] claim accuracy of $\pm$ 10°C based on experience. In fact, all that may be claimed is that measurements are within $\pm$ 10°C of the calibration curve. However, high quality thermocouples are known to be very reliable.

3.3 Procedure

3.3.1 Specimen Preparation

The 1/4 inch bar of Armco iron was merely cleaned with acetone to remove any surface grease before specimens were cut and weighed. The glass charging rod was raised, and a sample introduced from above by breaking a ground glass joint in the outlet line. The apparatus was purged thoroughly with commercial grade argon or nitrogen. An appropriate coil had been chosen previously and installed on the generator. The power was switched on. The specimen was levitated and then rapidly melted in the low conductivity inert gas. The specimen was held liquid for a short time and decarburised by the significant traces of oxygen impurity in the argon or nitrogen. The dissolved oxygen was subsequently removed by

changing over to pure hydrogen. The ability of hydrogen to remove dissolved oxygen is given in more detail in Table I, which shows that the practice of holding in hydrogen for 5 minutes more than guarantees complete deoxidation. During this time, any impurity of manganese and sulphur evaporated from the drop along with the oxygen. It is quite likely that any other trace elements, such as aluminum or copper, also vaporised from the iron. The resulting specimen was one of extremely high purity, despite the fact that no great expense had been incurred in purchasing the initial material. During the purification period, the conditions (power, temperature, etc.) were adjusted for a smooth changeover to the reactive gas, for which the needle valves were already set.

3.3.2 Obtaining Rate Curves

The hydrogen was cut off and simultaneously the H_2-H_2S mixture was switched on. The point of zero time was set when the H_2-H_2S gas mixture first contacted the drop, not when the valve was turned. Allowance was made for the small unavoidable space between valve and drop on the basis of plug flow through the swept volume. The drop was sulphurised at a constant temperature and constant flow rate for a certain period of time. On termination the copper mould was raised very closely to the drop, the power to the coil was switched off, the sample fell and was quenched to form a button in the base of the mould. The quenched sample was thoroughly cooled in a stream of hydrogen before removal from the reaction chamber.

This procedure was repeated with many specimens. The period of time in the H_2-H_2S mixture was varied. The periods were in the range of 1/2 to 50

minutes. Between samples the reaction tube and mould were cleaned by brushing. The whole procedure for obtaining a rate curve was repeated at various drop temperatures, at three gas flow rates, and using a variety of gas compositions.

Rate curves were also obtained for the transfer of sulphur from the sphere, into gases of hydrogen, helium and nitrogen. A sulphur-bearing drop to initiate these experiments was produced by constructing a rate curve in the manner described above. The sulphur content at any instant of time was then known. More specimens were levitated in H_2-H_2S mixtures and after a certain period of time, say 20 minutes, the sulphurising gas was switched over to the desulphurising gas. In this way the sulphur content of the drop at the start of sulphur removal could be predicted. Samples were quenched after various times in the desulphurising gas, taken for sulphur analysis and a second, but falling, rate curve obtained. When the desulphurising gas was pure hydrogen, great care was taken to ensure that the H_2-H_2S flow rate and the pure H_2 flow rate were identical and that the drop temperature was the same in both gases, (see Section 5.2.3 for need for identity).

3.3.3 Gas Sampling and Analysis

The device A in Figure 1, for taking samples of the H_2-H_2S mixtures is shown in more detail in Figure 6. The device was designed so that gas analysis could be carried out during the course of levitation. The sampling bulb was of known volume. It was filled for analysis at least five times through the duration required to establish a rate curve. The filled bulb was flushed out with helium at a very low flow rate for a period of fifty minutes. The hydrogen passed straight through the absorbing solution, which was agitated by a small magnetic stirrer. The hydrogen

sulphide was absorbed by the solution at the bubbler outlet.

The hydrogen sulphide was determined by a method based upon the technique of Kitchener et al[83]. Alkaline sodium hypochlorite solution was the absorbing reagent which oxidised the sulphide to sulphate. Care had to be taken with the alkalinity of the solution in order to ensure 100% oxidation[84] The solution was always made up to a pH of 14.4. Kitchener et al recommend boiling the solution after absorption to ensure that the oxidation is complete, but tests with and without boiling showed no discrepancy. The boiling step was abandoned. The solution was acidified with acetic acid and, after cooling, and iodometric titration against sodium thiosulphate was performed to determine the sulphate by difference. The results of the analysis were quoted, as is customary, as a ratio of partial pressures of H_2 and H_2S.

3.3.4 Analysis of Sulphur in Iron

The button samples produced by quenching in the copper mould were analysed for sulphur according to A.S.T.M. method E30-60T. The apparatus used was a Leco 518 analyser, which incorporated an inductive furnace rather than a resistance unit. The weighed specimen was placed in a zirconia crucible which had been fired previously to drive off any moisture or sulphur, and combusted by inductive heating in a stream of oxygen. The sulphur passed off as sulphur dioxide and was bubbled into the titration solution. Any free iodine in this solution was consumed according to:

$$SO_2 + I_2 + 2H_2O = H_2SO_4 + 2HI$$

The titration solution was potassium iodide in an excess of hydrochloric acid, in which the free iodine was generated continuously by additions of potassium iodate solution from a burette.

$$KIO_3 + 5KI + 6HCl = 6KCl + 3H_2O + 3I_2$$

Prior to analysis the analysing unit was always checked and calibrated against standards of known sulphur content. The standards were supplied by the N.B.S., numbers 129b and 133a, given in detail in N.B.S. Publication 260.

3.3.5 Sulphur Profiles

When a liquid iron-sulphur alloy solidifies the segregation of the sulphur in the solid is usually pronounced. This well known phenomenon has often prevented the production of homogeneous iron-sulphur alloys at room temperature. Only rapid quenching can prevent significant migration of the sulphur during the solidification process. If the speed of the quench is sufficiently rapid that sulphur segregation is eliminated, then the distribution of the sulphur in the solid is identical to the distribution in the liquid iron immediately prior to the quench. One method by which a high speed of quenching may be attained, is to supercool the liquid and then provide a means of nucleation which will initiate freezing. Levitation is ideally suited to such a method.

Specimens were levitated at a temperature of 1450°C, but in the liquid phase in an H_2-H_2S gas mixture. After various times of sulphurisation the drops were quenched. The first batch was quenched in the copper mould in the usual manner by switching off the power. The samples were taken for

sulphur analysis. The second batch of drops was quenched by nucleating the freezing process while the drops were still suspended in the coil. The spherical shape of the drops was retained in the solid phase. Some of the samples of the second batch were taken for analysis, from which a rate curve was established along with analyses of the first batch. Four other samples of the second batch, which were now known to be on the rising part of the rate curve, were mounted, sectioned and polished. On each of the four sections two diameters mutually at right angles were chosen. Each diameter was traversed for sulphur on the electron probe microanalyser. A count of the sulphur peaks gave the sulphur profile along any diameter.

CHAPTER 4

EXPERIMENTAL RESULTS

The immediate product of the experiments was, in most case, classical rate curves. The curves comprised the sulphur content of the iron drops and the periods of time in the appropriate gas stream. Subsequently, various calculations were performed with these raw experimental data as a basis. The calculations and their consequences will be discussed in Chapter 5. The purpose of the present chapter is to provide a written record of the original data in tabular form.

4.1 Sulphurisation in H_2-H_2S Mixtures

This section reports the data which pertain to the sulphur transfer from gas mixtures of H_2-H_2S to the initially-pure iron drops. Experiments were performed at four drop temperatures: 1500, 1600, 1675 and 1750°C. The gas flow rates used were 900, 2680 and 5070 cm^3 per minute. Various sulphur potentials of the gas phase were used but due to the nature of the supply, little control could be exercised over the composition prior to an experiment. However, the range of $\frac{PH_2S}{PH_2}$ ratio covered 0.00015 to 0.00895. The upper level corresponded to approximately 5% sulphur in the iron at equilibrium at 1600°C.

4.1.1 Drop Temperatures of 1600°C

Tables 2 to 10 show the results for sulphurising with nine different gas compositions, which are reported as PH_2S/PH_2 ratios. The drop temperature was 1600°C and the gas flow rate was 2680 cm^3 per min. in all cases. The tables are self-explanatory, except for two numbers which are reported below the columns and of which later mention will be made.

The weight of the specimen quoted is the mean of the weights of all the specimens in that table. As an example of the variation of the weights, Table 10 includes a column which shows the weight of each individual specimen.

At the lower flow rate of 900 cm^3 per min. three gas ratios were used to contruct Tables 11, 12 and 13, while at the same temperature Tables 14, 15 and 16 record the results at the higher flow rate of 5070 cm^3 per min.

4.1.2 Other Drop Temperatures

Other experiments were carried out at drop temperatures of 1500°C. While this temperature is below the melting point of pure iron, it may be above that of high sulphur-iron alloys. Consequently the liquid samples were, at least initially, in the supercooled state. Tables 17 and 18 give the results at a gas flow rate of 900 cm^3 per min.; Tables 19 and 20 are at 2680 cm^3 per min.; Tables 21 and 22 are at 5070 cm^3 per min.

With the drop-temperature at 1750°C results are shown for flow rates of 900 cm^3 per min. (Tables 23 and 24); of 2680 cm^3 per min. (Tables 25 and 26); and of 5070 cm^3 per min. (Table 27). The results of a single experiment at 1675°C, gas flow rate of 2680 cm^3 per min. and PH_2S/PH_2 ratio of 0.00523 are

shown in Table 28. During this single experiment, three additional "spot" samples were obtained with the same gas and flow rate. The temperatures were different from 1675°C and each sample was at steady state. The analyses of these three are not included in Table 28 since their purpose was quite separate from the purpose of the results presented here. They are presented, discussed and their purpose is outlined in Section 6.3.

A brief examination of all the tables will show that values of the constant B are missing from the tables at temperatures above 1600°C. Later it will be shown that a knowledge of the equilibrium constant K is required for the evaluation of this constant. The equilibrium above 1600°C is not known.

4.2 Desulphurisation

Sulphur was introduced into the pure iron sample by levitation in H_2-H_2S gas, under known conditions, so that after a certain period of time, say 20 minutes, the sulphur content was known. The sulphur was then removed from the drop by pure H_2, by inert gas, or by inert gas-H_2 mixtures. All desulphurisation experiments were performed at one temperature alone: 1600°C.

4.2.1 Desulphurisation by Pure Hydrogen

Three desulphurisation experiments were performed in pure H_2, one at each of the three gas flow rates. The results are shown in Tables 29, 30 and 31. Each set of data is compatible with a particular sulphurisation

experiment which was necessary as a source of sulphur-bearing drops. Table 29 at 900 cm^3 per min. is compatible with Table 13; Table 30 at 2680 cm^3 per min. with Table 7; and Table 31 at 5070 cm^3 per min. with Table 16.

4.2.2 Desulphurisation by Inert Gas

Desulphurisation of the drop by pure helium gave the results shown in Table 32, while Table 33 shows the rates helium, helium-hydrogen, and hydrogen. The composition of the helium-hydrogen mixture recorded in the table is that quoted by the gas supplier. The wide difference in the power of helium and of hydrogen as sulphur removers can easily be seen from the tabular results.

The removal of sulphur by nitrogen is listed in Table 34. The composition of the nitrogen-hydrogen mixture was measured by analysis using a gas chromatograph with a silica gel column. The volumetric flow rate is almost nineteen litres per minute which is much greater than any other flow rate used previously. The low conductivity of nitrogen dictated a high flow rate in order to maintain a sufficient rate of heat removal from the drop.

4.3 Sulphur Profiles

A total of 13 iron specimens were levitated at 1450°C in a H_2-H_2S gas mixture flowing at 1680 cm^3 per min. Of the total, four samples, although supercooled, were quenched in the normal manner in the copper mould after various times. The remainder were quenched after various times, while levitated within the coil, from the supercooled state. The solidification

process was initiated by any slight perturbation of the system. Of the nine solid spheres obtained in this way, five were taken for sulphur analysis along with the mould-quenched samples. Figure 7 shows the results through which an approximate curve has been drawn by eye.

From the figure, the sulphur content of each of the remaining four coil-quenched specimens may be crudely estimated. They are shown below together with their respective times in the H_2-H_2S mixture. The specimens are obviously from the steeply rising part of the curve and not from the steady state region.

Estimated sulphur content was 0.9% after 4 minutes

Estimated sulphur content was 1.0% after 5 minutes

Estimated sulphur content was 1.1% after 6 1/2 minutes

Estimated sulphur content was 1.2% after 8 minutes

The samples were mounted, sectioned along a diametric plane, and examined on the electron probe microanalyser for sulphur. Traverses were performed across two diameters, randomly chosen, but mutually at 90°. The size of the sulphide inclusions was constant along the two traverses, as was the frequency of the inclusions. Although the circular perimeter of the observed plane (i.e., the sphere's surface) was bevelled after polishing which made sighting difficult, no marked increase in sulphur was detected at the circumference. As the samples contained no impurities the sulphide peaks were very distinct. The peaks were easily counted from the chart output, which was quite conventional and hence need not be included.

The conclusion was confidently drawn that the sulphur distribution, at all times during sulphurisation, was homogeneous throughout the specimens.

CHAPTER 5

DISCUSSION OF RESULTS: KINETIC ASPECTS

In the main part of this chapter the remarks refer to the sulphurising of the drop in H_2-H_2S gases and the consequent rate curves which were produced. Where comments are included which pertain to other experiments, they are clearly marked as such. The results given in detail in the previous chapter are now discussed from a kinetic point of view; the thermodynamic aspects will be discussed in Chapter 6.

5.1 Interpretation of Transport Process

The objective of the analysis of the results was threefold:

(1) To confirm or deny the presence of a significant thermal diffusion flux.

(2) To explain the observed rates of sulphur transfer by a mechanistic model.

(3) To predict rates of transfer by means of the quantitative model which includes the thermal diffusion flux.

In order to initiate an explanation the potential mechanisms of transfer were scrutinized.

5.1.1 Transport Control

The sulphurisation of iron involves a number of elementary steps in series. These may be as follows:

(1) Transfer of hydrogen sulphide from the bulk of the gas to the interface by molecular and thermal diffusion, and convection.

(2) Adsorption of gaseous hydrogen sulphide onto the gas-metal interface.

(3) Reaction of hydrogen sulphide to hydrogen and sulphur on active sites.

(4) Desorption of sulphur from the active sites at the interface into liquid species.

(5) Transfer of dissolved sulphur from the interface to the bulk of the liquid by molecular diffusion and by convection.

(6) Other steps which involve the net motion of hydrogen: desorption and gas phase transfer.

The overall rate of transfer may be governed by a single step or by a combination of steps. The net rates of each step are equal.

The scheme of the steps is typical of that for any similar gas-liquid-metal system involving a simple chemical reaction. Other systems will vary slightly, particularly in the positioning of the chemical reaction in the sequence and in the number of parallel reaction steps if the reactants and products are multiple.

Before examining the sulphur rates in detail, certain qualitative evidence existed which gave an indication of the controlling steps. This evidence gave an insight into the various resistances involved, including which one may be the greatest.

Previous Experience. Other workers[25,26,27,29,33,79,85] who have passed various gases around metal spheres have found that the controlling step is usually mass transfer of some species in the gas phase. The overall rate

was controlled by transfer from the bulk gas to the interface. This step had a much greater resistance than the other steps. Equilibrium was assumed to exist at the interface. The bulk liquid composition was in equilibrium with the interfacial liquid composition. However, this evidence, although significant, is far from proof; the fact that the gas phase controls the overall rate of decarburisation in an Fe-C-O system does not mean that the same argument applies to the Fe-H_2-S system.

Liquid Stirring. The motion of a liquid metal which is caused by an electromagnetic field is well known. The levitation field creates internal motion within the drop. For a perfectly symmetric field and balanced drop, this motion would be regular. In practice the motion is extremely irregular. Confirmation of the speed and of the erratic nature of the motion was demonstrated by visual observation of any non-inductive particle (e.g., iron oxide) floating on the surface of the drop. A high speed film by Palmer[85], some frames of which are included in reference (85), admirably show the liquid motion. The liquid phase resistance was expected to be negligible since the large convective transfer of sulphur would provide large liquid phase transfer coefficients. The large coefficients applied for heat transfer as well as mass transfer; the temperature within the drop was expected to be uniform.

The convective forces of the internal motion cannot be evaluated. However, the limiting case in which they are zero may be calculated. The rate of sulphur transfer into a stagnant liquid drop by pure molecular diffusion

may be calculated for a given sulphur potential at the surface of the drop. The calculation is shown in Appendix I in detail, which concludes that the attainment of steady state is much more rapid than the measured rates shown in the tables of results. With the added liquid stirring which, in fact, enhances the diffusion coefficient, the rate of attainment of steady state would be even more rapid. Since the measured rates of sulphur transfer were so slow by comparison, it is most unlikely that the liquid phase transfer resistance had any influence at all on the overall rates of transfer.

Sulphur Profiles. The results given in Section 4.3 for the rapidly quenched supercooled drops showed sulphur homogeneity in the solid sphere. The horizontal sulphur profile may have originated from a sloping profile in the liquid which was destroyed and made horizontal by sulphur migration on solidification. However, this was improbable and the plausible explanation was that the sulphur was uniform before quenching. This argument implies negligible liquid phase resistance to the transfer of sulphur within the drop.

Iron Sulphide. At no time during sulphurisation was iron sulphide observed to form on the surface of the drop.

Reactions and Temperature. Although there are metallurgical examples of reactions -- some slags as reactants -- which are slow at temperatures of 1600°C, they are few. The reaction for the formation of sulphur from hydrogen sulphide is governed by rate constants which may be expected on an intuitive basis to be extremely large at temperatures of 1600°C.

Liquid Phase Desorption. From an intuitive view of the energies involved, the desorption of adsorbed sulphur from the interface to the liquid iron phase, may be considered as an easy step. The resistance of the desorption step is probably small and not likely to be a rate-controlling mechanism.

The qualitative evidence above collectively indicated that attention may be profitably directed towards the gas phase process, when searching for the controlling mechanism. With this in mind, the quantitative evidence is reviewed below.

A novel approach was applied for analysing the various transfer steps. The differential rate expression which described each step, was written for each step, and all expressions were set equal to the overall rate. The equations were manipulated in order to obtain a solution in terms of those members of the equations which were known. A solution was obtained for the various cases of rate control of the overall process. Full details of this analysis are given in Appendix 2, which has a form which may be applied to any gas-liquid system, levitation or crucible.

Step 1. If the flux of H_2S from the bulk of the gas mixture to the liquid surface were by pure diffusion, in the absence of convection, then Fick's law would apply. The radial component of the flux at any point would have the well known form

$$\text{Flux} = C \cdot D_{H2\text{-}H2S} \cdot \frac{d(xH_2S)}{dr} \qquad (5.1)$$

where r is any radial dimension from the centre of the drop in excess of r = a.

The concentration profiles are usually impossible to measure in most media. The mass transfer coefficient kg is therefore introduced. It is defined in terms of the mass flux at the interface (in the presence or absence of convection)

$$\text{Flux at the interface} = C.D_{H_2\text{-}H_2S} \cdot \frac{d(xH_2S)}{dr} = C.kg.\ (xH_2S_\infty - xH_2S_i) \qquad (5.2)$$

The mass transfer coefficient has analogy with the diffusion coefficient. It is generally independent of composition. However, it is a function of the physical properties of the gas and also of the geometry. Later mention will be made of the evaluation of total molar concentration C, and also the inclusion of a thermal diffusion component in equation (5.2). To introduce the thermal diffusion flux at this stage would be premature. Strictly speaking equation (5.17) applies for our situation. However, the omission of the effects of temperature differences in the gas mixture does not detract from the validity of the following analysis and it may facilitate clarity.

Step 2. The molecules of gaseous H_2S adsorb on active sites at the interface. The process is reversible and continuous and may be accompanied by the desorption of H_2S back to the gas, which must be considered.

$$\text{Flux} = k_1 \cdot x_{H_2S_i} \cdot \theta E - k_2 \cdot \theta_{H_2S} \tag{5.3}$$

The k's are the appropriate forward and reverse constants for the mechanism, and are similarly defined for the other steps. The θ's are the various fractions of the total active sites at the surface which are occupied by the various species (H_2S, H_2, S) or are vacant (E).

$$\theta_{H_2S} + \theta_{H_2} + \theta S + \theta E = 1 \tag{5.4}$$

Step 3. The chemical reaction is straight-forward if any single vacant site is all that is required for the forward reaction to proceed.

$$\text{Rate} = k_3 \cdot \theta_{H_2S} \cdot \theta E - k_4 \cdot \theta_{H_2} \cdot \theta S \tag{5.5}$$

Step 4. Sulphur is desorbed into the liquid iron.

$$\text{Rate} = k_5 \cdot \theta S - k_6 \cdot a_{Si} \cdot \theta E \tag{5.6}$$

Step 5. Liquid phase transfer of sulphur by diffusion and convection within the drop.

$$\text{Flux of sulphur} = k_L \cdot (a_{Si} - a_{S\infty}) \tag{5.7}$$

Step 6. There is a motion of hydrogen between the gas phase and the interface. The net rate must be equal to the rate of production by Step 3.

$$\text{Flux} = k_7 \cdot \theta H_2 - k_8 \cdot x H_{2i} \cdot \theta E \qquad (5.8)$$

The nature of the chemical reaction creates one molecule of sulphur for every molecule of hydrogen sulphide, hence the rate of any step may be conveniently expressed in terms of sulphur. The left-hand sides of equations (5.2), (5.3), (5.5) to (5.8) are equal to the overall rate, which is

$$\text{Overall rate} \cdot \frac{(\text{moles of sulphur})}{(\text{unit area})(\text{unit time})} = \frac{wt}{A.3200} \cdot \frac{d(\%S)}{dt} \qquad (5.9)$$

where A is the surface area of the drop;

t is any instant in time during sulphurisation.

The normal situation is to find values of the coefficients or rate constants by making other measurements including the overall rate. However, the process is usually thwarted by an inability to measure the intermediate parameters (i.e., θ and interfacial concentrations). Usually only the compositions at the extremes (i.e., bulk state) may be evaluated. The individual solution of each rate equation for each step is prevented. Any solution must be attempted using the bulk compositions only, which often prevents the achievement of a full solution. The introduction of any scientific technique, which permits the measurement of the interfacial properties during the course of a rate experiment, would be invaluable. Such a technique[12] may soon be available.

In the present sulphurisation studies the extreme compositions -- bulk gas ratio and bulk liquid sulphur content -- are the only compositions known. While a complete solution is impossible special cases where a certain step controls the overall rate may be expressed in terms of knowns by manipulation of the equations (Appendix 2). The products of the manipulation are shown briefly here.

Gas Phase Control Initial Rate.

$$\frac{wt}{A \cdot 3200} \cdot \left.\frac{d(\%S)}{dt}\right|_{t=0} = C \cdot kg\ (xH_2S_\infty) \qquad (5.10)$$

The initial transfer rate (at t = 0 for a drop initially free of sulphur) is directly proportional to the bulk gas sulphur potential. The initial slopes of rate curves which are obtained with different gas ratios, but otherwise identical conditions, would exhibit this linear dependence if the gas phase were, in fact, controlling.

In obtaining equation (5.10) equilibrium at the interface is assumed. By definition, gas phase control implies that the gas and liquid molecules adjacent at the interface are in equilibrium.

Adsorption Control Initial Rate.

$$\frac{wt}{A \cdot 3200} \cdot \left.\frac{d(\%S)}{dt}\right|_{t=0} = \frac{xH_2S_\infty \cdot k_1 \cdot k_7}{k_8 \cdot xH_2 + k_7} \qquad (5.11)$$

Unfortunately, the equilibrium is such that the changes in partial pressures of H_2 ($xH_{2i} \simeq xH_{2\infty} = xH_2$) are negligible for even large changes in partial pressure of H_2S in the bulk gas. For practical purposes, the initial transfer rate is directly proportional to the xH_2S_∞. The dependence of initial rate is thus the same for adsorption control as for gas phase control.

Chemical Reaction Control Initial Rate .

$$\frac{wt}{A \,.\, 3200} \cdot \left.\frac{d(\%S)}{dt}\right|_{t=0} = \frac{k_1.k_2.k_3.k_7.k_7.xH_2S_\infty}{\{k_2.k_7 + k_2.k_8.xH_2 + k_1.k_7.xH_2S_\infty\}^2} \qquad (5.12)$$

Desorption Control Initial Rate.

$$\frac{wt}{A \,.\, 3200} \cdot \left.\frac{d(\%S)}{dt}\right|_{t=0} = \frac{k_1.k_3.k_5.k_7.k_7.xH_2S_\infty}{k_1.k_3.k_7.k_7.xH_2S_\infty + k_2.k_4.k_8.k_8.xH_2.xH_2 + k_1.k_4.k_7.k_8.xH_2.xH_2S_\infty + k_2.k_4.k_7.k_8.xH_2} \qquad (5.13)$$

Liquid Phase Control.

$$\frac{wt}{A \,.\, 3200} \cdot \frac{d(\%S)}{dt} = k_L\,(a_{si} - a_{s\infty}) \qquad (5.14)$$

The condition of interfacial equilibrium permits a_{si} to be related to the gas, xH_2S_∞, at all times through the equilibrium constant.

$$\frac{wt}{A \cdot 3200} \cdot \left.\frac{d(\%S)}{dt}\right|_{t=0} = \frac{k_L \cdot xH_2S_\infty}{xH_{2\infty} \cdot K} \qquad (5.15)$$

Initial rates are again directly proportional to the gas composition. However, the constant of the proportionality k_L is dependent on liquid phase conditions only (independent of gas flow rate).

The condition that the interface is always at equilibrium for gas phase control and for liquid phase control is well illustrated by this analysis. By applying the conditions of either of the two controls, the mechanistic equations may be manipulated to yield:

$$\frac{xH_2S_i}{xH_{2i} \cdot a_{si}} = \frac{k_2 \cdot k_4 \cdot k_6 \cdot k_8}{k_1 \cdot k_3 \cdot k_5 \cdot k_7} \qquad (5.16)$$

The derivation of equation (5.16) is given in detail in Appendix 3. The right-hand side consists of constants which are dependent on temperature only. Equation (5.16) is thus a thermodynamic identity of the equilibrium condition. The right-hand side is analogous to an equilibrium constant which may apply at the interface at all times.

The next task after formulating the analysis was to compare the experimental data with the predictions of the analysis in the hope that the possibility of one type of control could be eliminated. The experiments shown

in Tables 2 to 10 at 1600°C and flow rate of 2680 cm^3 per min. were identical except for the bulk gas ratio. The initial rates of sulphur transfer to the pure drop were compared to the sulphur potential of the bulk gas mixture for these results. The comparison is shown in Figure 8 which clearly indicates the linear relationship. This is consistent with the analysis for gas phase control, control by the adsorption step, or by the liquid phase. Such a relationship would also be predicted when any of the three steps were in joint control. The slope of the line in Figure 8 is, of course, a measure of the rate constants or coefficients for that particular step, e.g., if there were gas phase control the initial rate would give kg, and then sulphur concentrations at greater times could be predicted using this kg. Having eliminated some steps, further proof is necessary to discriminate between the three possible steps.

The methods by which the rate constants or coefficients were evaluated will be discussed later in Section 5.2.1. At this early state it is sufficient merely to know that they were enumerated.

Two important properties of the coefficients were examined.

If the control were by the gas phase, forced convection would make significant contribution to the transfer of H_2S and so the coefficient would be a function of the gas velocity around the drop. On the other hand, the rate constant for the adsorption reaction, and the mass transfer coefficient for the liquid step, should be independent of the gas flow rate. The constants of the proportionality were compared at the three flow rates (at one drop

temperature). As an illustration, the values applying for Tables 11 to 13 were compared to the values for the experiments shown in Tables 2 to 10, which were in turn compared to values which were extracted from the data in Tables 14 to 16. The later table, Table 35, shows the comparison clearly. Since the gas compositions did not enter the dependence, average values over the range of compositions were taken, and these were compared for cases of constant drop temperature. The values were clearly dependent upon gas flow rate, which indicates the importance of the gas phase resistance. Furthermore, the values of the coefficient were approximately proportional to the square root of the gas flow rate which is in agreement with the empirical correlations for continuous phase mass transfer (Section 2.6.2). This evidence clearly suggests that all transfer resistances other than those for the gas phase are negligible.

The second examination was of the temperature dependence of the constants. Changes in temperature from 1500 to 1750°C created slight changes in the physical properties of the gas and the liquid which, in turn, would affect the values of kg and k_L. However, this effect would be quite small. In contrast, the dependence of an adsorption rate constant, say k_1, upon temperature is large, probably exponential. The changes in k_1 from 1500 to 1750°C would be by a factor in excess of two. A crude calculation of this change is shown in Appendix 4, which is based upon the likely exponential relationship between adsorption constant and temperature. The experimental coefficients did not exhibit this magnitude of change with temperature. The

unchanging values of the rate coefficients from 1500 to 1750°C is additional evidence of gas phase control.

On the basis of the large amount of evidence discussed, the conclusion was drawn that the overall rate of sulphur transfer was controlled by the transfer of H_2S in the gas phase. Further discussion and interpretation of the experimental results are made on the basis that this conclusion is valid.

5.1.2 Thermal Diffusion Flux

Traditionally thermal diffusion fluxes have been studied in the classical two bulb experiment, in which the gas mixtures were allowed to reach steady state before analysing for the degree of separation of the components. In metallurgical studies where thermal diffusion was thought to be important, the consequences of thermal diffusion on the experimental variables have received attention rather than the thermal diffusion flux itself. These two situations have led to a popular misconception; thermal diffusion is thought of as an equilibrium, or at most, a static effect in which gases are permanently segregated. However, it is in fact a dynamic effect, and is appropriately classified as kinetic. The temperature gradient is a driving force which gives rise to a molecular motion which occurs at a finite speed. The flux may well be a function of time-dependent parameters, and hence itself may change with time. When thermal diffusion is discussed it must be considered at all times of a rate experiment, not just at steady state.

The significance of thermal diffusion was illustrated very clearly in the sulphurisation experiments by comparing the steady state sulphur

content of the drop with that predicted from the gas analysis. The equilibrium sulphur content was found by using Chipman's relationship[78] for the particular gas mixture flowing past the drop. The comparison is graphically illustrated in Figure 9, which contains the data of Table 8 at 1600°C. This form of rate curve and the discrepancy between the sulphur content predicted from gas analysis and the measured content, was found for all experiments at 1500 and 1600°C. Figure 9 is typical and illustrates the magnitude of the discrepancy relative to the total sulphur in the iron. At steady state, equilibrium existed across the gas-liquid interface. The gas very close to the liquid surface was in equilibrium with the sulphur in the liquid. The amount of H_2S adjacent to the drop therefore must have been lower than the amount in the bulk H_2-H_2S mixture. This was caused by continual migration of the H_2S molecules away from the hot gas at the surface towards the cold bulk gas. Thermal diffusion of H_2 molecules was equal and opposite. At steady state this migration at the surface was balanced by the convective flux of H_2S towards the drop. A dynamic, but time-independent, state existed in the gas.

The flux of H_2S due to thermal diffusion, significant at steady state, was present at all times. The net flux of H_2S comprised two components. The convective flux (molecular, forced, natural) was given by equation (5.2), to which the second component of flux was added:

$$\text{Net flux of } H_2S = C \cdot k_g \cdot (x_{H_2S_\infty} - x_{H_2S_i}) - N_T \qquad (5.17)$$

The thermal diffusion flux, N_T, is given by equations (2.11) and (2.12)

$$N_T = D_{H2-H2S} \cdot k_T \cdot C \cdot \text{grad ln } T \qquad (5.18)$$

Note that the two fluxes in equation (5.17) are in opposite directions.

Equation (5.18) applies at any instant in time or space. In order to find the degree of segregation created by the flux over a space coordinate or length which has different temperatures at its extremities, the equation must be integrated. The integration is difficult, but fortunately, is not necessary. Our interest is restricted to the flux at a special location. The thermal diffusion flux at the gas-metal interface is the flux which is relevant to the overall rate of sulphurisation. The flux is normal to the surface and so the driving force reduces to the radial component of the temperature gradient. Equation (5.17) becomes

$$\text{Net flux of } H_2S = C \cdot k_g \, (x_{H_2S_\infty} - x_{H_2S_i}) - \left\{ \frac{D_{H2-H2S} \cdot k_T \cdot C \cdot \frac{dT}{dr}}{T} \right\}_i \qquad (5.19)$$

The usual difficulty in integrating equations of the form of equation (5.18) is that the thermal diffusion ratio k_T is not a constant. This is one area where the similarity between the molecular diffusion coefficient for a binary gas at moderate pressures and the thermal diffusion coefficient no longer holds. The ratio k_T is dependent upon the gas composition. A clue to the form of the dependence may be now briefly mentioned. For an equimolar binary mixture the value of k_T is finite. Consider mixtures which are increasingly rich in one component. In the limiting case as the pure gas is approached k_T must tend towards zero. Thermal diffusion does not occur

in a pure gas. The functional dependence upon composition has yet to be truly identified. It may be complex[47,51] if full account of the structure of the molecules is taken, or it may be simple if a working relationship is required. Furry et al[86] were the first to suggest for a binary mixture of A and B that:

$$k_T = \alpha \cdot x_A \cdot x_B \qquad (5.20)$$

where α is a constant, independent of composition, usually referred to as the thermal diffusion factor.

Equation (5.20) is widely accepted as a reliable approximation[50] of the complex methods for predicting k_T. It predicts that k_T is zero for each pure component and has a maximum value for equimolar concentrations. The small numbers of experimentally determined values of k_T for various gas combinations that do exist, confirm that equation (5.20) is sufficiently accurate for most purposes. Methods which are based upon the kinetic theory of gases are available for calculating values of α. Like the molecular diffusion coefficient, α is temperature dependent.

The basis for equation (5.17) was equation (5.2) which was derived for an isothermal gas. Temperature gradients existed in the gas around the levitated drop and the driving force for convective transfer of H_2S extended between the two limits of the temperature difference. This created the problem of what molar concentration to use for the gas. On the basis of gas ideality, the molar concentrations at room temperature and 1600°C differ greatly. The present day knowledge does not provide a solution of theoretical origin. However, practical circumstances have led to a reliable answer. Single

valued properties are chosen which have the same net effect on the overall transfer as the changing values. These are defined as those evaluated at an effective temperature, T_f (see equation (2.16)):

$$T_f = \frac{T_i + T_\infty}{2} \tag{5.21}$$

The total molar concentration C_f evaluated at T_f, was used to replace C in equation (5.19). The final flux equation which should apply for our experiments was:

$$\frac{wt}{A \cdot 3200} \cdot \frac{d(\%S)}{dt} =$$

$$C_f \cdot kg \cdot (xH_2S_\infty - xH_2S_i) - \left(\frac{D_{H2-H2S} \cdot \alpha \cdot xH_2S \cdot xH_2 \cdot C}{T} \cdot \frac{dT}{dr} \right)_i \tag{5.22}$$

Note that this equation, with the thermal diffusion flux included, reduces at time zero to equation (5.10).

5.2 Proof of Flux Equation

The proposed flux equation (5.22) and its derivation have firm foundation. Various consequences of this equation were examined. It was tested to see how well it agreed with the experimental data. A comparison between the experiment and equation (5.22) for particular situations is made below.

5.2.1 Methods of Solution

In equation (5.22) certain members of the thermal diffusion term remained constant over the period of any particular sulphurisation experiment. At any fixed temperature, all the terms except the mole fractions were constant. For the range of gas mixtures employed, the changes in the mole fraction of hydrogen at the interface were negligible in comparison to the changes in xH_2S_i. Hence, xH_{2i} could be taken as a constant. A collective constant b, was defined:

$$b = \frac{D_{H2\text{-}H2S} \cdot \alpha \cdot xH_2}{T} \cdot \frac{dT}{dr} \qquad (5.23)$$

$$\frac{wt}{A \cdot 3200} \cdot \frac{d(\%S)}{dt} = C_f \cdot kg \cdot (xH_2S_\infty - xH_2S_i) - (C \cdot b \cdot xH_2S)_i \qquad (5.24)$$

The term b, although not a mass transfer coefficient, is analogous to kg and has the same units. Both were found to be slightly temperature dependent. Both were strong functions of flow rate. The most important member of b is the temperature gradient at the interface which defies direct measurement.

At drop temperatures where the equilibrium constant is known, xH_2S_i can be calculated from the analysis of the sulphur in the iron, (%S). The flux equation has two unknowns, kg and b. It was solved and their values found by the four methods described below.

Method One. At zero time xH_2S_i was zero, kg could be found if the left hand side of the flux equation were known. Values of the equilibrium constant

were not involved with initial rates.

At large times the left hand side was zero, and b was given in terms of kg. Values of the equilibrium constant were necessary to obtain b.

A graphical plot was made of the sulphur in the iron versus time. The initial slope to give kg was taken from a line through the early points. At the other extreme, the obviously steady state points were averaged and the mean value used to find b. The validity of the two values was checked by solving the flux equation at all times between the two extremes. Agreement at the intermediate times over the whole length of the rate curve, within experimental error, verified the form of the equation. Needless to say, this method suffered from the lack of accuracy common to all graphical techniques which involve differentiation.

Method Two. The flux equation was integrated to yield an analytical solution when the assumption was made that the activity coefficient was constant and independent of the sulphur concentration. At low sulphur concentrations (i.e., particularly close to zero time) the activity coefficient was not far removed from unity.

$$\frac{wt}{A \,.\, 3200} \,.\, \frac{d(\%S)}{dt} = \tag{5.25}$$

$$C_f \,.\, kg \,.\, \left(xH_2S_\infty - \frac{K.PH_{2i}.f_s.\%S}{P_T} \right) - \left(\frac{C.b.K.PH_{2i}.f_s.\%S}{P_T} \right)_i$$

where P_T is the total atmospheric pressure.

Integrate with f_s constant:

$$(\%S) = \beta 1 \cdot \left[1 - \exp\left(\frac{-A.3200.t.\beta 2}{wt}\right)\right] \qquad (5.26)$$

where constant, $\beta 1 = \dfrac{C_f.kg.xH_2S_\infty.P_T}{C_f.kg.K.PH_{2i}.f_s + (C.b.K.PH_2.f_s)_i}$

where constant, $\beta 2 = \dfrac{C_f.kg.K.PH_{2i}.f_s}{P_T} + \left(\dfrac{C.b.K.PH_2.f_s}{P_T}\right)_i$

A curve fitting technique was used to search for values of constant $\beta 1$ and constant $\beta 2$ in equation (5.26) to give the best fit of the experimental points. The criterion for the best fit was the minimum sum of the squares of differences between predicted and measured values of sulphur content in the drop. From the values of $\beta 1$ and $\beta 2$, kg and b were extracted given the equilibrium constant. These were put into equation (5.24), which was solved numerically with the true dependence of the activity coefficient included. The advantage of this method was that the search pattern for kg and b and the numerical integration were separated.

Method Three. The integration and the search pattern were combined but the search reduced to one variable. The steady state sulphur content was found by averaging the obviously steady state values. The left hand side of the flux equation was set equal to zero and b expressed in terms of the unknown kg. The flux equation had now only one unknown parameter. It was solved at all times by a finite difference technique while simultaneously searching

for the value of the one unknown which gave the best fit to the experimental data by a least squares criterion.

Method Four. The final method was to integrate equation (5.24) by finite differences with simple marching steps, while searching for the values of kg and b which gave the best fit to the data. The two-variable search pattern was the Hooke and Jeeves[87] technique. The computer programme for the search is described in detail in Appendix 3 of Pang's thesis[88]. This method had the advantage that all the experimental points were taken into account along the whole of the rate curve. The objective function (the error) of the search had only one minimum and yielded unique values of kg and b.

All four methods gave similar results, but those of method four were considered to be the most reliable because of the advantage mentioned. The results of method four only will be included in this thesis.

5.2.2 Solutions at 1600°C

The flux equation was first compared with the nine experiments at 1600°C and gas flow rate of 2680 cm^3 per min. (Tables 2 to 10). There is little to be gained from including all nine graphical comparisons here -- one example is chosen. The experiment at a gas ratio of 0.00250 (Table 3) is shown in Figure 10. The curve shown is the solution of the flux equation for kg = 39.6 and b = 23.6. The agreement is excellent and typical of that found in the other nine experiments. The line shown in Figure 9 is the

numerical solution of the points in Table 8. The values of kg and b found are summarised below.

$\frac{PH_2S}{PH_2} \times 10^3$ ratio	kg	b
= 1.86	= 38.9 cm. per s.	= 24.0 cm. per s.
" = 2.50	" = 39.6 "	" = 23.6 "
" = 3.61	" = 40.3 "	" = 25.9 "
" = 3.99	" = 40.4 "	" = 24.1 "
" = 4.29	" = 42.5 "	" = 25.3 "
" = 5.32	" = 41.3 "	" = 23.7 "
" = 5.72	" = 41.4 "	" = 22.8 "
" = 6.44	" = 41.1 "	" = 22.0 "
" = 7.47	" = 39.1 "	" = 21.7 "
	Average = 40.5 "	Average = 23.7 "

The excellent agreement of each curve over the range of gas compositions demonstrated, not only the applicability of the model, but also that the approximate functional dependence of thermal diffusion upon composition was sufficiently accurate.

At the lower flow rate of 900 cm^3 per min. the three sets of data were equally well fitted by the flux equation's solution. Of the three, (Tables 11 to 13) the experiment at gas ratio of 0.00215 is shown in Figure 11. The values which gave the best predicted curve were:

$\frac{PH_2S}{PH_2} \times 10^3$ ratio = 1.56	kg = 20.7 cm. per s.	b = 16.1 cm. per s.
" " = 2.15	" = 22.5 "	" = 19.3 "
" " = 4.96	" = 21.0 "	" = 18.3 "
	Average = 21.4 "	Average = 17.9 "

At the same temperature of 1600°C three rate curves (Tables 14 to 16) were obtained at a flow rate of 5070 cm^3 per min. The one at a gas ratio of 0.00186 is shown in Figure 12 with the closest fitting curve which resulted from the solution of the flux equation. The values of kg and b were:

$\frac{PH_2S}{PH_2} \times 10^3$ ratio = 1.86	kg = 44.2 cm. per s.	b = 31.3 cm. per s.
" " = 5.72	" = 48.0 "	" = 29.3 "
" " = 6.39	" = 47.1 "	" = 30.9 "
	Average = 46.4 "	Average = 30.5 "

The variation in composition of the H_2-H_2S was circumvented by confining attention to the average values only of kg and b. As was expected, the mass transfer coefficient increased with increasing gas velocity as the contribution of forced convection was enlarged. The increasing flow rate also produced more heat removal from the drop, which led to steeper temperature gradients at the interface and so caused increases in the values of b.

5.2.3 Desulphurisation in Hydrogen

Before discussing the sulphurisation results at the other temperatures, the results for the removal of sulphur from the drop appropriately fit into the discussion at this stage. The rate curves for sulphur removal provided final and additional proof of the gas phase control and of the validity of the flux equation. Three rate curves were obtained, one at each flow rate and all at 1600°C; the one at 2680 cm^3 per min. (Table 30) was plotted in Figure 13. The points showing the increasing sulphur content were those of Table 7 for an H_2-H_2S gas with a ratio of 0.00532. The curve through the points was the best solution of the flux equation, for which kg and b were found. After 20 minutes the gas was switched to pure H_2 but temperature and flow rate were held constant. The points of the falling rate curve were obtained. The change in physical properties in switching from H_2-H_2S to H_2 was negligible. The values of kg and b found for the rising curve applied for the falling curve. However, the direction of gaseous convective flux was changed. For sulphurisation, the convective flux and thermal diffusion flux were in opposition. For desulphurisation, both terms on the right hand side of equation (5.24) became negative. With kg = 41.3 and b = 23.7 cm. per s., equation (5.24) with xH_2S_∞ set at zero was integrated by a finite difference technique. The starting point for the integration was taken as the sulphur content at 20 minutes which was predicted by the sulphurising curve (as opposed to the point or points). The falling curve on Figure 13 shows the solution, which is in excellent agreement with the experimental points.

The experimental points for pure H_2 flowing at 900 cm^3 per min. (Table 29) are shown in Figure 14. The starting samples were provided by the H_2-H_2S rate curve which are listed in Table 13. The parameters which were found to apply were kg = 21.0 and b = 18.3 cm per s. Equation (5.24) was solved with these values when both fluxes were negative, to give the falling rate curve shown in Figure 14. Experiment and model were again in agreement. Solutions were also obtained at other values of b (with the same kg), to illustrate the effect of the thermal diffusion flux. Of particular interest is the curve for b = -18.3 cm. per s., which represents the effect of not changing the direction of the fluxes.

The H_2-H_2S data in Table 16 gave the rate curve shown in Figure 15 for a flow rate of 5070 cm^3 per min. The parameters for the closest curve were found to be kg = 47.1 and b = 30.9 cm. per s., and they applied for the pure H_2 data shown in Table 31. The experimental points of Table 31 are shown in Figure 15 along with the predicted curve obtained by integrating equation (5.24) for sulphur removal.

5.2.4 Solutions at Other Temperatures

The approach described above for the experiments at 1600°C was applied to all the work at 1500°C. Values of the equilibrium constant were known at 1500°C and so equation (5.24) could be solved. The values of kg and b which gave the best fit to the experimental data were obtained. Some of the curves which gave the minimum sum of the squares of the differences are shown graphically. Of the two experiments at a flow rate of 900 cm^3 per min. (Tables 17 and 18) the experimental points at the gas ratio

of 0.00654 (Table 18), are shown in Figure 16. The curve shown represents kg = 21.5 and b = 17.3 cm per s.

The two experiments at a flow rate of 2680 cm^3 per min. are in Tables 19 and 20. Figure 17 shows the data of Table 19 along with the calculated curve.

The highest flow rate, 5070 cm^3 per min. (Tables 21 and 20) Figure 18, was drawn to show the agreement between the curve and the data at a gas ratio of 0.00219 (Table 21).

The experiments and calculations which have been discussed so far are summarised in Table 35. Every experiment is shown and the calculated values of kg and b are included. The independence of the two coefficients and of the PH_2S/PH_2 ratio is apparent. Average values, over the ranges of gas compositions, were calculated and these are listed in the table. From this point onwards the average values are the ones to be examined.

Table 35 is a very comprehensive table and is a numerical synopsis of the kinetic data and their interpretation. The experiments at drop temperatures of 1750 and 1675°C are included. At these temperatures, the equilibrium constants were not known. Values of b therefore could not be calculated and are absent from Table 35.

The average values in Table 35 allowed the effect of flow rate and drop temperature to be examined. The increase in velocity past the drop created steeper concentration and temperature gradients which enlarged the values of kg and b, (see equations (5.2) and (5.23). With the flow rate constant the increases in temperature created small increases in kg. This was due to small changes in physical properties of the gas and/or, an increase in the natural convection component of mass transfer. Changes in values of b with temperature

were not measured with sufficient precision to make any general statements.

5.3 Calculation of Mass Transfer Coefficients, kg

The control of mass transfer by the gas phase resistance and the form of the flux equation (5.24) have been proved. In so doing, the coefficients kg and b were evaluated; as a secondary matter their numerical values were examined. A comparison was made between them and values which could be calculated a priori.

Methods for calculating heat and mass transfer coefficients for flow around spheres were discussed in Section 2.6.2. Some of the difficulties were outlined. The suggested equations were used to calculate values of kg which may be expected to apply for the levitated drop.

All the physical properties were evaluated at the effective film temperature T_f. The actual values and their method of calculation are given in detail in Appendix 5. The values were first used in the Ranz and Marshall correlation (equation 2.14), even though the correlation was not derived for a non-isothermal gas around the drop. In the absence of any contribution due to natural convection values of kg, or the more universal Sherwood number, were calculated. The introduction of the concept of T_f overcame the problem of physical properties; the evaluation of the approach velocity of the gas was complicated. The correlation assumes that the approach velocity is uniform and extends over a cross-section that is large relative to the drop. The annulus which was formed between the levitated sphere and the reaction tube in cross-section, reduced the area for gas flow significantly. Therefore,

the velocity of the gas was increased as it passed the equator of the sphere. The presence of this wall effect almost certainly gave higher mass transfer rates than would have occurred if the reaction tube were of infinite radius. The correlation was applied using both the superficial approach velocity and the velocity through the annulus.

The contribution of forced convection to mass transfer may have been enhanced by increases in local velocity close to the drop. These were caused by volumetric expansion of the gas as it was heated by the proximity of the hot drop. The argument was proposed therefore, that the velocity may be calculated at room temperature or at T_f.

The limits of the range of Re which resulted are as follows:

Minimum flow rate: 900 cm^3 per min.

Approach velocity at room temperature, no wall effect: Re ≈ 1

Velocity at T_f, wall effect: Re ≈ 5

Maximum flow rate: 5070 cm^3 per min.

Approach velocity at room temperature, no wall effect: Re ≈ 5

Velocity at T_f, wall effect: Re ≈ 26

The experimental mass transfer coefficients were converted into Sherwood numbers, Sh, and were compared with some of the calculated values in Table 36.

A cursory examination of the levitation apparatus led to the conclusion that natural convection effects were pronounced. The large temperature differences between the gas at the interface and the gas in bulk created densities which were of the order of six-fold different. However, a more thorough examination of the convection currents showed that a quick look at

temperature difference alone may be extremely misleading.

Earlier levitation workers[25,26,27,29,30,79,85] elected to allow for natural convection by the use of the correlation of Steinberger and Treybal[68] which is given in equation (2.15). Although there are many other correlations in the literature, each with its own vices and virtues, this equation was chosen for use here as an illustrative example and to permit easy comparison with the earlier workers. Some of the values of Sh predicted by this correlation are shown in Table 36.

While the agreement between the experimental values and the values calculated by any of the empirical methods is poor, the very fact that all the numbers are of the same order of magnitude is gratifying. The agreement is much better than was originally anticipated, when all the factors mitigating against the correlations were considered.

The values of the Sh calculated with and without natural convection were close, indicating that free convection was a small effect despite the steep temperature gradients. (Changes in density due to the composition of the gas were negligible.) The explanation is that the Gr is relatively small. Although the change in density, as the ratio ρ_∞/ρ_i, was large, the change $(\rho_\infty-\rho_i)\,\rho_f$ was small for a gas which was predominantly hydrogen. The parameter Gr dictates the magnitude of natural convection, not the temperature differences alone. The relative importance (in contrast to magnitude) of natural convection in any system depends upon the contribution to the total convection: it must be compared with the forced convection. The comparison is readily afforded by the ratio Gr/Re^2. Narasimhan[69] found that:

Natural convection is negligible for $\frac{Gr}{Re^2}$ less than 0.2

Forced convection is negligible for $\frac{Gr}{Re^2}$ greater than 80

For a 1 gram drop of iron at 1600°C in hydrogen, the Gr was approximately 10, which gave the following ratios:

For Re = 1, then $\frac{Gr}{Re^2} = 10$

For Re = 26, then $\frac{Gr}{Re^2} = 0.015$

Even though the values of Re were small, the ratio above still indicated that natural convection was small relative to forced convection in most experiments.

Some of the earlier levitation workers have expressed their final results as mass transfer coefficients rather than quote them as Sherwood numbers. The advantage of using Sh is illustrated in Table 34. All the values of the Sh were close to 2. The contributions of both natural and forced convection were small. However, the special limiting case of Sh = 2, for pure molecular diffusion, is true only for isothermal conditions. In the presence of changing physical properties Sh can be shown to equal values other than 2, (Appendix 6). Hence, in using the correlations evaluated at T_f, not only may the forced and natural convective terms be in error but also the ordinary diffusion term.

The correlations were derived for mass transfer by convection and diffusion alone in the absence of thermal diffusion. Strictly speaking, the presence of thermal diffusion due to temperature gradients affects the composi-

tion gradients (and vice versa). In this way, the mass transfer coefficient has a slight dependence upon the flux due to thermal diffusion. This interactive effect is probably small, since the experimental values of kg remained constant as the magnitude of the thermal diffusion flux was changed at constant temperature and gas flow rate. However, theoretically the dependence does exist.

The proposal of an equation which correlated the experimental mass transfer coefficients or the search for an existing correlation which gave better agreement, was not the object of this thesis. Improved methods of prediction will probably become available in the future. They will correctly describe the effects of temperature gradients; they will probably show that the forced convection and natural convection contributions are not separate terms which may be independently added as in equation (2.15). However, at this stage the Ranz and Marshall type correlations have been proved quite adequate for order of magnitude calculations.

5.4 Calculation of Thermal Diffusion Constants, b

In the previous section, one of the pair of constants which the solution of the flux equation provided was compared with values predicted by semi-empirical correlations. Similar attempts were made to compare the thermal diffusion constant b, with values which were derived from other sources. The values of b up to this stage were experimental numbers without fundamental significance. They had the same units as kg, and incidently were of the same order of magnitude. However, not only did b permit the correc-

tion for the thermal diffusion error in experiments, but also it could be used to predict the thermal diffusion factor α. In equation (5.23), the molecular diffusion coefficient can be computed from the kinetic theory of gases, which would enable α to be calculated if the interfacial temperature gradient were known. The following analysis was proposed to estimate the temperature gradient at the surface.

Electromagnetic stirring in the liquid creates a uniform temperature distribution in the drop as well as a homogeneous sulphur profile. The molar concentration gradient in the gas phase creates mass transfer, to which the heat transfer is analogous when created by a temperature profile which is free from effects of radiation. For a gas which is primarily hydrogen, very little radiant energy is absorbed by the molecules surrounding the drop. The temperature gradients are due to convection and conduction only. The mechanism which facilitates mass transfer is the same mechanism which facilitates the non-radiant heat removal from the surface of the drop. The analogy between heat and mass transfer is complete if we neglect spatial variations of physical properties in the gas phase. The analogy between heat and mass fluxes must now be placed on a quantitative basis.

One easily understood way to illustrate the relationship between the two fluxes is to examine the empirical correlations. Equation (2.13) applies for heat transfer without natural convection. It may be written in general terms including a contribution by natural convection as:

$$Nu = 2.0 + F(Re,Pr) + F'(Gr,Pr) \tag{5.27}$$

$$Nu = 2.0 + F(Re) \cdot Pr^{y} + F'(Gr) \cdot Pr^{y^*} \tag{5.28}$$

where F and F' merely represent some functional dependence. The indices y and y* may not be accurately known, or equal, but are of the order of 1/3 or 1/4. For most gases the Pr and the Sc are approximately unity, which suppresse the effect of the index. Approximate the index to a reasonable value, say 1/3. Equation (2.15) for mass transfer may be written:

$$Sh - 2.0 = F(Re) \cdot Sc^{1/3} + F'(Gr) \cdot Sc^{1/4} \qquad (5.29)$$

$$\frac{Sh - 2.0}{Nu - 2.0} \approx \left[\frac{Sc}{Pr}\right]^{1/3} \qquad (5.30)$$

The term (Sh - 2.0) represents mass transfer by forced and natural convection. These same convective forces cause the heat transfer which is represented by (Nu - 2.0). Thus, Sh and Nu may be related through ratio of $(Sc/Pr)^{1/3}$ when evaluated at the mean film temperature. In this way, the heat transfer coefficient, h, may be evaluated from the experimental measurements of the mass transfer coefficient kg.

The convective heat flux Q, from the drop to the bulk of the gas, is given by:

$$Q = h \cdot (T_i - T_\infty) \qquad (5.31)$$

This overall flux must be the same flux (non-radiant) that is conducted from the surface of the drop in the radial direction:

$$Q = -\left(k \cdot \frac{dT}{dr}_i\right) \qquad (5.32)$$

where the thermal conductivity k, of the gas is evaluated at the surface temperature. The radial temperature gradient at the interface is then substituted into equation (5.23) and the thermal diffusion factor found at any value of b.

The above sequence was followed using the average values of kg and b at the three gas flow rates at temperature of 1500 and 1600°C. The six values of α are shown in Table 37 and are compared with the theoretical value of α. Theoretically predicted values of α at 1500 and 1600°C were approximately equal when calculated at one atmosphere by a method based upon the kinetic theory of gases. Further details of the method are outlined in Appendix 7. In view of the tenuous nature of the heat-mass transfer analogy, the agreement between experimental and theoretical values of α is better than had been anticipated. There are no measured values of α for H_2-H_2S mixtures at these temperatures reported in the scientific literature, and so no further comparison may be made.

A variation on the argument outlined above is to calculate the convective heat transfer coefficient h, directly from a popular empirical correlation (e.g., equation 2.13). Large errors may be introduced as a consequence but, on the other hand, there is no necessity for experimental measurements of the mass transfer coefficient.

5.5 Desulphurisation by Inert Gases

The knowledge which has been gained recently about the sulphur transfer in hydrogen was applied to the inert gases. The rates of desulphurisation in helium and nitrogen are shown in Tables 32, 33 and 34. The presence of small amounts of hydrogen greatly enhanced the rates indicating that desulphurisation of steel melts by inert gas on an industrial basis is doomed if the initial trials with hydrogen are unsuccessful. An attempt was made to predict the rate of sulphur removal and as an example, the results of Table 32 were chosen.

The transfer rates were assumed to be gas phase controlled and interfacial equilibrium was presumed to apply. The sulphur vapour was assumed to transfer completely through to the bulk gas of the helium even though this part of the gas may be well below the condensation point. The sulphur species in the vapour was taken as S_2 and the equilibrium for the surface reaction was given by:

$$\frac{1}{2} \cdot S_2(\text{gas}) = S \text{ (dissolved in iron)} \qquad (5.33)$$

$$K_s = \frac{a_S}{(PS_2)^{1/2}} \qquad (5.34)$$

The value of K_s was taken from page 525 of Elliott and Gleiser[89]. The flux equation, which ignored any thermal diffusion was:

$$\frac{wt}{A \cdot 3200} \cdot \frac{d(\%S)}{dt} \cdot \frac{1}{2} = [kg.C_f.(x_i - x_\infty)]_{\text{for } S_2 \text{ vapour}} \qquad (5.35)$$

Mole fraction of S_2 in the bulk gas was zero, and at the interface it was calculated from equation (5.34). The flux equation was solved for various values of the mass transfer coefficient. One value was calculated from Ranz and Marshall correlation (equation 2.14) with an approach velocity at room temperature. All physical properties were evaluated at T_f. The correlation yielded a value of 3.2 for the Sherwood number. A second value of Sh = 4 was found when allowance for a contribution by natural convection was made (equation 2.15). The rates of desulphurisation which would be predicted by these two values of Sh are shown in Figure 19 which also shows the points measured experimentally. The calculated curves and the measured data are widely different. Figure 19 also includes two curves which show the rates of desulphurisation that correspond to Sh = 10 and Sh = 13. These higher values of Sherwood number give closer agreement with the experimental points.

In any gas-liquid mass transfer experiment in which there is disagreement between the measured rates and those predicted by empirical correlations, the cause is usually that the correlation is inapplicable. This reasoning suggests that the predictions based upon gas phase considerations alone are incorrect in the present study because the experiment itself is not the gas phase controlled. However, if significant resistances to transfer did exist other than in the gas phase, then the measured rates would be less than the empirically predicted rates. Figure 19 shows the reverse. The discrepancy in the present study therefore, is not caused by the assumption that desulphurisation may be treated as pure evaporation.

Earlier evidence in this thesis has shown that the predictions of the empirical correlations may be unreliable in non-isothermal conditions. This may be the cause of the discrepancy in Figure 19. However, the discrepancy appears exceptionally large and suggests some other cause. The evidence is consistent with the hypothesis that the sulphur vapour was condensing in the gas film prematurely, before reaching the bulk gas state where room temperature prevailed. The condensation occurred at some location between the normal boiling point of sulphur and room temperature. This location would be dictated by the vapour pressure - temperature relationship of sulphur and the actual partial pressure in the gas. The concentration gradient of the sulphur vapour was thereby increased and enhanced transfer rates consequently were created. Unfortunately, our present day knowledge is insufficient to express this enhancement on a quantitative basis.

CHAPTER 6

DISCUSSION OF RESULTS: THERMODYNAMIC ASPECTS

6.1 Introduction

The previous chapter was concerned with the kinetic aspects of the sulphurisation process. The interpretation of the results and the analysis of the behaviour were undertaken with an explanation of the kinetic events as the primary objective. The information which the interpretation produced applied at all times of the whole process, including the special case of large times. The present chapter will discuss the equilibrium condition of the experiments. The discussion will represent a very general example of a classical interpretative technique: that is, the measurement of equilibrium data by means of kinetic experiments.

The flux equation which correctly describes the transfer process contains three parameters:

(1) the mass transfer coefficient, kg,

(2) the thermal diffusion constant, b (comprising α and dT/dr),

(3) the equilibrium relationship at the interface, K.

With experimental data available and a knowledge of K, the equation has been solved to yield values of kg and b. Unfortunately, the rule that knowledge of any one of the three values permits evaluation of the other two, is not true in general. If kg and b are known initially by some means

then it should be possible to evaluate K. The method is the converse to what was done in Chapter 5 and is outlined below.

6.2 Evaluation of K from Rate Curves

Rates of sulphurisation were measured at 1675°C (Table 28) and also at 1750°C for the three different flow rates (Tables 23 - 27). On the basis that Chipman's[78] results could not be extrapolated to temperatures above 1600°C, values of K were not known for these six experiments. Values of the mass transfer coefficient were found, in effect, from the initial rate data. Values which applied for each rate curve are shown in Table 35, which indicates no values of b. A method was necessary by which the known values of b at 1500 and 1600°C could be extrapolated to higher temperatures.

The measured values of b at 1500 and 1600°C showed no significant trend with temperature. In view of the nature of the components of the collective constant, a slight dependence of b on temperature had been anticipated originally. Over the narrow range of 100°C this dependence was not verified by experiment which, therefore, dictated that values of b at the higher temperatures be taken as the average of the values at 1500 and 1600°C.

At flow rate of 900 cm^3/ min., average b = 17.2 cm. per sec.

At flow rate of 2680 cm^3/min., average b = 24.2 cm. per sec.

At flow rate of 5070 cm^3/min., average b = 31.2 cm. per sec.

The values of the activity coefficient f_s for sulphur dissolved in iron were assumed to be constant over the temperature range. It was known to

be the same at 1500, 1550 and 1600°C. It was likely to have a similar value at 1750°C.

For each of the six rate curves, the steady state sulphur content of the drop was averaged from the points which were obviously at steady state. The left hand side of the flux equation (equation 5.24) was set equal to zero. The values of kg, b and f_s were substituted which permitted the solution for K. As a check, the known parameters were inserted in the full flux equation which was then integrated from time equal to zero. The integration, which produced weight percent sulphur in iron against time, was compared to the original experimental points over the whole time period.

The six values of K, each of which represents an independent measurement, are shown in Table 38. Figure 20 shows them in graphical form.

A final word is necessary here in order to clarify any ambiguity which may exist over the experimental basis for the calculated values of K. The values which have been found are values at one gas composition alone. The concept of log K' -- that is, extrapolation to infinite dilution over a gas composition range (Section 2.7) -- has not been employed here. Secondly existing values of the activity coefficient were necessary to find values of K. The author is well aware of these facts. The importance of Figure 20 is not in the numerical values which it shows at 1675 and 1750°C, but in the method by which it was derived. A means has been demonstrated by which true equilibrium constants may be measured for a gas-metal system even though thermal diffusion errors are present. The experimental efficiency of this method is demonstrated in the following section.

6.3 Evaluation of K from "Spot" Measurements

The method for evaluating the equilibrium constant was described above. The power of this method in terms of experimental efficiency was illustrated by three discrete measurements. Immediately after constructing the rate curve at a flow rate of 2680 cm^3 per min., and drop temperature of 1675°C (Table 28), three individual samples of iron were levitated in the known H_2-H_2S until steady state, (30 minutes). The drop temperatures were 1650 and 1700°C to straddle the range on each side of 1675°C; the third temperature was 1550°C which was chosen as a check value since K at 1550°C was already known but had never been used so far. The sulphur content of the samples was found to be:

At 1550°C, sulphur content of drop was 1.87%

At 1650°C, sulphur content of drop was 1.61%

At 1700°C, sulphur content of drop was 1.64%

The mass transfer coefficient was known to vary slightly with temperature. The value at 1675°C was kg = 42.0 cm. per s. For the other temperatures, this value was proportioned according to the pattern established in Table 35. The known values of kg, b, xH_2S_∞ were substituted into equation (5.24) at steady state to yield three values of xH_2S_i. In turn the true equilibrium constant was found from the three sulphur compositions.

At 1550°C, equilibrium constant was 0.00234

At 1650°C, equilibrium constant was 0.00270

At 1700°C, equilibrium constant was 0.00266

The three "spot" values of K are shown against the reciprocal of T in Figure 21. Although the findings of Chipman were indirectly necessary to calculate a "spot" K value at 1550°C, the agreement between the two values is excellent. The assumption that b may be taken as constant over this temperature range introduced only a very small error. The three points in Figure 21 represent a net experimental duration of only 90 minutes.

6.4 Comparison of K with other Measurements

The equilibria of the Fe-H_2-H_2S system has been studied by various workers over the last thirty-five years. The merits and defects of the studies were discussed in Section 2.7, which drew the conclusion that only the recent thermodynamics reported by Chipman[78] were essentially devoid of error. Notwithstanding, the past studies have been collected together on Figure 22 and this allows a graphical comparison of all the equilibria in existence, including the values found in the present project. The levitation results are in fair agreement with the data reported in the literature, which gives strong confirmation to the method by which they were derived.

The results obtained in the present project lie below the extended straight line through Chipman's three points at 1500, 1550 and 1600°C. The explanation is that slight dissociation of the hydrogen sulphide occurs at temperatures in excess of 1600°C. Trace amounts of other sulphurous gases are formed as products of the molecular dissociation. This suggests that the dissolution of sulphur in the iron was no longer a single chemical reaction

at the higher drop temperatures. The traditional linear relationship between the equilibrium constant and the reciprocal of temperature can be derived only when two conditions are satisfied. The heat of the chemical reaction must remain constant and the stoichiometry of the reaction must remain unchanged as the temperature is varied; only then is the linearity preserved. For H_2S the heat of the reaction may or may not have changed as temperatures above 1600°C were encountered. However, the stoichiometry certainly changed when molecular dissociation occurred. The multiple reaction caused deviation from the straight line proportionality as the number of H_2S molecules at the surface was slightly depleted. Some of the equilibria measurements by the early workers shown in Figure 22 make no allowance for the slight dissociation at the higher temperatures. These measurements may be corrected by using the free energies involved in the dissociation to correct for the small change in H_2S content at the metal surface. This correction would move the values of K into closer agreement with those of this study.

CHAPTER 7

INTERPRETATION OF EXISTING DATA

7.1 Introduction

The foregoing chapters have given emphasis to the method of interpretation of levitation data rather than to the numerical values which were produced by such interpretation. An attempt will be made in this chapter to demonstrate application of the method and yet, at the same time, produce meaningful numerical values which may be compared to known values.

Equilibria in various systems have been measured by the levitation technique. Often, errors due to thermal diffusion have been present. An example is the work of Larche[21,90]. The example is excellent for the purposes of our demonstration because the data are extensive and well recorded, and secondly, because the task may be attempted by two approaches: experimental and non-experimental.

Larche studied the thermodynamics of the ternary system Fe-O-Cr with levitation melting. In so doing, the oxygen contents of iron drops (without chromium) became available when at steady state with various H_2-H_2O mixtures and various CO-CO_2 mixtures. The equilibrium constants calculated from these measurements, particularly in H_2-H_2O gas, were clearly in error due to thermal diffusion in the gas mixture close to the drop surface. For this reason, further work with the iron-oxygen binary contacting H_2-H_2O was abandoned. The subsequent measurements with the ternary to give the chromium

oxygen interaction parameter were successful. Fortunately, the authors have included the initial data in the absence of chromium and it is to this inclusion that our attention is directed.

7.2 Equilibria under H_2-H_2O Gas

The levitation apparatus for the oxygen study was very similar to that used for the present sulphur study. The details of the apparatus and the experimental conditions are well recorded. The experimental information gathered in the present study is directly applicable for accurate correction of any error caused by thermal segregation of the hydrogen and the water vapour.

On the basis that the rate of the reaction

$$H_2(gas) + \underline{O}\ (\text{dissolved in liquid iron}) = H_2O\ (gas)$$

was controlled by the transfer of water vapour from the bulk gas to the drop surface, an analogy with equations (5.23) and (5.24) may be drawn. If thermal diffusion flux is significant, then at steady state we may write:

$$0 = kg_o \cdot C_{fo} \cdot (xH_2O_\infty - xH_2O_i) - (E.C_o.xH_2.xH_2O)_i \qquad (7.1)$$

where the constant, $E = \alpha_{H2-H2O} \cdot D_{H2-H2O} \cdot \frac{dT}{dr} \cdot \frac{1}{T}$ (7.2)

Complete rate curves were not provided by Larche. Steady state values only were measured, at drop temperatures of 1550, 1600, 1650, 1700

and 1750°C. Many of the dimensions of the apparatus were identical to those of the present study. The gas flow rate past the drop was 1 litre per min. The major component of the mixture was hydrogen which gives further similarity to the H_2-H_2S mixture, and in particular, the absorption of radiant energy can be ignored. The similarity of diffusion, forced and natural convection in the gases meant that these mass transfer mechanisms were identified by the same Sherwood numbers for both systems when at identical flow rates and drop temperatures. The Sh for each temperature of Larche's study could be predicted from the sulphurisation experiments, and hence kg_o became available. The analogy between heat and mass transfer is invoked as before, which permits the calculation of Nu and subsequently $(dT)/(dr)_i$. Physical properties, including the thermal diffusion factor for hydrogen-water vapour mixtures, may be calculated by the same methods shown in Appendices 5 and 7. Values of E are found for each of the five drop temperatures.

Unlike the constant b, the term E has been defined so that it does not include either of the mole fractions of the two gaseous components. The quantity of water vapour in the mixture was significant and in some cases xH_2 was removed from unity, unlike xH_2 in the H_2-H_2S mixtures. Although the hydrogen was by far the major component, in equation (7.1) the term of xH_2 had to be replaced by $(1 - xH_2O)$. For each of the many values of bulk gas composition, equation (7.1) is solved for the corresponding value of xH_2O_i. In turn, this may be compared with the measured oxygen content in the iron to yield an equilibrium constant

$$K_o = \frac{PH_2O_i}{PH_{2i} \cdot (\%\underline{O})} \qquad (7.3)$$

In this way, K_o was found for every steady state that had been measured, and the average was taken. This was performed for each of the five temperature levels studied, which comprised a total of 42 levitated samples. Some of the salient values which the preceding calculation produced are listed in Table 39.

A graphical presentation is made in Figure 23 which illustrates with more clarity the correction for the error due to thermal segregation. For purposes of comparison four other studies[91,92,93,94] of the same system are included, which clearly indicate the validity of the correction. A comprehensive comparison with all other works is given in the original references[21,90].

7.3 Equilibria Under CO-CO_2 Gas

The above example served to show how accurate equilibria may be extracted from data containing thermal diffusion errors. The key to the accuracy of the method was the reliable and accurate values of kg which had been found by experiment for the particular system in use. Whenever accuracy is desired in the prediction of equilibrium constants, kg should be found experimentally and if K is known at one particular temperature, b should be found experimentally. However, an approximate assessment of any system may

be made on a basis which is non-experimental. Such an assessment is recommended for any future levitation study and should be undertaken prior to the commencement of the levitation programme. The information which is provided will assist in designing the laboratory programme. The approach to follow is outlined below. It has been followed for the case of liquid iron levitated in mixtures of $CO-CO_2$ gas at steady state.

1) Assume gas phase control and formulate an explanation of the mechanism similar to equations (7.1) and (7.2). For the dissolution of oxygen in iron from $CO-CO_2$ mixtures, this would be:

$$O = kg'.C'_f.(xCO_{2\infty}-xCO_{2i}) - (E'.C'.xCO.xCO_2)_i \qquad (7.4)$$

$$E' = \alpha_{CO-CO2} \cdot D_{CO-CO2} \cdot \frac{dT}{dr} \cdot \frac{1}{T} \qquad (7.5)$$

The primed variables refer specifically to the $CO-CO_2$ system.

2) Calculate the appropriate physical properties and from them Sh by a Ranz-Marshall type correlation. An estimate of the contribution by natural convection must be included if it is significant.

3) Calculate the gas phase mass transfer coefficient.

4) Calculate the gas phase (convective) heat transfer, i.e., Nu by use of a correlation for heat loss which is analogous to the correlation used for mass transfer.

5) Step 4 provides the heat transfer coefficient, followed by the convective heat flux, from which the interfacial temperature gradient is found.

6) Calculate E'.

7) Compare the magnitudes of the convective flux and the thermal diffusion flux in order to estimate the characteristics of the experiment which is to be undertaken in the future.

8) For the $CO-CO_2$ data which have been gathered, the gas composition at the interface may be found for each corresponding gas analysis in the bulk. The equilibrium constant is calculated by comparison with the oxygen dissolved in the levitated drop.

$$K_{CO-CO2} = \frac{PCO_{2i}}{PCO_i \cdot (\%\underline{O})} \qquad (7.6)$$

The above approach is approximate but even so, may be informative to any proposed levitation study. The approach was used to examine the $CO-CO_2$ data of Larche[21,90]. The equilibrium constants originally measured were in error due to thermal diffusion. The error was corrected and the comparison is shown in Figure 24. The correction, although approximate, has moved the original values towards closer agreement with the earlier and widely accepted measurements reported by Gokcen[95]. As would be anticipated the error due to thermal diffusion in the $CO-CO_2$ mixtures is smaller than that in the H_2-H_2O mixtures.

CHAPTER 8

DISCUSSION OF ERRORS

8.1 Sulphur Content of Levitated Drops

The errors in the laboratory measurements were estimated by means of replicas which were produced under supposedly identical conditions. A qualitative examination of the rate curves indicated that scatter of the results was small. Much of the error suppression was due to:

1) factors which are inherent within the levitation technique,
2) the use of the two-colour pyrometer in preference to total radiation pyrometry.

Even though the accuracy of the results was deemed to be high on an intuitive basis, a true estimate of the errors must be expressed on a quantitative basis.

During the normal course of experiments certain reproducibility checks were carried out. At a drop temperature of 1600°C and an H_2-H_2S gas flow rate of 2680 cm^3 per min. seven samples were levitated, each for a half minute. The subsequent sulphur analysis yielded a mean sulphur content of 0.2442%. On the basis that the errors were normally distributed, the distribution was characterised by a standard deviation of 0.0050. One unit of standard deviation, expressed as a percentage of the mean, was 2.05%.

A second batch of seven replicas was made under the same conditions as the first batch, at half minute durations. The two batches were produced

on separate occasions between which the laboratory apparatus was shut down completely and vacated. The second batch had a mean of 0.2443% sulphur and a standard deviation of 0.0054 which represented 2.23% of the mean.

The two batches were examined to question whether they were drawn from the same population. The two means were compared by a t-test. The two variances were compared by an F-test. The difference in the means, and the difference in the variances, were not significant. The passage of time, shut down and start up (including removal of the coil from the generator) therefore did not introduce any new effects.

A third batch of seven replicas was made for a levitation period of one minute. The mean of the batch was found to be 0.4652% sulphur and the standard deviation was 0.0045 (or 0.97% of the mean value).

A fourth batch of replicas was made at 1600^{o}C and a flow rate of 2680 cm^{3} per min., each sample being held for 20 minutes in the sulphurising gas before quenching. Eighteen samples had a mean of 1.786% sulphur, one standard deviation was 0.026 (or 1.44% of the mean).

The above replicate batches gave a measure of the combined variations in temperature, gas flow rate, time and sulphur analysis which may have occurred about some mean value. The absolute values of the measured variables were considered to be accurate. The pyrometer was calibrated frequently against high quality thermocouples which, in addition, were checked against the melting point of iron. The flow meter was calibrated against a wet test meter, which is a constant displacement device for which the swept volume is known. The electric clock gave accurate increments of time. The accuracy of the sulphur analyser was demonstrated by performing sulphur analysis on N.B.S. steel standards which are the most reliable standards available commercially.

8.2 Error in Coefficients, kg and b

Tables 2 to 10 represent nine rate experiments performed under identical conditions of temperature and flow rate, with various H_2-H_2S gas mixtures. These experiments provide replicas of the mass transfer coefficient kg and the thermal diffusion constant b. The nine values of kg have an arithmetic mean value of 40.51 cm. per s. and, if distributed normally, have a standard deviation of 1.13. The mean value of b is 23.69 cm. per s. with 1.31 standard deviation. The ultimate product of the variables measured during the laboratory procedure is the value of each of the two coefficients. The errors which were present in kg and b may thus be used to characterise the net errors of the total experiment.

The method by which kg and b were found gave equal importance to each experimental point on the sulphurisation rate curve. In so doing, the best pair of values for a rate expression was found as a combination, not as two mutually independent entities. For any one rate curve the errors in kg are incorporated into the value of b. An effective way to illustrate the sensitivity of b with respect to kg, and with respect to the experimental measurements, is given below.

A rate curve was selected at random. At 1600^{o}C and flow rate of 2680 cm^3 per min. Table 3 was chosen. The values of kg and b which gave the closest agreement between the experimental data and the rate equation were already known. Holding kg constant at the best value, b was perturbed and the consequent rate equation compared with the data. The comparison was made by a least squares criterion. The process was then repeated after perturbing the mass transfer coefficient. Values of kg were chosen which were distributed

(at say, $\pm$ two units of standard deviation) about the already known best estimate of kg. The comparison which was finally produced is shown in Figure 25. Numerical values of b are sensitive to kg, and similarly the values of kg are sensitive to b. Perturbations of either coefficient cause significant shifts in the closeness of the fit between the curve provided by the rate equation and the experimental points. The curve through the loci of the minimum sum of the squares of the differences is not shallow; it has its own minimum which is distinct.

An attempt was made to separate the errors in kg from the errors in b. An alternative way to describe the attempt would be that it provides an estimate of the error which may be anticipated in b, if the true value of kg were already available. The mean value was taken of the nine mass transfer coefficients which had been found for the identical conditions of 1600^{o}C and flow rate of 2680 cm^{3} per min. (Tables 2 to 10). In view of the number of experiments performed in order to obtain this mean, it is very reliable and may be supposed to be an accurate estimate of the true value. This mean was presumed to apply to each of the nine rate experiments from which it had been derived. A search was performed to find the value of b which now gave closest agreement to each individual set of rate data. The nine new values of b had a mean of 23.71 cm. per s. with a standard deviation of 1.40. These two numbers were compared with those applying for the original values of b shown previously. The use of an accurate value of kg has not reduced the scatter in the estimates of b, in fact, the variance has been marginally increased. Removal of errors in the mass transfer coefficient did not improve the accuracy of b. Quite a degree of independence must exist therefore, between the errors in the estimates of kg and errors in the estimates of b.

CHAPTER 9

SUMMARY AND CONCLUSIONS

1. An apparatus has been constructed. Its operation has demonstrated that the levitation technique can be used for controlled kinetic studies which involve gas-liquid metal interaction. In particular, the controlling and widening of the range of experimental conditions may be achieved by the appropriate choice from a selection of many varied electromagnetic coils.

2. The overall rates of mass transfer from mixtures of H_2-H_2S to a sphere of liquid iron were found to be gas phase controlled. The mass transfer coefficients were measured experimentally.

3. Measured values of Sherwood number and values predicted by available mass transfer correlations were compared. The correlations are recommended for calculating the order of magnitude of the mass transfer coefficients which may apply for any proposed levitation study.

4. The significant contribution of this study was the demonstration and isolation of the presence of thermal diffusion.

5. The thermal diffusion fluxes which occur in a cold binary gas mixture surrounding a hot levitated drop were expressed on a quantitative basis. The thermal diffusion fluxes were incorporated into an explanation of the

rates of sulphur transfer into the drop.

6. The convective forces in the gas phase give rise to both mass transfer and heat transfer. Heat conduction and mass diffusion are similar. The mechanism which created the mass transfer was the self-same mechanism which created heat transfer. Advantage was taken of this situation to evaluate the temperature gradients at the drop surface and subsequently, to predict the thermal diffusion factor α for the H_2-H_2S binary gas mixture at elevated temperatures.

7. The levitation technique's expedience for measurement of thermodynamic relationships in certain metallurgical systems has always been well known, but has been handicapped by gas phase segregation at steady state. A method by which the degree of thermal separation of the gaseous components may be estimated has been developed. Existing data for steady state gas-liquid iron compositions, which were in error due to thermal diffusion, have been corrected. Equilibrium constants for the Fe-H_2-H_2S system were measured at temperatures above 1600^{o}C. There is now scope for measuring gas-liquid phase equilibria by the levitation technique where previously this technique was considered unsuitable.

8. Rates of evaporation of sulphur from the liquid iron surface into a cold inert gas stream were measured. They have been presented for record here. The rates were higher than had been predicted. The acceleration may have been caused by premature condensation of the sulphur vapour in the thermal layer around the drop.

REFERENCES

1. Muck, O.: German Patent, 1923, No. 422004.
2. Okress, E.C., Wroughton, D.M., Comenetz, G., Brace, P.H. and Kelly, J.C.R.: J. App. Phys., 1952, 23, 545.
3. Polonis, D.H. and Parr, J.G.: Trans. A.I.M.E., 1954, 200, 1148.
4. Sunderland, M.: M.Eng. Thesis, McMaster University, October, 1967.
5. Cooper, C.F., George, C.M. and Hopkins, S.W.J.: Special Ceramics of British Ceramic Research Association, 1962, page 49.
6. Comenetz, G. and Salatka, J.W.: J. Electrochem. Soc., 1958, 105, 673.
7. Bunshah, R.F. and Juntz, R.S.: University of California, U.C.R.L.-7913, 1964.
8. Begley, R.J., Comenetz, G., Flinn, P.A. and Salatka, J.W.: Rev. Sci. Inst., 1959, 30, 38.
9. Shiraishi, S.Y. and Ward, R.G.: Can. Met. Quart., 1964, 3, 117.
10. El-Mehairy, A.E. and Ward, R.G.: Trans. A.I.M.E., 1963, 227, 1226.
11. Hulsey, W.J.: Research and Development Report of the U.S.A.E.C., Number Y-1413, Issued 26-April-1963.
12. Murarka, R., Hamielec, A.E., Fraser, M.E. and Lu, W-K.: Met. Trans. A.I.M.E., 1971, 2, 817.
13. Smith, P.N. and Ward, R.G.: Can. Met. Quart., 1966, 5, 77.
14. Svyazhin, A.G., Vishkarev, A.F. and Yavoyskiy, V.I.: Russian Metallurgy, (Metally), 1968, 5, 47.
15. Turkdogan, E.T., Grieveson, P. and Darken, L.S.: J. Phys. Chem., 1963, 67, 1647.

16. Robertson, D.G.C., Roberts, O.G. and Jenkins, A.E.: Trans. A.I.M.E., 1969, 245, 2413.

17. Distin, P.A., Whiteway, S.G. and Masson, C.R.: Can. Met. Quart., 1971, 10, 13.

18. Caryll, D.B. and Ward, R.G.: J.I.S.I., 1967, 205, 28.

19. Kershaw, P.: Ph.D. Thesis, McMaster University, September, 1968.

20. Shiraishi, S.Y.: M.Sc. Thesis, McMaster University, May, 1966.

21. Larche, F.C.L.: M.Sc. Thesis, McMaster University, August, 1968.

22. Toop, G.W. and Richardson, F.D.: Proc. Symp. Advances in Extractive Metallurgy, Inst. Mining and Metallurgy, April 1967, page 181.

23. Dondelinger, J.G., Kay, D.A.R. and McLean, A.: Met. Trans. A.I.M.E., 1971, 2, 3203.

24. Gomersall, D.W.: Ph.D. Thesis, McMaster University, September, 1967.

25. Baker, L.A., Warner, N.A. and Jenkins, A.E.: Trans. A.I.M.E., 1964, 230, 1228.

26. Baker, L.A., Warner, N.A. and Jenkins, A.E.: Trans. A.I.M.E., 1967, 239, 857.

27. Kaplan, R.S. and Philbrook, W.O.: Trans. A.I.M.E., 1969, 245, 2195.

28. Distin, P.A. and Whiteway, S.G.: Can. Met. Quart., 1970, 9, 419.

29. Distin, P.A., Hallett, G.D. and Richardson, F.D.: J.I.S.I., 1968, 206, 821.

30. Distin, P.A.: Ph.D. Thesis, University of London, April, 1967.

31. Baker, R.: J.I.S.I., 1967, 205, 637.

32. Baker, L.A. and Ward, R.G.: J.I.S.I., 1967, 205, 714.

33. Vig, S.K. and Lu, W-K.: J.I.S.I., 1971, 209, 630.

34. Gomersall, D.W., Shiraishi, S.Y. and Ward, R.G.: J. Aust. Inst. Metals, 1965, 10, 220.

35. Ito, K. and Sano, K.: Trans. I.S.I. Japan, 1969, 9, 465.

36. Mori, K. and Suzuki, K.: Trans. I.S.I. Japan, 1970, 10, 232.

37. Peters, R.J.W., Masson, C.R. and Whiteway, S.G.: Trans. Faraday Soc., 1965, 61, 1745.

38. Rony, P.R.: The Electromagnetic Levitation of Metals, University of California, Report U.C.R.L.-11411, May 7th, 1964.

39. Hulsey, W.J.: M.Sc. Thesis, University of Tennessee, 1963.

40. Rostron, A.J.: Science J., 1967, 3, No. 7, 69.

41. Harris, B. and Jenkins, A.E.: J. Sci. Instruments, 1959, 36, 238.

42. Lewis, J.C., Neumayer, H.R.J. and Ward, R.G.: J. Sci. Instruments, 1962, 39, 569.

43. Peifer, W.A.: J. of Metals, 1965, 17, 487.

44. Fromm, E. and Jehn, H.: Brit. J. Appl. Phys., 1965, 16, 653.

45. Hatch, A.J. and Smith, W.E.: J. Appl. Phys., 1967, 38, 742.

46. Booth, A.R. and Charles, J.A.: Nature, 1966, 212, 750.

47. Chapman, S. and Cowling, T.G.: The Mathematical Theory of Non-Uniform Gases, Cambridge University Press.

48. Chapman, S. and Dootson, F.: Phil. Mag., 1917, 33, 248.

49. Present, R.D.: Kinetic Theory of Gases, McGraw Hill Book Company, 1958.

50. Clark-Jones, R. and Furry, W.H.: Rev. of Mod. Phys., 1946, 18, No. 2, 151.

51. Gillespie, L.J.: J. Chem. Phys., 1939, 7, 530.

52. Frankel, S.P.: Phys. Rev., 1940, 57, 661.

53. Gillespie, L.J.: J. Chem. Phys., 1939, 7, 438.

54. DeGroot, S.R.: Thermodynamics of Irreversible Processes, North Holland Publishing Co., 1958.

55. Denbigh, K.G.: The Thermodynamics of the Steady State: Methuen and Company, Monographs on Chemical Subjects, 1951.

56. Dastur, M.N. and Chipman, J.: Disc. Faraday Soc., 1948, No. 4, 100.

57. Darken, L.S. and Gurry, R.W.: J. Amer. Chem. Soc., 1945, 67, 1398.

58. Richardson, F.D. and Alcock, C.B.: Nature, 1951, 168, 661.

59. Alcock, C.B.: Inter. J. Appl. Radiation and Isotopes, 1958, 3, 135.

60. Kontopoulos, A.: Ph.D. Thesis, McMaster University, January, 1971.

61. Delancey, G.B. and Chiang, S.H.: A.I.Ch.E.J., 1968, 14, 664.

62. Grew, K.E. and Ibbs, T.L.: Thermal Diffusion in Gases, Cambridge University Press, 1952.

63. Glasstone, S.: Sourcebook on Atomic Energy, Van Nostrand, 3rd Edition, 1967.

64. Robertson, D.G.C. and Jenkins, A.E.: Proc. International Conference in Metallurgy and Materials Science, University of Pennsylvania, September, 1969. Published by Plenum Press, 1970.

65. Sano, N. and Matsushita, Y.: Trans. I.S.I. Japan, 1971, 11, 232.

66. Ranz, W.E. and Marshall, W.R.: Chem. Eng. Prog., 1952, 48, 141.

67. Ranz, W.E. and Marshall, W.R.: Chem. Eng. Prog., 1952, 48, 173.

68. Steinberger, R.L. and Treybal, R.E.: A.I.Ch.E.J., 1960, 6, 227.

69. Narasimhan, C.: Ph.D. Thesis, McGill University, April, 1966.

70. Chipman, J. and Ta Li: Trans. A.S.M., 1937, 25, 435.

71. Skelly, H. and White, J.: J.I.S.I., 1947, 155, 201.

72. Morris, J.P. and Williams, A.J.: Trans. A.S.M., 1949, 41, 1425.

73. Sherman, C.W., Elvander, H.I. and Chipman, J.: Trans. A.I.M.E., 1950, 188, 334.

74. Cordier, J.A. and Chipman, J.: Trans. A.I.M.E., 1955, 202, 905.

75. Adachi, A. and Morita, Z.: Tech. Rept. Osaka University, Japan, 1958, 8, 385.

76. Yoshii, C. and Sasaki, K.: Japan Soc. Sci. Promotion, 19th Tech. Com. Rept., 8131-206 (May, 1966).

77. Fuwa, T., Ban-ya, S. and Yoshida, K.: Japan. Soc. Sci. Promotion, 19th Tech. Com. Rept., 8130-205 (May, 1966).

78. Chipman, J. and Ban-ya, S.: Trans. A.I.M.E., 1968, 242, 940.

79. Glen, C.G. and Richardson, F.D.: Proc. Intern. Conference in Metallurgy and Materials Science, University of Pennsylvania, September, 1969, Plenum Press, 1970.

80. Turkdogan, E.T.: Trans. A.I.M.E., 1964, 230, 740.

81. Szekely, J. and Hills, A.W.D.: Int. J. Heat Mass Transfer, 1969, 12, 11.

82. Szekely, J. and Hills, A.W.D.: Chem. Eng. Sci., 1964, 19, 79.

83. Kitchener, J.A., Liberman, A., and Spratt, D.A.: Analyst., 1951, 76, 509.

84. Dunicz, B.L. and Rosenquist, T.: Anal. Chem., 1952, 24, 404.

85. Palmer, A.R.: Ph.D. Thesis, Imperial College of University of London, January, 1971.

86. Furry, W.H., Jones, R.C. and Onsager, L.: Phys. Rev., 1939, 55, 1083.

87. Hooke, R. and Jeeves, T.A.: J. Assn. for Comp. Mach., 1961, 8, 212.

88. Pang, K-H.: Ph.D. Thesis, McMaster University, March, 1970.

89. Elliott, J.F. and Gleiser, M.: Thermochemistry for Steelmaking, Volume II, Addison-Wesley Publishing Co., 1963.

90. Larche, F.C.L. and McLean, A.: to be published in J.I.S.I.

91. Averin, V.V., Polyakov, A.Y. and Samarin, A.M.: Izv. Akad. Nauk. S.S.S.R., Otd. Tekhu Nauk., 1955, 3, 90.

92. Gokcen, N.A., Belton, G.R. and Tankins, E.S.: Trans. A.I.M.E., 1964, 203, 820.

93. Floridis, T.P. and Chipman, J.: Trans. A.I.M.E., 1958, 212, 549.

94. Kontopoulos, A., Kay, D.A.R. and McLean, A.: to be published in Met. Trans. A.I.M.E.

95. Gokcen, N.A.: Trans. A.I.M.E., 1956, 206, 1558.

96. Crank, J.: The Mathematics of Diffusion, Oxford University Press, 1956.

97. Belton, G.R. and McCarron, R.L.: Trans. A.I.M.E., 1969, 245, 1161.

98. Bird, R.B., Stewart, W.E. and Lightfoot, E.N.: Transport Phenomena, John Wiley and Sons, 1966.

99. Reid, R.C. and Sherwood, T.K.: The Properties of Gases and Liquids, McGraw-Hill, 1958.

100. Kirshenbaum, A.D. and Cahill, J.A.: Trans. A.I.M.E., 1962, 224, 816.

101. Hirschfelder, J.O., Curtiss, C.F. and Bird, R.B.: Molecular Theory of Gases and Liquids, John Wiley and Sons, 1954.

102. Vlasov, S.M., Devyatykh, G.G. and Tsinovoi, Y.N.: Zhur. Fiz. Khim., 1968, 42, 2745.

APPENDIX I

DIFFUSION OF SULPHUR WITHIN A STAGNANT DROP OF LIQUID IRON

The rates of sulphur transfer may be calculated theoretically for certain limiting cases. Such extreme situations, while not realistic, are informative. One limiting case is that of liquid phase control of the overall rate in the absence of any internal motion within the liquid. Suppose that the gas phase resistance were negligible, that the rate constants for the chemical reaction were large, and interfacial equilibrium existed at all times.

The transfer of material from the drop surface into the liquid by radial diffusion is given by an equation of continuity of the form:

$$\frac{\partial S}{\partial t} = D_{Fe\text{-}S} \cdot \left(\frac{\partial^2 S}{\partial r^2} + \frac{2}{r} \cdot \frac{\partial S}{\partial r} \right)$$

where S represents some measure of the concentration of sulphur in the iron,

t is time,

$D_{Fe\text{-}S}$ is the molecular diffusion coefficient for sulphur in iron,

r is the radial coordinate drawn from the sphere's centre at which r = zero.

The boundary conditions are known which permit an analytical solution to this one-dimensional problem. Full details of the method of solution

are given in Chapter 6 of Crank[96], which presents a solution in a general, non-dimensional form. The total mass of sulphur (or concentration) which has diffused into the drop at $t = \infty$ (i.e., steady state) is defined as M_∞. The mass of sulphur (or concentration) which is present in the sphere at any instant in time is defined as M_t. The solution for the case of a sphere initially free of sulphur is shown in Figure 26.

The diffusion coefficient for the iron-sulphur binary at 1600°C is given as 1.7×10^{-4} cm^2 per s. by Belton and McCarron[97]. The radius of the sphere, (a), is taken as 0.34 cm. After only six minutes the quantity of sulphur inside the drop is 99% of the total that is given by the steady state equilibrium with the infinite concentration sink surrounding the drop surface.

The case for liquid phase control for a non-stagnant drop may be similarly solved. The solution may be identical, with the exception that the diffusion coefficient is enlarged. It is quite likely that the irregular internal liquid motion within a levitated drop creates an apparent enhancement of D_{Fe-S} of some orders of magnitude. This would have the effect of greatly expanding the upper (real time) scale of Figure 26, while the curve remained fixed. The attainment of steady state would be considerably more rapid than in a drop free from imposed convective forces.

APPENDIX 2

ANALYSIS OF TRANSFER MECHANISMS

The overall process of transport from the bulk of the gas mixture to the bulk of the liquid iron is divided into steps. A mechanism for each step is presumed. The rate of each step is expressed mathematically. These mechanisms and expressions are described in Chapter 5. The same nomenclature is used in this Appendix.

The flux of H_2S from the bulk gas to the gas-liquid interface is by molecular diffusion, forced and natural convection.

$$\frac{wt}{A \cdot 3200} \cdot \frac{d(\%S)}{dt} = \text{Flux} = C.kg.(xH_2S_\infty - xH_2S_i) \qquad (5.2)$$

If thermal diffusion makes a contribution to transport in this step, the above equation is written as:

$$\text{Flux} = C \cdot kg \cdot (xH_2S_\infty - xH_2S_i) - (C \cdot b \cdot xH_2S)_i \qquad (5.24)$$

The object of this appendix is to illustrate the approach to a typical metallurgical mass transfer process. The scheme of the analysis and the final results are not affected by the inclusion or the exclusion of the thermal diffusion term. For clarity, it may be excluded here.

The gaseous H_2S molecules adsorb onto active sites at the interface.

$$\text{Flux} = k_1 \cdot x_{H_2S_i} \cdot \theta E - k_2 \cdot \theta_{H_2S} \tag{5.3}$$

The chemical reaction takes place among adsorbed species.

$$\text{Flux} = k_3 \cdot \theta_{H_2S} \cdot \theta E - k_4 \cdot \theta_{H_2} \cdot \theta S \tag{5.5}$$

Sulphur is desorbed from the interface into the liquid phase.

$$\text{Flux} = k_5 \cdot \theta S - k_6 \cdot a_{si} \cdot \theta E \tag{5.6}$$

Transfer of sulphur from the interface into the bulk liquid is by diffusion and convection.

$$\text{Flux} = k_L (a_{si} - a_{s\infty}) \tag{5.7}$$

The stoichiometry of the reaction which relates the fluxes of H_2S and S, also relates the flux of H_2 from the reaction sites.

$$\text{Flux} = k_7 \cdot \theta_{H_2} - k_8 \cdot x_{H_{2i}} \cdot \theta E \tag{5.8}$$

For the overall process with no accumulation of material, the rate of each step is the same. Typical of most transfer processes, the intermediate parameters defy measurement in the laboratory. The values of θ's are unknown although their sum is unity. Only the bulk compositions may be

measured. The elimination of θ's is necessary. This may be achieved for certain limiting cases, so that the only unknowns remaining are the rate coefficients. Chosen examples are shown below.

Gas Phase Control

Initially there is no sulphur in the liquid and $a_{Si} = 0$. Equilibrium exists at the interface and $xH_2S_i = 0$. Equation (5.2) becomes:

$$\text{Flux} \Big|_{t=0} = C.kg.xH_2S_\infty$$

Adsorption Control

The adsorption step provides a very high resistance to transfer compared to the other steps. In equation (5.3) k_1 and k_2 are relatively small numbers. In contrast, the mechanisms of the other steps take place very readily. The forward flux and reverse flux in the other steps are both extremely large. For practical purposes, equations (5.5), (5.6) and (5.8) are approximated:

$$k_3 \cdot \theta H_2S \cdot \theta E \approx k_4 \cdot \theta H_2 \cdot \theta S$$

$$k_5 \cdot \theta S \approx k_6 \cdot a_{Si} \cdot \theta E$$

$$k_7 \cdot \theta H_2 \approx k_8 \cdot xH_{2i} \cdot \theta E$$

Simultaneous solution for each θ-term is performed, followed by substitution in equation (5.3), which becomes:

$$\text{Flux} = \frac{k_1 \cdot k_3 \cdot k_5 \cdot k_7 \cdot xH_2S_i - k_2 \cdot k_4 \cdot k_6 \cdot k_8 \cdot a_{Si} \cdot xH_{2i}}{k_3 \cdot k_6 \cdot k_7 \cdot a_{Si} + k_3 \cdot k_5 \cdot k_8 \cdot xH_{2i} + k_4 \cdot k_6 \cdot k_8 \cdot xH_{2i} \cdot a_{Si} + k_3 \cdot k_5 \cdot k_7}$$

For adsorption control, the interfacial compositions may be replaced by the bulk compositions of gas and liquid. The special case of zero time for a liquid initially free of sulphur reduces the above equation.

$$\text{Flux}\Big|_{t=0} = \frac{k_1 \cdot k_7 \cdot xH_2S_\infty}{k_8 \cdot xH_{2\infty} + k_7} \qquad (5.11)$$

Chemical Reaction Control

If the overall rate of transfer is controlled by the rate of the chemical reaction, a similar argument to that for the adsorption step above may be applied. Equation (5.5) must be evaluated. This is achieved by:

$$k_1 \cdot xH_2S_i \cdot \theta E \simeq k_2 \cdot \theta H_2S$$

$$k_5 \cdot \theta S \simeq k_6 \cdot a_{Si} \cdot \theta E$$

$$k_7 \cdot \theta H_2 \simeq k_8 \cdot xH_{2i} \cdot \theta E$$

Eliminate the θ's and substitute into equation (5.5).

$$\text{Flux} = \frac{k_1 . k_2 . k_3 . k_5 . k_5 . k_7 . k_7 . xH_2S_i - k_2 . k_2 . k_4 . k_5 . k_6 . k_7 . k_8 . a_{Si} . xH_{2i}}{(k_2 . k_5 . k_7 + k_2 . k_6 . k_7 . a_{Si} + k_2 . k_5 . k_8 . xH_{2i} + k_1 . k_5 . k_7 . xH_2S_i)^2}$$

This equation reduces to equation (5.12) at zero time.

The process may be repeated for cases of liquid phase desorption control and of convective transfer control into the bulk liquid. In this way, the rate of the process may be expressed in terms of parameters which can be controlled and measured in the laboratory. By comparison with the experimental evidence, a particular rate controlling step can be identified. In some cases the form of the solution may be such that the rate coefficients can be numerically evaluated.

Joint Control

The experimental data may indicate that control is not by a single step in the overall process. More than one mechanism may be jointly controlling the rate. The situation is now more complex. A solution is still possible for certain cases and is shown here for joint control by gas phase transport and adsorption.

$$\text{Flux} = C . kg . (xH_2S_\infty - xH_2S_i) = k_1 . xH_2S_i . \theta E - k_2 . \theta H_2S$$

Eliminate xH_2S_i:

$$\text{Flux} = \frac{C.kg.k_1.\theta E.xH_2S_\infty - C.kg.k_2.\theta H_2S}{C.kg + k_1.\theta E}$$

In order to evaluate the θ's the same reasoning as before is applied.

$$k_3.\theta H_2S.\theta E \simeq k_4.\theta S.\theta H_2$$

$$k_5.\theta S \simeq k_6.a_{Si}.\theta E$$

$$k_7.\theta H_2 \simeq k_8.\theta E.xH_{2i}$$

$$a_{Si} \simeq a_{S\infty}$$

Evaluate the θ's and substitute in the equation for the flux.

$$\text{ux} = \frac{C.kg.k_1.k_3.k_5.k_7.xH_2S_\infty - C.kg.k_2.k_4.k_6.k_8.a_{S\infty}.xH_{2\infty}}{C.kg.k_3.k_5.k_7+k_1.k_3.k_5.k_7+C.kg.k_3.k_5.k_8.xH_{2\infty}+C.kg.k_4.k_6.k_8.a_{S\infty}.xH_{2\infty}+C.kg.k_3.k_6.k_7.a_S}$$

This above equation for joint control reduces to the two solutions obtained earlier, when the conditions for the limiting cases of gas phase control alone and of adsorption control alone are applied to it.

APPENDIX 3

GAS PHASE OR LIQUID PHASE CONTROL: INTERFACIAL EQUILIBRIUM

The five steps of the transfer process were outlined in the preceding appendix. By definition, if the process is gas phase controlled or is liquid phase controlled (or jointly by both) then equilibrium exists at the interface at all times. The analysis of the preceding appendix readily leads to this condition in algebraic terms.

If the resistance is high in the gas or liquid phase, the same argument applied in Appendix 2 may be employed in the intermediate steps. As before equations (5.3), (5.5), (5.6) and (5.8) may be approximated to:

$$k_1 \cdot x_{H_2S_i} \cdot \theta E \simeq k_2 \cdot \theta_{H_2S}$$

$$k_3 \cdot \theta_{H_2S} \cdot \theta E \simeq k_4 \cdot \theta_{H_2} \cdot \theta S$$

$$k_5 \cdot \theta S \simeq k_6 \cdot a_{Si} \cdot \theta E$$

$$k_7 \cdot \theta_{H_2} \simeq k_8 \cdot x_{H_{2i}} \cdot \theta E$$

The four identities above are manipulated to eliminate θ's, and are rearranged to give:

$$\frac{x_{H_2S_i}}{x_{H_{2i}} \cdot a_{Si}} = \frac{k_2 \cdot k_4 \cdot k_6 \cdot k_8}{k_1 \cdot k_3 \cdot k_5 \cdot k_7}$$

APPENDIX 4

VARIATION OF ADSORPTION RATE CONSTANT WITH TEMPERATURE

The rate constants for chemisorption or chemical reactions may be expressed by the well known Arrhenius equation:

$$k' = A' \cdot \exp\left(-\frac{Ea}{RT}\right)$$

The rate constant k', is independent of external conditions such as gas flow rate in our case, but is dependent upon temperature as shown. The frequency factor A', is independent of temperature. The universal gas constant is 1.988 cal. per mole ^{o}K. The activation energy Ea, is not known, but for purposes of a proportional comparison an order of magnitude is quite sufficient. As an example, suppose that Ea = 25,000 cal. per mole. At a temperature of $1500^{o}C$, $T = 1773^{o}K$.

$$\frac{k'}{A'} = \exp\frac{-25,000}{1.988 \times 1773} = \exp - 7.092$$

$$\ln\left(\frac{k'}{A'}\right)\Bigg|_{1500} = -7.092$$

At a temperature of $1750^{o}C$, $T = 2023^{o}K$.

$$\frac{k'}{A'} = \exp \frac{-25,000}{1.988 \times 2023} = \exp -6.216$$

$$\ln \left(\frac{k'}{A'} \right) \Bigg|_{1750} = -6.216$$

Effect of this temperature change on the rate constant:

$$\ln \left(\frac{k'}{A'} \right) \Bigg|_{1750} - \ln \left(\frac{k'}{A'} \right) \Bigg|_{1500} = -6.216 + 7.092$$

$$\ln \left(\frac{k'_{1750}}{k'_{1500}} \right) = + 0.876$$

The ratio $$\frac{k'_{1750}}{k'_{1500}} = 2.4$$

APPENDIX 5

PHYSICAL PROPERTIES

Diffusion Coefficient

The kinetic theory of gases has led to the development of various methods for calculation of many physical properties of gases. For low density gases, the equations for prediction of properties are very reliable. They were used here for estimating some of the gaseous properties at various elevated temperatures. The diffusion coefficient was predicted from page 511 of reference 98 (also Chapter 8 of reference 99) which gives for binary gas mixtures at one atmosphere of pressure, that:

$$D_{H2-H2S} = \frac{0.001858 \cdot T^{3/2} \cdot \left(\frac{1}{MH2} + \frac{1}{MH2S}\right)^{1/2}}{\sigma^2_{H2-H2S} \cdot \Omega_{D.H2-H2S}}$$

where MH2 = 2 and MH2S = 34 and the Lennard-Jones parameters of σ and Ω_D are available.

Typical values calculated were:

D_{H2-H2S} at $300^{o}K$ = 0.684 cm^2 per s.

D_{H2-H2S} at $1100^{o}K$ = 6.29 cm^2 per s.

D_{H2-H2S} at $1900^{o}K$ = 15.5 cm^2 per s.

The wide variation of this physical property with temperature is worthy of note. The effects of the non-isothermal conditions around the levitate drop are by no means insignificant.

Viscosity

A similar type of relationship is given by references 98 and 99 for estimating the viscosity of monatomic and diatomic gases. For the range H_2-H_2S ratios used in the experiments, the viscosity was essentially that of pure hydrogen.

$$\mu = \frac{2.669 \times 10^{-5} \cdot (M.T)^{1/2}}{\sigma^2 \cdot \Omega_\mu}$$

At 1100^oK, $\mu = 20.9 \times 10^{-5}$ gram. per cm. s.

Thermal Conductivity

The thermal conductivity is shown in reference 98, page 255 and reference 99, Chapter 7 to be:

$$k = \frac{1.989 \times 10^{-4} \cdot (T/M)^{1/2}}{\sigma^2 \cdot \Omega_k}$$

As before, the collision diameter, σ, and the collision integral, Ω_k, are well tabulated. The above equation applies only for monatomic gases at low pressure and must be corrected for polyatomic gases such as hydrogen. The Eucken correction factor for hydrogen was 1.255.

At 1100°K, thermal conductivity is

$$9.74 \times 10^{-4} \frac{\text{cal. cm.}}{\text{cm}^2 \text{ . s . }^{\circ}\text{K}}$$

At 1900°K, thermal conductivity is

$$13.9 \times 10^{-4} \frac{\text{cal. cm.}}{\text{cm}^2 \text{ . s . }^{\circ}\text{K}}$$

Density

The density of hydrogen is widely recorded over ranges of temperature and pressure. The records show it very closely approaches ideal behaviour. The values of density used for calculations here were those provided by the suppliers of the hydrogen gas. The values showed very close agreement with the various other values quoted in the scientific literature. When calculating certain parameters, e.g., gas velocity past the levitated drop, at intermediate temperatures, ideality was assumed.

At 1100°K the density is

$$2.23 \times 10^{-5} \text{ gram. per cm.}^3$$

Density of Liquid Iron

Values for the density of liquid iron were taken from the measurements of Kirshenbaum and Cahill[100] who used the immersed-sinker method for density measurements over a wide temperature range starting at the melting point. Their findings were expressed by:

$$\rho_d = 8.523 - (8.358 \times 10^{-4}) \cdot T$$

which gives the density in gram. per cm^3 for the temperature in ^oK.

APPENDIX 6

MOLECULAR DIFFUSION TO AND FROM A SPHERE

SHERWOOD NUMBER = 2

In general, the equations of continuity and of energy have not been solved simultaneously for heat and mass transfer to three-dimensional bodies. However, analytical solutions for certain limiting cases are available. One such case is the steady state transfer of material by molecular diffusion (c.f., evaporation of a pure liquid) from a sphere. Similar heat transfer from a solid sphere by conduction alone is fully understood. Both solutions are valid only when the physical properties of the surrounding medium remain constant. The two methods of solution are combined here and allowance, although approximate, is made for the dependence of the two salient physical properties upon temperature.

Molecular Diffusion . Constant Diffusion Coefficient

The steady state flux of material in the radial direction from the sphere's surface is:

$$\text{Mass Flux} = - D \cdot \frac{dC}{dr}$$

where D is the diffusion coefficient,

C is the concentration of the diffusing species in the surrounding medium,

r is the radial coordinate for which r=0 at the sphere's centre and r=a at the sphere's surface.

All symbols used in this appendix are specific to this appendix alone.

In the absence of material accumulation or generation, the total radial mass flow, ZI, is:

$$ZI = - 4\pi r^2 \cdot D \cdot \frac{dC}{dr}$$

Integrate with constant D:

$$\int_{r=a}^{r=r} \frac{ZI}{4\pi r^2} \cdot dr = - D \cdot \int_{C=C_i}^{C=C} \frac{dC}{dr}$$

$$- \frac{ZI}{4\pi} \cdot \left(\frac{1}{r} - \frac{1}{a} \right) = - D \cdot (C - C_i)$$

Far away from the drop, $r = \infty$, $C = C_\infty$. Therefore

$$\frac{ZI}{4\pi} \cdot \frac{1}{a} = - D \cdot (C_\infty - C_i)$$

Eliminate the unknown, ZI:

$$1 - \frac{a}{r} = \frac{C - C_i}{C_\infty - C_i}$$

This equation may be expressed in dimensionless terms where:

$$C^* = \frac{C - C_i}{C_\infty - C_i} \quad \text{and} \quad r^* = \frac{r}{a}$$

Therefore,

$$1 - \frac{1}{r^*} = C^*$$

At the surface of the sphere where $r^* = 1$, we have:

$$Sh = 2 \cdot \frac{dC^*}{dr^*}$$

Therefore

$$Sh = 2$$

A similar approach for heat conduction may be followed to show that Nu = 2. This approach is followed below without the condition of constant thermal conductivity. It is not carried to completion, but merely to the point of providing the temperature distribution around the drop.

Heat Conduction . Changing Thermal Conductivity

Steady state heat flux radially from the sphere is:

$$\text{Heat Flux} = - k \cdot \frac{dT}{dr}$$

The total heat flow, Z2, is:

$$Z2 = - 4\pi r^2 \cdot k \cdot \frac{dT}{dr}$$

The thermal conductivity k, changes with temperature. The absolute values of k are not required, merely the functional dependence upon temperature. The dependence may be approximate to a square root (see Appendix 5) for purposes of this illustration.

$$k = Z3 \cdot T^{1/2}$$

where Z3 is some constant of proportionality.

Integrate:

$$\int_{r=a}^{r=r} \frac{Z2}{4\pi r^2} \cdot dr = - Z3 \cdot \int_{T=T_i}^{T=T} T^{1/2} \cdot dT$$

$$- \frac{Z2}{4\pi} \cdot \left(\frac{1}{r} - \frac{1}{a} \right) = - Z3 \cdot \frac{2}{3} \cdot \left(T^{3/2} - T_i^{3/2} \right)$$

Far away from the drop, $r = \infty$, $T = T_\infty$. Therefore:

$$\frac{Z2}{4\pi} \cdot \frac{1}{a} = - Z3 \cdot \frac{2}{3} \cdot (T_\infty^{3/2} - T_i^{3/2})$$

Eliminate the unknowns, Z2 and Z3:

$$1 - \frac{a}{r} = \frac{T^{3/2} - T_i^{3/2}}{T_\infty^{3/2} - T_i^{3/2}}$$

The temperature distribution around the sphere is now known. This profile is assumed to be fixed and will apply regardless of any other transport process that may occur. In other words, any interaction is ignored.

Molecular Diffusion . Changing Diffusion Coefficient

Molecular diffusion is now superimposed. Now however, allowance is made for the dependence of the diffusion coefficient upon temperature, on the basis of the already known temperature profile. Again, the absolute values of D are not necessary. The dependence of the diffusion coefficient upon temperature (see Appendix 5) may be approximated by:

$$D = Z4 \cdot T^{3/2}$$

where Z4 is another constant of proportionality.

Again the molecular diffusion in the radial direction gives rise to a mass flux of:

$$\text{Mass Flux} = - D \cdot \frac{dC}{dr}$$

$$\text{Total Mass flow, } Z5 = - 4\pi r^2 \cdot Z4 \cdot T^{3/2} \cdot \frac{dC}{dr}$$

Integrate:

$$\int_{r=a}^{r=r} \frac{Z5}{4\pi r^2} \cdot \frac{1}{Z4 . T^{3/2}} \cdot dr = - \int_{C=C_i}^{C=C} dC$$

where $T = f(r)$ is the previously found temperature distribution.

$$\frac{Z5}{4\pi . Z4} \cdot \left(\frac{-1}{aT_i^{3/2} - aT_\infty^{3/2}} \right) \cdot \ln \left(\frac{aT_i^{3/2} - aT_\infty^{3/2} + rT_\infty^{3/2}}{rT_i^{3/2}} \right)$$

$$= - (C - C_i)$$

Far away from the drop, $r = \infty$, $C = C_\infty$.

$$\frac{Z5}{4\pi . Z4} \cdot \left(\frac{-1}{aT_i^{3/2} - aT_\infty^{3/2}} \right) \cdot \ln \left(\frac{T_\infty^{3/2}}{T_i^{3/2}} \right) = - (C_\infty - C_i)$$

Eliminate the unknowns, Z4 and Z5:

$$\frac{\ln\left(\frac{aT_i^{3/2} - aT_\infty^{3/2} + rT_\infty^{3/2}}{rT_i^{3/2}}\right)}{\ln\left(\frac{T_\infty^{3/2}}{T_i^{3/2}}\right)} = \frac{C - C_i}{C_\infty - C_i}$$

As before $C^* = \frac{C - C_i}{C_\infty - C_i}$ and $r^* = \frac{r}{a}$

Therefore:

$$\frac{dC^*}{dr^*} = \frac{1}{\ln\left(\frac{T_\infty^{3/2}}{T_i^{3/2}}\right)} \cdot \frac{T_\infty^{3/2} - T_i^{3/2}}{\frac{r}{a}\left(T_i^{3/2} - T_\infty^{3/2} - \frac{rT_\infty^{3/2}}{a}\right)}$$

Taking our situation, in which $T_\infty = 296^oK$ and $T_i = 1873^oK$, the equation above may be evaluated at the drop surface where $r = a$.

$$\left.\frac{dC^*}{dr^*}\right|_{r^*=1} = 0.339$$

Therefore Sh = 0.68

For the severe non-isothermal conditions around the drop and their consequent effect upon the physical properties, the Sh may be far removed from the isothermal value of 2 for pure molecular diffusion.

APPENDIX 7

THERMAL DIFFUSION FACTOR, α

A method for calculation of the thermal diffusion coefficient or factor of binary gas mixtures is given by Hirschfelder et al[101]. The equation stems from the kinetic theory treatment and it is used here. The calculation is lengthy but is explained very clearly in Chapter 8[101].

The original derivation includes a slight dependence upon composition of the gas.

$$\alpha = \frac{(S^{(1)} \cdot xH_2 - S^{(2)} \cdot xH_2S)}{X_\lambda + Y_\lambda} \cdot \frac{6C^*_{H2-H2S} - 5}{6\lambda_{H2-H2S}}$$

The terms X, Y, λ, and C* are defined and evaluated according to Hirschfelder. For most gas pairs, the terms $S^{(1)}$ and $S^{(2)}$ are opposite in sign and of the same order of magnitude. This is true for H_2-H_2S mixtures, and so the term in brackets shows negligible variation and gives values of α which are constant over the range of concentrations used in this study.

Evaluation of α for H_2 - H_2S at 1500, 1600 and 1750°C showed that the effect of temperature changes over this narrow range was negligible. One value is sufficient for the whole range.

$$\alpha = 0.71$$

An estimate of the reliability of this method of calculation was obtained by comparison with a known rare value. Vlasov et al[102] measured the thermal diffusion factor for a mean mixture of 90% H_2 and 10% H_2S in a two bulb experiment at atmosphere pressure. The temperatures of the hot and cold bulbs were respectively 293°K and 195°K. Their measurements gave α = 0.33. Calculation by the method of reference 101 for the same mixture at a mean temperature of 244°K gave α = 0.35.

TABLE 1

OXYGEN REMOVAL FROM LEVITATED DROPS

Specimens of Armco iron were held at approximately 1600 °C with a gas flowrate of approximately 2 litres per minute.

	OXYGEN CONTENT p.p.m.
Specimen not levitated.	665
Melt in helium, immediately quench.	549
Melt in helium, immediately quench in H_2.	7
Melt in helium, hold in H_2 for 1 min.	9
Melt in helium, hold in H_2 for 2 min.	6
Melt in helium, hold in H_2 for 3 min.	1
Melt in helium, hold in H_2 for 4 min.	1
Melt in helium, hold in H_2 for 5 min.	2
Melt in helium, hold in H_2 for 7.5 min.	0
Melt in helium, hold in H_2 for 10 min.	0

N.B. The lowest six values of oxygen content are as-read from the oxygen analyser. They are inside the error band about the zero-setting of the analysing instrument.

TABLE 2

SULPHURISATION IN H2-H2S

SPECIMEN TEMPERATURE = 1600 CENTIGRADE

*VOLUMETRIC FLOWRATE = 2680 ML. PER MINUTE

**GAS COMPOSITION = .00186

ATMOSPHERIC PRESSURE = 758.1 M.M.MERCURY

WEIGHT OF SPECIMEN = .9722 GRAMS

TIME MINUTES	SULPHUR WT.PERCENT
0.0	0.000
.5	.108
.5	.106
1.0	.183
1.5	.246
2.0	.285
2.5	.338
3.0	.369
3.5	.404
4.0	.428
5.0	.459
7.0	.514
10.0	.550
15.0	.563
20.0	.569
25.0	.563
30.0	.558
35.0	.563
40.0	.561
45.0	.541
50.0	.559

MASS TRANSFER COEFFICIENT = 38.85 CM.PER SECOND

VALUE OF THE CONSTANT B = 24.01 CM.PER SECOND

*Wherever volumetric flowrates are quoted they are the as-measured values at room temperature and pressure.

**Wherever gas compositions are quoted they are as the ratio $\frac{PH_2S}{PH_2}$

TABLE 3

SULPHURISATION IN H2-H2S

SPECIMEN TEMPERATURE = 1600 CENTIGRADE
VOLUMETRIC FLOWRATE = 2680 ML. PER MINUTE
GAS COMPOSITION = .00250
ATMOSPHERIC PRESSURE = 758.2 M.M.MERCURY
WEIGHT OF SPECIMEN = .9697 GRAMS

TIME MINUTES	SULPHUR WT.PERCENT
0.0	0.000
.5	.138
1.0	.201
1.5	.346
2.0	.392
2.5	.461
3.0	.529
4.0	.595
5.0	.634
7.0	.710
10.0	.732
15.0	.768
20.0	.766
25.0	.761
30.0	.771
35.0	.777
40.0	.766
45.0	.777
50.0	.770

MASS TRANSFER COEFFICIENT = 39.59 CM.PER SECCND
VALUE OF THE CONSTANT B = 23.63 CM.PER SECOND

TABLE 4

SULPHURISATION IN H2-H2S

SPECIMEN TEMPERATURE = 1600 CENTIGRADE
VOLUMETRIC FLOWRATE = 2680 ML. PER MINUTE
GAS COMPOSITION = .00361
ATMOSPHERIC PRESSURE = 762.9 M.M.MERCURY
WEIGHT OF SPECIMEN = .9663 GRAMS

TIME MINUTES	SULPHUR WT.PERCENT
0.0	0.000
.5	.243
1.0	.388
1.5	.500
2.0	.606
2.5	.658
3.0	.735
4.0	.840
5.0	.910
6.0	.951
7.0	1.01
8.0	1.06
10.0	1.09
12.0	1.10
14.0	1.10
16.0	1.12
18.0	1.13
20.0	1.12
20.0	1.12
25.0	1.13
30.0	1.11
35.0	1.11
40.0	1.14
45.0	1.10

MASS TRANSFER COEFFICIENT = 40.34 CM.PER SECOND
VALUE OF THE CONSTANT B = 25.92 CM.PER SECOND

TABLE 5

SULPHURISATION IN H2-H2S

SPECIMEN TEMPERATURE = 1600 CENTIGRADE
VOLUMETRIC FLOWRATE = 2680 ML. PER MINUTE
GAS COMPOSITION = .00399
ATMOSPHERIC PRESSURE = 760.0 M.M.MERCURY
WEIGHT OF SPECIMEN = .9389 GRAMS

TIME MINUTES	SULPHUR WT.PERCENT
0.0	0.000
.3	.088
.3	.223
.5	.215
2.0	.655
3.0	.847
4.0	.972
6.0	1.13
8.0	1.23
10.0	1.24
12.5	1.25
15.0	1.24
15.0	1.27
17.5	1.26
20.0	1.26
20.0	1.27
30.0	1.28
30.0	1.26
40.0	1.26
40.0	1.27

MASS TRANSFER COEFFICIENT = 40.44 CM.PER SECOND
VALUE OF THE CONSTANT B = 24.09 CM.PER SECOND

TABLE 6

SULPHURISATION IN H2-H2S

SPECIMEN TEMPERATURE = 1600 CENTIGRADE.
VOLUMETRIC FLOWRATE = 2680 ML. PER MINUTE
GAS COMPOSITION = .00429
ATMOSPHERIC PRESSURE = 760.0 M.M.MERCURY
WEIGHT OF SPECIMEN = .9687 GRAMS

TIME MINUTES	SULPHUR WT.PERCENT
0.0	0.000
1.5	.606
2.5	.936
3.3	.945
5.0	1.17
7.0	1.20
8.0	1.37
10.0	1.20
12.0	1.34
15.0	1.35
17.0	1.36
18.0	1.39
20.0	1.40
20.0	1.37
20.0	1.40
25.0	1.42
30.0	1.39
35.0	1.38
40.0	1.39

MASS TRANSFER COEFFICIENT = 42.52 CM.PER SECOND
VALUE OF THE CONSTANT B = 25.27 CM.PER SECOND

TABLE 7

SULPHURISATION IN H2-H2S

SPECIMEN TEMPERATURE = 1600 CENTIGRADE
VOLUMETRIC FLOWRATE = 2680 ML. PER MINUTE
GAS COMPOSITION = .00532
ATMOSPHERIC PRESSURE = 757.1 M.M.MERCURY
WEIGHT OF SPECIMEN = .9489 GRAMS

TIME MINUTES	SULPHUR WT.PERCENT
0.0	0.000
.5	.278
1.0	.555
1.5	.766
2.0	.879
3.0	1.14
4.0	1.29
5.0	1.42
6.0	1.52
8.0	1.65
10.0	1.65
12.0	1.76
15.0	1.75
18.0	1.74
20.0	1.77
20.0	1.77
25.0	1.73
30.0	1.78
35.0	1.77
40.0	1.78

MASS TRANSFER COEFFICIENT = 41.25 CM.PER SECOND
VALUE OF THE CONSTANT B = 23.74 CM.PER SECOND

TABLE 8

SULPHURISATION IN H2-H2S

SPECIMEN TEMPERATURE = 1600 CENTIGRADE
VOLUMETRIC FLOWRATE = 2680 ML. PER MINUTE
GAS COMPOSITION = .00572
ATMOSPHERIC PRESSURE = 758.8 M.M.MERCURY
WEIGHT OF SPECIMEN = .9786 GRAMS

TIME MINUTES	SULPHUR WT.PERCENT
0.0	0.000
.5	.305
1.0	.552
1.5	.731
2.0	.933
2.5	1.05
3.0	1.22
3.5	1.39
4.0	1.46
5.0	1.61
7.0	1.76
10.0	1.85
15.0	1.91
20.0	1.94
25.0	1.94
30.0	1.87
35.0	1.95
40.0	1.94
45.0	1.94
50.0	1.95

MASS TRANSFER COEFFICIENT = 41.41 CM.PER SECOND
VALUE OF THE CONSTANT B = 22.75 CM.PER SECOND

SULPHURISATION IN H2-H2S

SPECIMEN TEMPERATURE = 1600 CENTIGRADE

VOLUMETRIC FLOWRATE = 2680 ML. PER MINUTE

GAS COMPOSITION = .00644

ATMOSPHERIC PRESSURE = 762.0 M.M.MERCURY

WEIGHT OF SPECIMEN = .9400 GRAMS

TIME MINUTES	SULPHUR WT.PERCENT
0.0	0.000
.5	.474
1.0	.720
1.5	.861
2.0	1.04
2.1	1.17
2.2	1.19
2.4	1.25
2.5	1.26
3.0	1.38
4.0	1.61
4.4	1.66
5.0	1.76
5.0	1.73
6.0	1.94
7.0	1.94
8.0	2.04
10.0	2.14
10.0	2.10
12.0	2.14
13.5	2.30
16.0	2.19
20.0	2.21
20.0	2.27
25.0	2.33
30.0	2.24
35.0	2.21
40.0	2.24
50.0	2.23

MASS TRANSFER COEFFICIENT = 41.06 CM.PER SECOND

VALUE OF THE CONSTANT B = 22.01 CM.PER SECOND

TABLE 10

SULPHURISATION IN H2-H2S

SPECIMEN TEMPERATURE = 1600 CENTIGRADE
VOLUMETRIC FLOWRATE = 2680 ML. PER MINUTE
GAS COMPOSITION = .00747
ATMOSPHERIC PRESSURE = 758.8 M.M.MERCURY
WEIGHT OF SPECIMEN = .9896 GRAMS

TIME MINUTES	SULPHUR WT.PERCENT	INDIVIDUAL WEIGHTS - GRAMS
0.0	0.000	
.5	.479	0.9890
1.0	.746	0.9850
1.5	.970	0.9815
2.0	1.20	0.9878
2.5	1.38	0.9876
3.0	1.56	0.9865
4.0	1.76	0.9923
5.0	2.05	0.9942
7.0	2.26	0.9932
10.0	2.48	1.0014
15.0	2.53	0.9919
20.0	2.62	0.9997
25.0	2.66	0.9953
30.0	2.66	0.9867
35.0	2.70	0.9914
40.0	2.61	0.9789
45.0	2.73	0.9882
50.0	2.56	0.9846

MASS TRANSFER COEFFICIENT = 39.07 CM.PER SECOND
VALUE OF THE CONSTANT B = 21.70 CM.PER SECOND

TABLE 11

SULPHURISATION IN H2-H2S

SPECIMEN TEMPERATURE = 1600 CENTIGRADE
VOLUMETRIC FLOWRATE = 900 ML. PER MINUTE
GAS COMPOSITION = .00156
ATMOSPHERIC PRESSURE = 748.0 M.M.MERCURY
WEIGHT OF SPECIMEN =1.2203 GRAMS

TIME MINUTES	SULPHUR WT.PERCENT
0.0	0.000
.5	.034
1.0	.078
2.0	.136
3.0	.194
4.0	.239
5.0	.278
6.0	.301
8.0	.345
10.0	.352
12.5	.394
15.0	.424
17.5	.419
20.0	.429
25.0	.433
30.0	.432

MASS TRANSFER COEFFICIENT = 20.72 CM.PER SECOND
VALUE OF THE CONSTANT B = 16.10 CM.PER SECOND

TABLE 12

SULPHURISATION IN H2-H2S

SPECIMEN TEMPERATURE = 1600 CENTIGRADE
VOLUMETRIC FLOWRATE = 900 ML. PER MINUTE
GAS COMPOSITION = .00215
ATMOSPHERIC PRESSURE = 756.6 M.M.MERCURY
WEIGHT OF SPECIMEN = .9705 GRAMS

TIME MINUTES	SULPHUR WT.PERCENT
0.0	0.000
.5	.056
.5	.059
1.0	.114
1.5	.173
2.0	.223
2.5	.256
3.0	.298
3.5	.330
4.0	.362
5.0	.409
7.0	.478
10.0	.537
15.0	.563
20.0	.577
25.0	.593
30.0	.593
35.0	.590
40.0	.585
45.0	.584
50.0	.581

MASS TRANSFER COEFFICIENT = 22.51 CM.PER SECOND
VALUE OF THE CONSTANT B = 19.31 CM.PER SECOND

TABLE 13

SULPHURISATION IN H2-H2S

SPECIMEN TEMPERATURE = 1600 CENTIGRADE
VOLUMETRIC FLOWRATE = 900 ML. PER MINUTE
GAS COMPOSITION = .00496
ATMOSPHERIC PRESSURE = 752.5 M.M.MERCURY
WEIGHT OF SPECIMEN = .9731 GRAMS

TIME MINUTES	SULPHUR WT.PERCENT
0.0	0.000
.5	.145
1.0	.292
1.5	.416
2.0	.546
2.5	.668
3.0	.674
5.0	.936
7.0	.890
10.0	1.17
15.0	1.33
20.0	1.39
20.0	1.41
25.0	1.47
30.0	1.45
40.0	1.42
45.0	1.43
50.0	1.43

MASS TRANSFER COEFFICIENT = 21.02 CM.PER SECOND
VALUE OF THE CONSTANT B = 18.30 CM.PER SECOND

TABLE 14

SULPHURISATION IN H2-H2S

SPECIMEN TEMPERATURE = 1600 CENTIGRADE
VOLUMETRIC FLOWRATE = 5070 ML. PER MINUTE
GAS COMPOSITION = .00186
ATMOSPHERIC PRESSURE = 758.9 M.M.MERCURY
WEIGHT OF SPECIMEN = .9710 GRAMS

TIME MINUTES	SULPHUR WT.PERCENT
0.0	0.000
.5	.113
.5	.111
1.0	.199
1.5	.264
2.0	.314
2.5	.355
3.0	.387
3.5	.418
4.0	.436
5.0	.478
7.0	.515
10.0	.529
15.0	.539
20.0	.539
25.0	.531
30.0	.536
35.0	.535
40.0	.542
45.0	.543
50.0	.541

MASS TRANSFER COEFFICIENT = 44.21 CM.PER SECOND
VALUE OF THE CONSTANT B = 31.32 CM.PER SECOND

TABLE 15

SULPHURISATION IN H2-H2S

SPECIMEN TEMPERATURE = 1600 CENTIGRADE
VOLUMETRIC FLOWRATE = 5070 ML. PER MINUTE
GAS COMPOSITION = .00572
ATMOSPHERIC PRESSURE = 758.8 M.M.MERCURY
WEIGHT OF SPECIMEN = .9818 GRAMS

TIME MINUTES	SULPHUR WT.PERCENT
0.0	0.000
.5	.509
1.0	.705
1.5	.888
2.0	1.01
2.5	1.14
3.0	1.33
3.5	1.41
4.0	1.48
5.0	1.55
7.0	1.67
10.0	1.85
15.0	1.88
20.0	1.89
25.0	1.89
30.0	1.91
35.0	1.86
40.0	1.89
45.0	1.91
50.0	1.89

MASS TRANSFER COEFFICIENT = 47.96 CM.PER SECOND
VALUE OF THE CONSTANT B = 29.34 CM.PER SECOND

TABLE 16

SULPHURISATION IN H2-H2S

SPECIMEN TEMPERATURE = 1600 CENTIGRADE
VOLUMETRIC FLOWRATE = 5070 ML. PER MINUTE
GAS COMPOSITION = .00639
ATMOSPHERIC PRESSURE = 757.7 M.M.MERCURY
WEIGHT OF SPECIMEN = .9732 GRAMS

TIME MINUTES	SULPHUR WT.PERCENT
0.0	0.000
.5	.378
1.0	.745
1.5	.955
2.0	1.14
2.5	1.33
3.0	1.46
4.0	1.62
5.0	1.71
7.0	1.91
10.0	2.02
15.0	2.15
20.0	2.08
20.0	2.15
25.0	2.15
30.0	2.08
35.0	2.14
40.0	2.05
45.0	1.98
50.0	2.08

MASS TRANSFER COEFFICIENT = 47.06 CM.PER SECOND
VALUE OF THE CONSTANT B = 30.91 CM.PER SECOND

TABLE 17

SULPHURISATION IN H2-H2S

SPECIMEN TEMPERATURE = 1500 CENTIGRADE
VOLUMETRIC FLOWRATE = 900 ML. PER MINUTE
GAS COMPOSITION = .00250
ATMOSPHERIC PRESSURE = 759.7 M.M.MERCURY
WEIGHT OF SPECIMEN = .9754 GRAMS

TIME MINUTES	SULPHUR WT.PERCENT
0.0	0.000
.5	.081
1.0	.121
1.5	.189
2.0	.237
2.5	.290
3.0	.355
4.0	.433
5.0	.493
7.0	.641
10.0	.677
15.0	.779
20.0	.817
25.0	.853
26.0	.838
30.0	.832
35.0	.844
40.0	.857
45.0	.855
45.0	.867
50.0	.846

MASS TRANSFER COEFFICIENT = 19.91 CM.PER SECOND
VALUE OF THE CONSTANT B = 14.91 CM.PER SECOND

TABLE 13

SULPHURISATION IN H2-H2S

SPECIMEN TEMPERATURE = 1500 CENTIGRADE

VOLUMETRIC FLOWRATE = 900 ML. PER MINUTE

GAS COMPOSITION = .00654

ATMOSPHERIC PRESSURE = 758.7 M.M.MERCURY

WEIGHT OF SPECIMEN = .9513 GRAMS

TIME MINUTES	SULPHUR WT.PERCENT
0.0	0.000
.5	.218
1.0	.404
1.5	.559
2.0	.707
2.0	.720
2.5	.826
3.0	.963
4.0	1.28
5.0	1.35
5.0	1.44
6.0	1.51
7.0	1.55
8.0	1.76
9.0	1.88
10.0	1.98
11.0	1.96
12.0	2.04
14.0	2.13
16.0	2.20
18.0	2.30
20.0	2.30
20.0	2.24
25.0	2.38
30.0	2.41
35.0	2.43
41.0	2.39
45.0	2.45
50.0	2.42

MASS TRANSFER COEFFICIENT = 21.48 CM.PER SECOND

VALUE OF THE CONSTANT B = 13.34 CM.PER SECOND

TABLE 19

SULPHURISATION IN H2-H2S

SPECIMEN TEMPERATURE = 1500 CENTIGRADE
VOLUMETRIC FLOWRATE = 2680 ML. PER MINUTE
GAS COMPOSITION = .00015
ATMOSPHERIC PRESSURE = 754.7 M.M.MERCURY
WEIGHT OF SPECIMEN = .9688 GRAMS

TIME MINUTES	SULPHUR WT.PERCENT
0.0	0.000
.5	.007
1.0	.016
1.5	.022
2.0	.027
2.5	.030
3.0	.033
3.5	.035
4.0	.039
7.0	.045
10.0	.046
15.0	.048
25.0	.050
35.0	.049
40.0	.050
45.0	.050
50.0	.050

MASS TRANSFER COEFFICIENT = 40.94 CM.PER SECOND
VALUE OF THE CONSTANT B = 28.85 CM.PER SECOND

TABLE 20

SULPHURISATION IN H2-H2S

SPECIMEN TEMPERATURE = 1500 CENTIGRADE
VOLUMETRIC FLOWRATE = 2680 ML. PER MINUTE
GAS COMPOSITION = .00186
ATMOSPHERIC PRESSURE = 756.6 M.M.MERCURY
WEIGHT OF SPECIMEN = .9687 GRAMS

TIME MINUTES	SULPHUR WT.PERCENT
0.0	0.000
.5	.123
1.0	.194
1.5	.285
1.5	.260
2.0	.327
2.5	.366
3.0	.412
3.5	.449
4.0	.470
5.0	.516
7.0	.561
10.0	.616
11.5	.637
15.0	.626
20.0	.651
25.0	.654
30.0	.648
35.0	.655
40.0	.649
45.0	.652
50.0	.672

MASS TRANSFER COEFFICIENT = 39.47 CM.PER SECOND
VALUE OF THE CONSTANT B = 24.28 CM.PER SECOND

TABLE 21

SULPHURISATION IN H2-H2S

SPECIMEN TEMPERATURE = 1500 CENTIGRADE
VOLUMETRIC FLOWRATE = 5070 ML. PER MINUTE
GAS COMPOSITION = .00219
ATMOSPHERIC PRESSURE = 759.7 M.M.MERCURY
WEIGHT OF SPECIMEN = .9773 GRAMS

TIME MINUTES	SULPHUR WT.PERCENT
0.0	0.000
.5	.194
1.0	.298
1.5	.380
2.0	.444
2.5	.500
3.0	.530
4.0	.606
4.5	.610
5.0	.664
6.0	.673
7.0	.705
10.0	.768
15.0	.780
20.0	.782
25.0	.760
30.0	.781
35.0	.787
40.0	.771
45.0	.781
50.0	.785

MASS TRANSFER COEFFICIENT = 48.57 CM.PER SECOND
VALUE OF THE CONSTANT B = 31.82 CM.PER SECOND

TABLE 22

SULPHURISATION IN H2-H2S

SPECIMEN TEMPERATURE = 1500 CENTIGRADE
VOLUMETRIC FLOWRATE = 5070 NL. PER MINUTE
GAS COMPOSITION = .00639
ATMOSPHERIC PRESSURE = 759.1 M.M.MERCURY
WEIGHT OF SPECIMEN = .9935 GRAMS

TIME MINUTES	SULPHUR WT.PERCENT
0.0	0.000
.5	.362
1.0	.820
1.5	1.07
2.0	1.18
2.5	1.38
3.0	1.45
4.0	1.70
5.0	1.80
7.0	2.05
10.0	2.30
15.0	2.41
20.0	2.42
25.0	2.37
30.0	2.39
35.0	2.43
40.0	2.49
45.0	2.41
50.0	2.41

MASS TRANSFER COEFFICIENT = 43.39 CM.PER SECOND
VALUE OF THE CONSTANT B = 32.54 CM.PER SECOND

TABLE 23

SULPHURISATION IN H2-H2S

SPECIMEN TEMPERATURE = 1750 CENTIGRADE
VOLUMETRIC FLOWRATE = 900 ML. PER MINUTE
GAS COMPOSITION = .00148
ATMOSPHERIC PRESSURE = 753.9 M.M.MERCURY
WEIGHT OF SPECIMEN =1.1993 GRAMS

TIME MINUTES	SULPHUR WT.PERCENT
0.0	0.000
.5	.029
1.0	.066
2.0	.121
3.0	.184
4.0	.222
5.0	.255
6.0	.293
8.0	.328
10.0	.345
12.5	.363
15.0	.380

MASS TRANSFER COEFFICIENT = 21.90 CM.PER SECOND

TABLE 24

SULPHURISATION IN H2-H2S

SPECIMEN TEMPERATURE = 1750 CENTIGRADE
VOLUMETRIC FLOWRATE = 900 ML. PER MINUTE
GAS COMPOSITION = .00895
ATMOSPHERIC PRESSURE = 749.8 M.M.MERCURY
WEIGHT OF SPECIMEN =1.1381 GRAMS

TIME MINUTES	SULPHUR WT.PERCENT
0.0	0.000
.5	.167
1.0	.440
2.0	.864
3.0	1.18
4.0	1.40
5.0	1.62
6.0	1.89
8.0	2.18
10.0	2.44
12.5	2.54
15.0	2.62
17.5	2.75
20.0	2.69
25.0	2.70
30.0	2.69
40.0	2.80
50.0	2.90

MASS TRANSFER COEFFICIENT = 24.23 CM.PER SECOND

TABLE 25

SULPHURISATION IN H2-H2S

SPECIMEN TEMPERATURE = 1750 CENTIGRADE
VOLUMETRIC FLOWRATE = 2680 ML. PER MINUTE
GAS COMPOSITION = .00241
ATMOSPHERIC PRESSURE = 759.8 M.M.MERCURY
WEIGHT OF SPECIMEN = .9621 GRAMS

TIME MINUTES	SULPHUR WT.PERCENT
0.0	0.000
.5	.131
1.0	.232
1.5	.311
2.0	.369
2.5	.431
3.0	.469
4.0	.529
5.0	.583
7.0	.631
10.0	.655
15.0	.662
20.0	.670
25.0	.671
30.0	.666
35.0	.670
40.0	.670
45.0	.661
50.0	.663

MASS TRANSFER COEFFICIENT = 42.55 CM.PER SECOND

TABLE 26

SULPHURISATION IN H2-H2S

SPECIMEN TEMPERATURE = 1750 CENTIGRADE
VOLUMETRIC FLOWRATE = 2680 ML. PER MINUTE
GAS COMPOSITION = .00747
ATMOSPHERIC PRESSURE = 756.7 M.M.MERCURY
WEIGHT OF SPECIMEN = .9731 GRAMS

TIME MINUTES	SULPHUR WT.PERCENT
0.0	0.000
.5	.364
1.0	.705
1.5	.974
2.0	1.18
2.5	1.36
3.0	1.51
4.0	1.71
5.0	1.83
7.0	2.08
10.0	2.20
15.0	2.34
20.0	2.26
25.0	2.31
30.0	2.24
35.0	2.31
40.0	2.29
45.0	2.33
50.0	2.27

MASS TRANSFER COEFFICIENT = 42.72 CM.PER SECOND

TABLE 27

SULPHURISATION IN H2-H2S

SPECIMEN TEMPERATURE = 1750 CENTIGRADE
VOLUMETRIC FLOWRATE = 5070 ML. PER MINUTE
GAS COMPOSITION = .00747
ATMOSPHERIC PRESSURE = 758.6 M.M.MERCURY
WEIGHT OF SPECIMEN = .9912 GRAMS

TIME MINUTES	SULPHUR WT.PERCENT
0.0	0.000
.3	.301
.8	.752
1.3	1.02
1.8	1.26
2.3	1.39
3.0	1.53
4.0	1.74
5.0	1.88
7.0	2.03
10.0	2.22
15.0	2.20
20.0	2.16
25.0	2.27
30.0	2.23
33.2	2.23
35.0	2.27
45.0	2.22
50.0	2.22

MASS TRANSFER COEFFICIENT = 49.94 CM.PER SECOND

TABLE 28

SULPHURISATION IN H2-H2S

SPECIMEN TEMPERATURE = 1675 CENTIGRADE
VOLUMETRIC FLOWRATE = 2680 ML. PER MINUTE
GAS COMPOSITION = .00523
ATMOSPHERIC PRESSURE = 759.0 M.M.MERCURY
WEIGHT OF SPECIMEN = .9770 GRAMS

TIME MINUTES	SULPHUR WT.PERCENT
0.0	0.000
.5	.262
.5	.275
1.0	.571
1.5	.649
2.0	.812
2.5	.943
3.0	1.04
5.0	1.34
7.0	1.52
10.0	1.65
15.0	1.58
20.0	1.60
25.0	1.60
30.0	1.55
35.0	1.58
40.0	1.56
50.0	1.60

MASS TRANSFER COEFFICIENT = 42.02 CM.PER SECOND

DESULPHURISATION WITH PURE HYDROGEN

SPECIMEN TEMPERATURE = 1600° CENTIGRADE AT ALL TIMES

TABLE 29

FLOWRATE = 900 ML. PER MINUTE

WEIGHT = 0.9731 GRAMS

TIME MINUTES	SULPHUR WT.PERCENT
0.	1.40
2.	1.02
3.	0.756
4.	0.578
6.	0.390
8.	0.245
10.	0.143
12.	0.087
14.	0.064
17.	0.016
20.	0.007
25.	< 0.005

TABLE 30

FLOWRATE = 2,680 ML. PER MINUTE

WEIGHT = 0.9489 GRAMS

TIME MINUTES	SULPHUR WT.PERCENT
0.	1.76
2.	0.821
3.	0.615
4.	0.376
5.	0.231
6.	0.196
8.	0.062
10.	0.027
12.5	0.013
15.	0.006
17.5	< 0.005
20.	< 0.005

TABLE 31

FLOWRATE = 5,070 ML. PER MINUTE

WEIGHT = 0.9732 GRAMS

TIME MINUTES	SULPHUR WT.PERCENT
0.	2.09
2.	0.908
3.	0.573
4.	0.359
5.	0.206
6.	0.135
7.	0.078
8.	0.050
9.	0.030
10.	0.018
12.	0.008
15.	<0.005

TABLE 32

DESULPHURISATION WITH INERT GASES

SPECIMEN TEMPERATURE = 1600° CENTIGRADE

VOLUMETRIC FLOWRATE = 2,960 ML. PER MINUTE

GAS COMPOSITION - PURE HELIUM

WEIGHT OF SPECIMEN = 0.8864 GRAMS

TIME MINUTES	SULPHUR WT.PERCENT
0.	2.23
5.	2.22
10.	2.04
12.5	2.08
15.	1.83
17.5	1.98
20.	1.90
22.5	1.93
25.	1.78
27.5	1.81
30.	1.81
30.	1.75
35.	1.71
40.	1.71
50.	1.55

TABLE 33

DESULPHURISATION WITH INERT GASES

SPECIMEN TEMPERATURE = 1600° CENTIGRADE

VOLUMETRIC FLOWRATE = 3,340 ML. PER MINUTE

GAS COMPOSITION a) PURE HELIUM
b) HELIUM - HYDROGEN
c) PURE HYDROGEN

WEIGHT OF SPECIMEN = 1.0966 GRAMS

TIME MINUTES	SULPHUR WT.PERCENT
PURE HELIUM	
0.	1.47
10.	1.42
20.	1.38
30.	1.31
40.	1.28
50.	1.16
60.	1.10
94% HELIUM - 6% HYDROGEN	
0.	1.47
3.	1.36
5.	1.28
7.	1.26
10.	1.17
12.	1.08
15.	0.977
20.	0.868
25.	0.748
PURE HYDROGEN	
0.	1.47
2.	0.755
3.	0.457
4.	0.313
6.	0.126
8.	0.019
10.	0.009
12.	< 0.005
15.	< 0.005

TABLE 34

DESULPHURISATION WITH INERT GASES.

SPECIMEN TEMPERATURE = 1600° CENTIGRADE

VOLUMETRIC FLOWRATE = 18,900 ML. PER MINUTE

GAS COMPOSITION a) PURE NITROGEN

b) NITROGEN - HYDROGEN

WEIGHT OF SPECIMEN = 1.0353 GRAMS

TIME MINUTES	SULPHUR WT. PERCENT
PURE NITROGEN	
0.	1.88
15.	1.80
25.	1.71
35.	1.70
45.	1.58
55.	1.50
65.	1.37
92% NITROGEN - 8% HYDROGEN	
0.	1.88
3.	1.79
5.	1.70
10.	1.61
14.	1.52
20.	1.39
25.	1.18
30.	1.07
40.	0.878
50.	0.611
60.	0.498

TABLE 35

GAS FLOW RATE cm^3 / minute	DROP TEMP. °C	RATIO $\frac{P_{H_2S} \times 10^3}{P_{H_2}}$	kg cm/sec	AVERAGE VALUE kg cm/sec	b cm/sec	AVERAGE VALUE b cm/sec
900	1500	2.50	19.92	20.7	14.91	16.1
900	1500	6.54	21.48		17.35	
900	1600	1.56	20.72		16.10	
900	1600	2.15	22.51	21.4	19.31	17.9
900	1600	4.96*	21.03		18.31	
900	1750	1.48	21.90	23.1		
900	1750	8.95	24.23			
2680	1500	0.15	40.94	40.2	28.85	26.6
2680	1500	1.86	39.47		24.29	
2680	1600	1.86	38.86		24.01	
2680	1600	2.50	39.60		23.64	
2680	1600	3.61	40.34		25.92	
2680	1600	3.99	40.44		24.10	
2680	1600	4.29	42.52	40.5	25.28	23.7
2680	1600	5.32*	41.26		23.75	
2680	1600	5.72	41.41		22.75	
2680	1600	6.44	41.07		22.01	
2680	1600	7.47	39.08		21.71	
2680	1675	5.23	42.02	42.0		
2680	1750	2.41	42.55	42.6		
2680	1750	7.47	42.73			
5070	1500	2.19	48.57	46.0	31.83	32.2
5070	1500	6.39	43.39		32.54	
5070	1600	1.86	44.21		31.32	
5070	1600	5.72	47.96	46.4	29.34	30.5
5070	1600	6.39*	47.07		30.91	
5070	1750	7.47	49.95	49.9		

SYNOPSIS OF EXPERIMENTAL RESULTS IN TABLES 2 TO 28.

TABLE 36

	TEMPERATURE °C	FLOW RATE cm^3 per min.		
		900	2680	5070
BY EXPERIMENT	1500	2.49	4.83	5.53
	1600	2.38	4.51	5.16
	1750	2.29	4.23	4.95
RANZ-MARSHALL APPROACH VELOCITY AT ROOM TEMP. NO WALL EFFECT	1500	2.68	3.17	3.59
	1600	2.66	3.13	3.55
	1750	2.62	3.07	3.48
RANZ-MARSHALL VELOCITY AT T_f + WALL EFFECT	1500	3.50	4.60	5.57
	1600	3.48	4.56	5.52
	1750	3.45	4.49	5.44
APPROACH VELOCITY AT ROOM TEMP. NO WALL EFFECT NATURAL CONVECTION	1500	3.56	3.96	4.34
	1600	3.53	3.89	4.24
	1750	3.47	3.81	4.14

COMPARISON OF MEASURED SHERWOOD NUMBERS WITH VALUES CALCULATED BY CORRELATIONS ON THREE DIFFERENT BASES.

TABLE 37

FLOW RATE cm^3 per min.	DROP TEMPERATURE	THERMAL DIFFUSION FACTOR
900	1500	0.61
2680	1500	0.48
5070	1500	0.54
900	1600	0.57
2680	1600	0.46
5070	1600	0.52
Theoretical value of α = 0.71		

VALUES OF THERMAL DIFFUSION FACTOR FOR BINARY GAS MIXTURE OF HYDROGEN - HYDROGEN SULPHIDE FOUND BY EXPERIMENT AT DROP TEMPERATURES OF 1500 AND 1600°C.

TABLE 38

DROP TEMPERATURE	GAS FLOWRATE $cm.^3$ per min.	K	Log K
1750	5070	0.00287	-2.54
1750	2680	0.00285	-2.55
1750	2680	0.00285	-2.55
1750	900	0.00261	-2.58
1750	900	0.00271	-2.57
1675	2680	0.00273	-2.56

Average value of K at 1750°C = 0.00278

Average Log K at 1750°C = -2.56

VALUES OF THE EQUILIBRIUM CONSTANT FOUND FROM SIX INDEPENDENT EXPERIMENTAL RATE CURVES AT 1675 AND 1750°C.

TABLE 39

CORRECTION OF EQUILIBRIA FOR IRON DROPS LEVITATED IN HYDROGEN - WATER VAPOUR GAS MIXTURES.

DATA OF LARCHE			CALCULATED BY PRESENT STUDY		
NUMBER OF SAMPLES	TEMPERATURE OF IRON DROP °C	LOG OF EQUILIBRIUM CONSTANT	kg_o cm. per s.	E cm. per s.	MEAN VALUE OF K_o
8	1550	0.821	16.1	13.0	4.59
8	1600	0.723	16.5	13.4	3.57
10	1650	0.591	16.8	13.8	2.62
9	1700	0.482	17.2	14.2	2.04
7	1750	0.396	17.6	14.7	1.67
42					

LARCHE'S EQUATION :- $\text{Log } K_o = \frac{7054}{T} - 3.16$

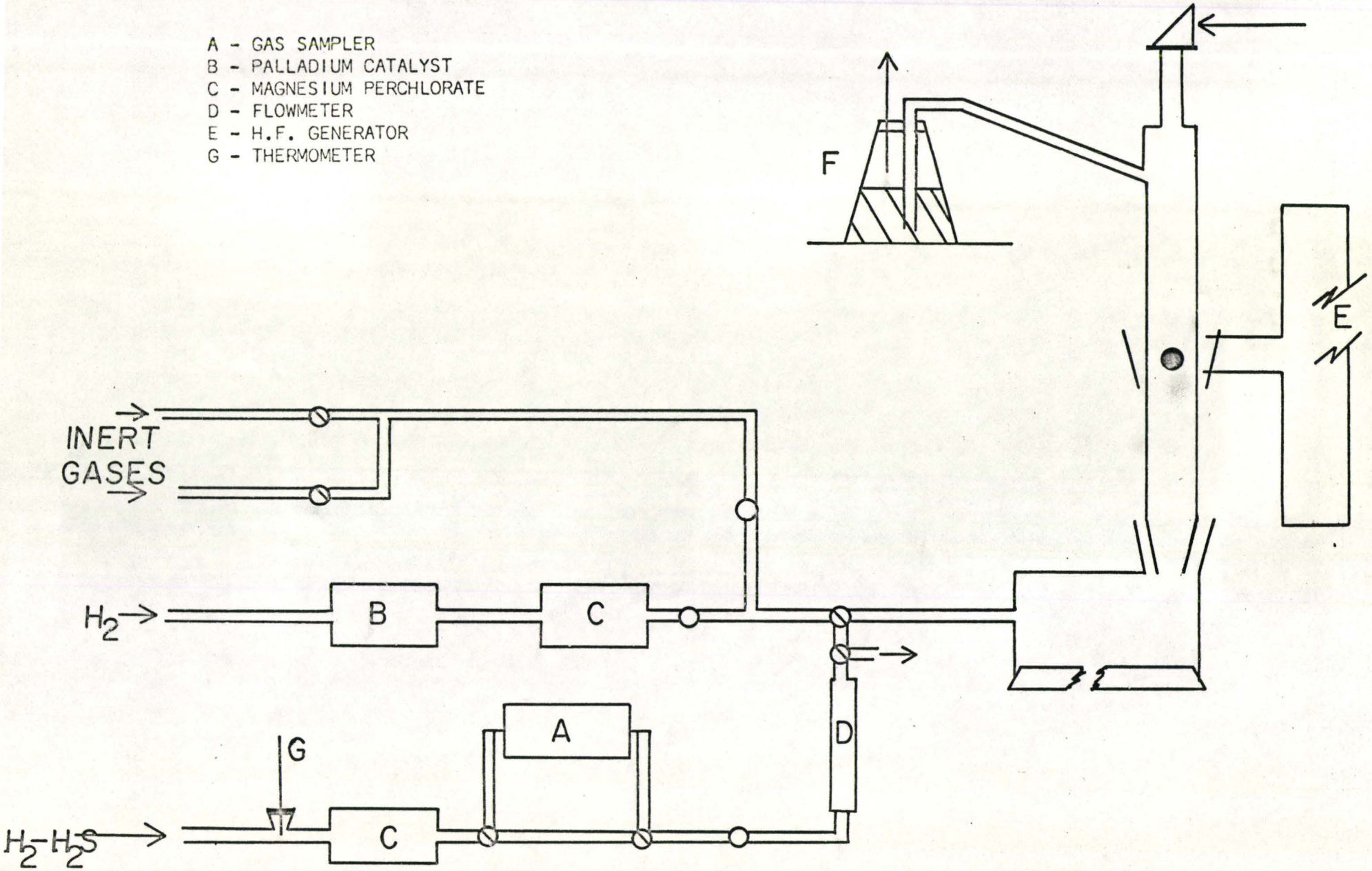

FIGURE 1 Schematic Illustration of the Overall Apparatus

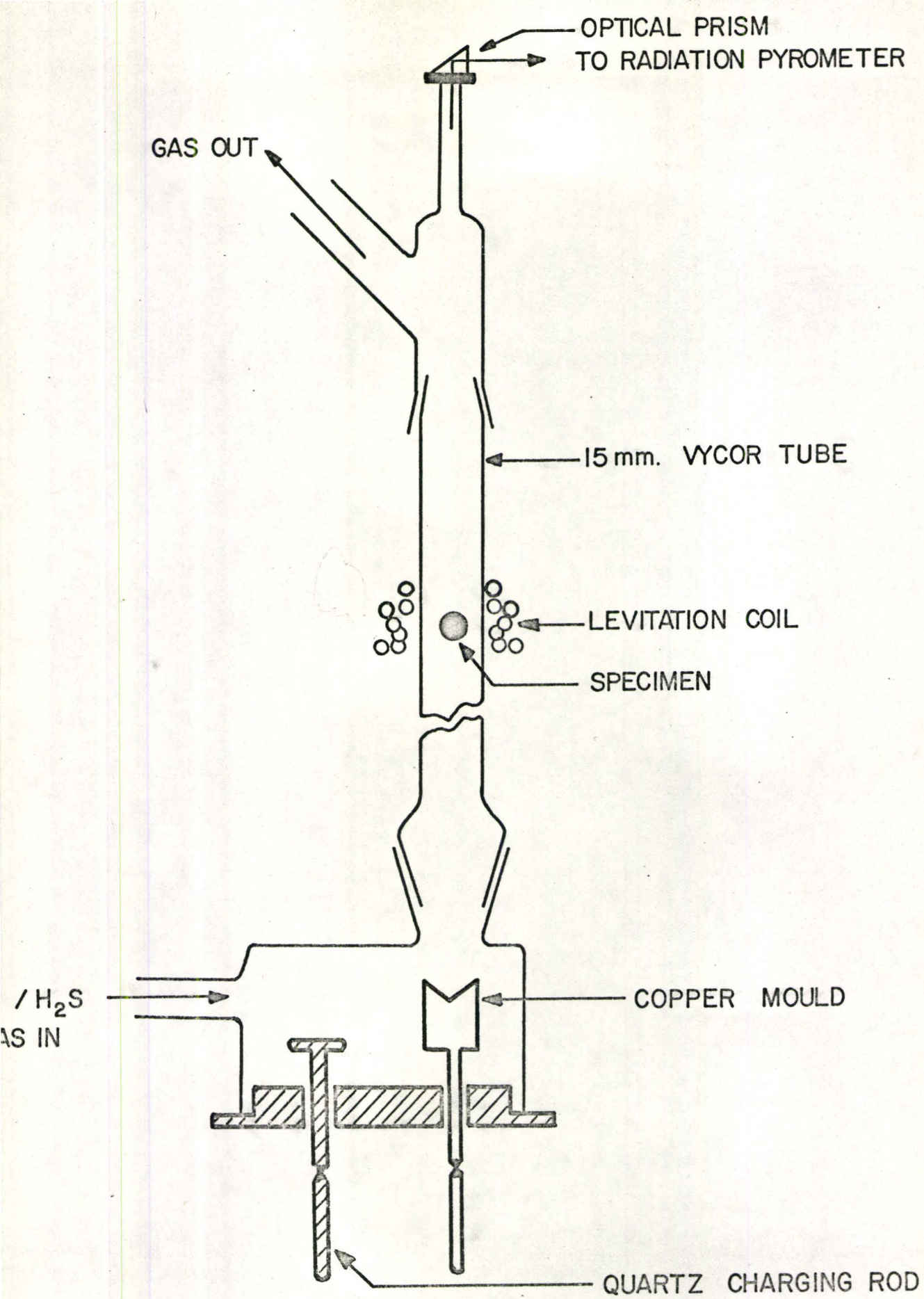

FIGURE 2 Diagram of the Levitation Tube and Charging Arrangement

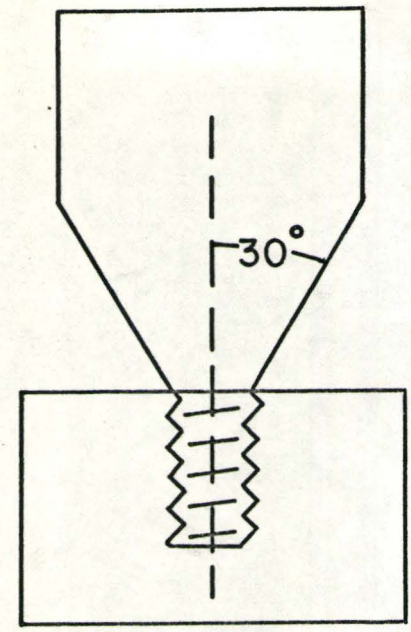

BRASS FORMER

SCHEMATIC COIL

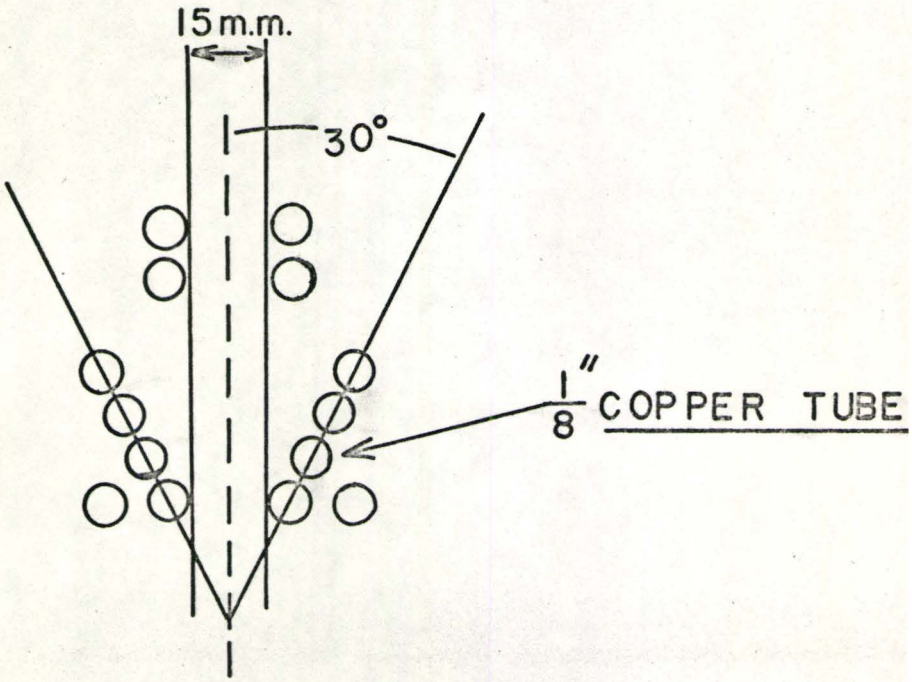

FIGURE 3 Cross-section of a Typical Levitation Coil and the Former on which it was wound

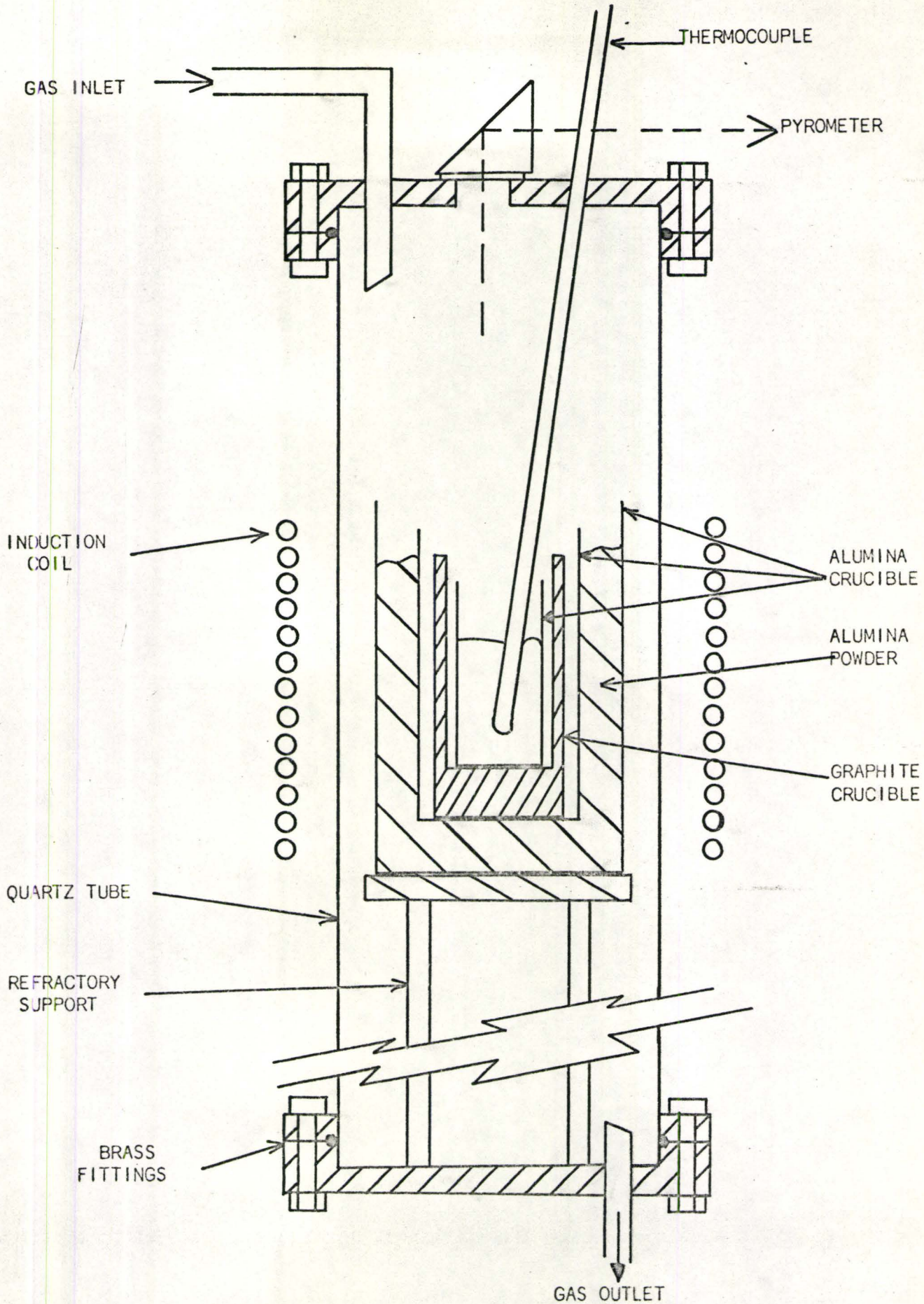

FIGURE 4 Apparatus for Calibration of Pyrometer on a Liquid Iron Melt

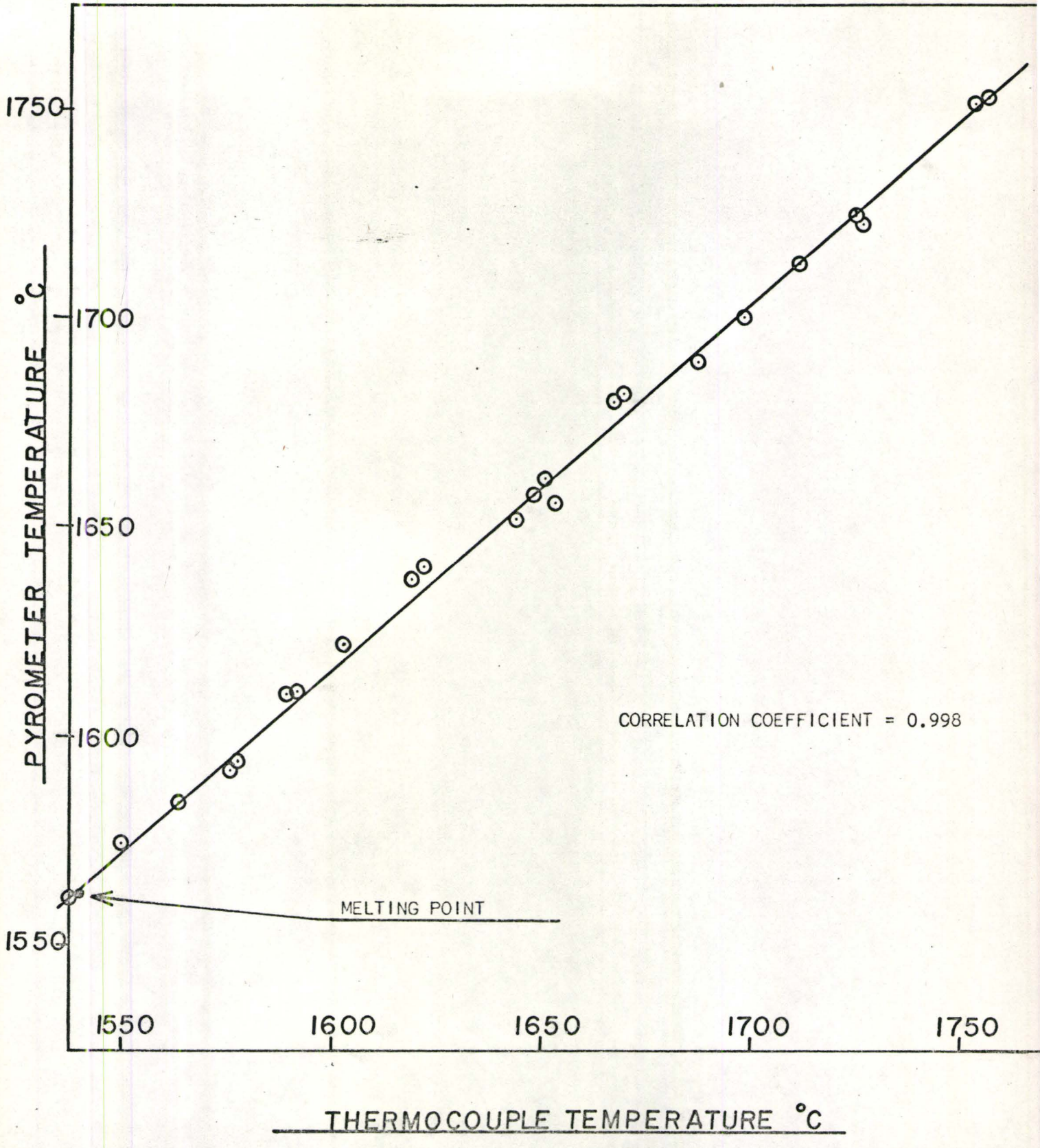

FIGURE 5 Calibration Curve for Pyrometer against Thermocouple

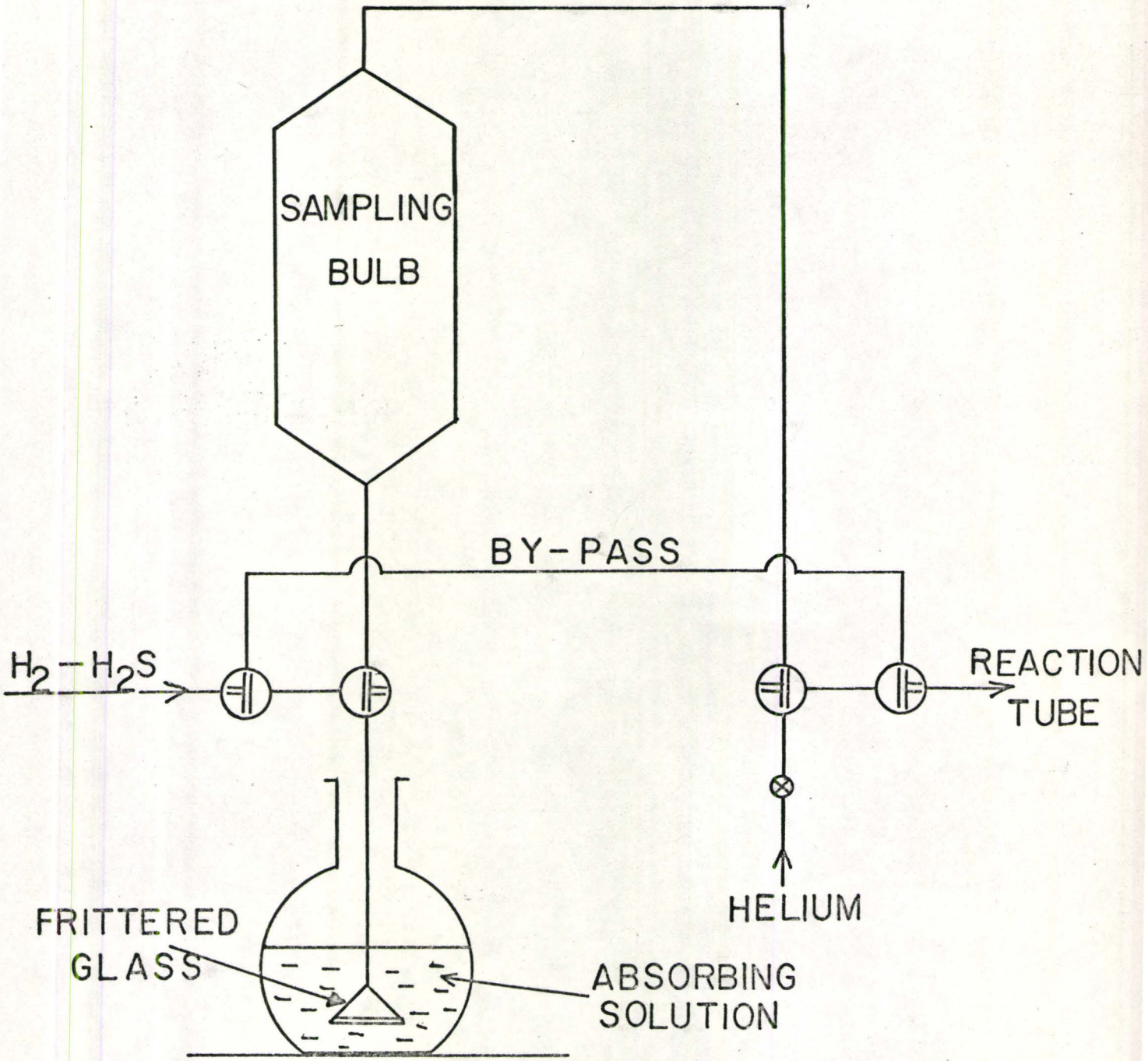

GAS SAMPLING ARRANGEMENT

FIGURE 6 Cross-section of Device for taking Samples of the Gas Mixtures for Analysis

FIGURE 7 Sulphur Content of Supercooled Drops for Rapid Quenching
Drop Temperature - $1450_3^{\circ}C$
Gas Flowrate - 1680 cm.^{3} per min.

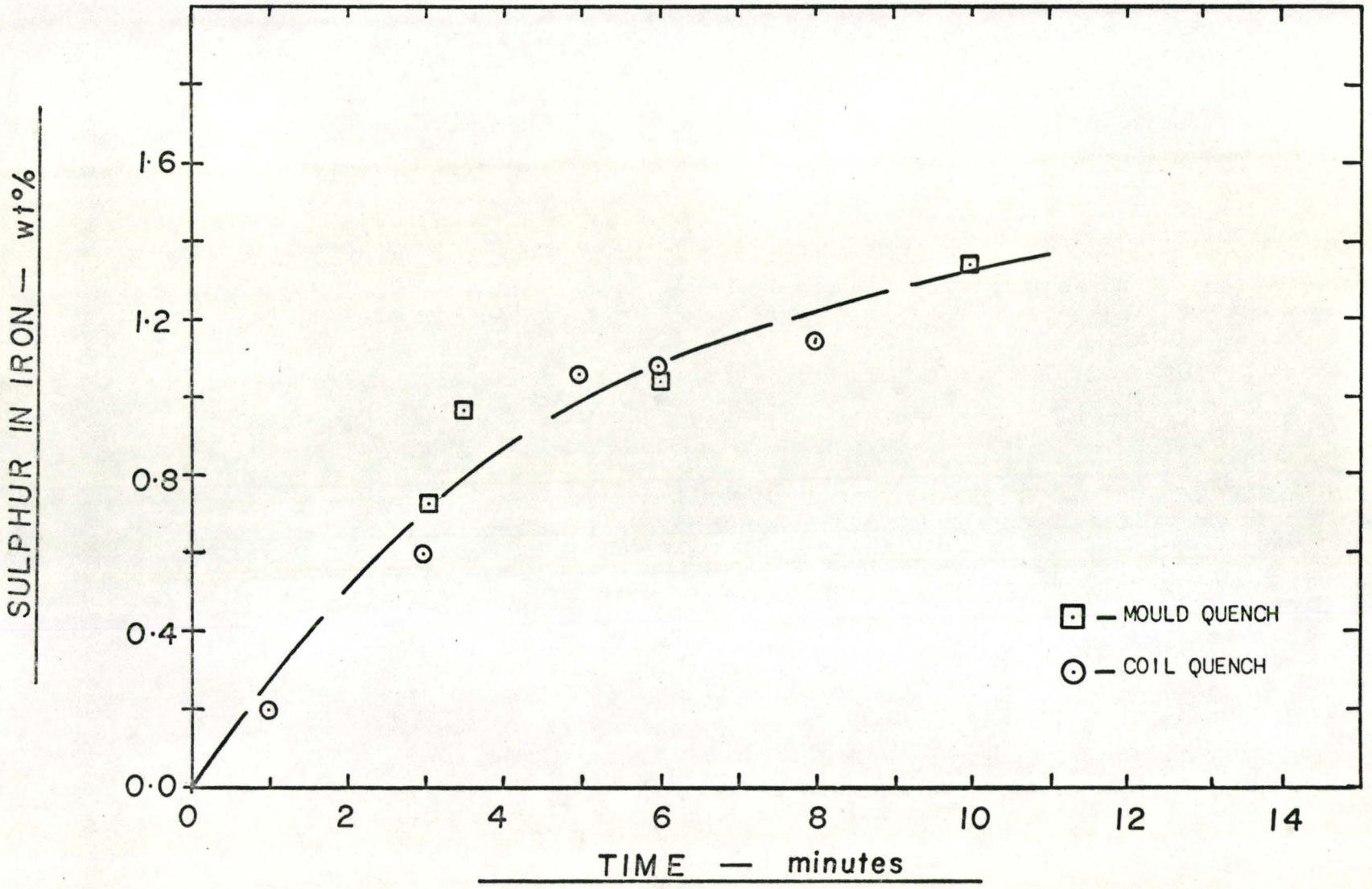

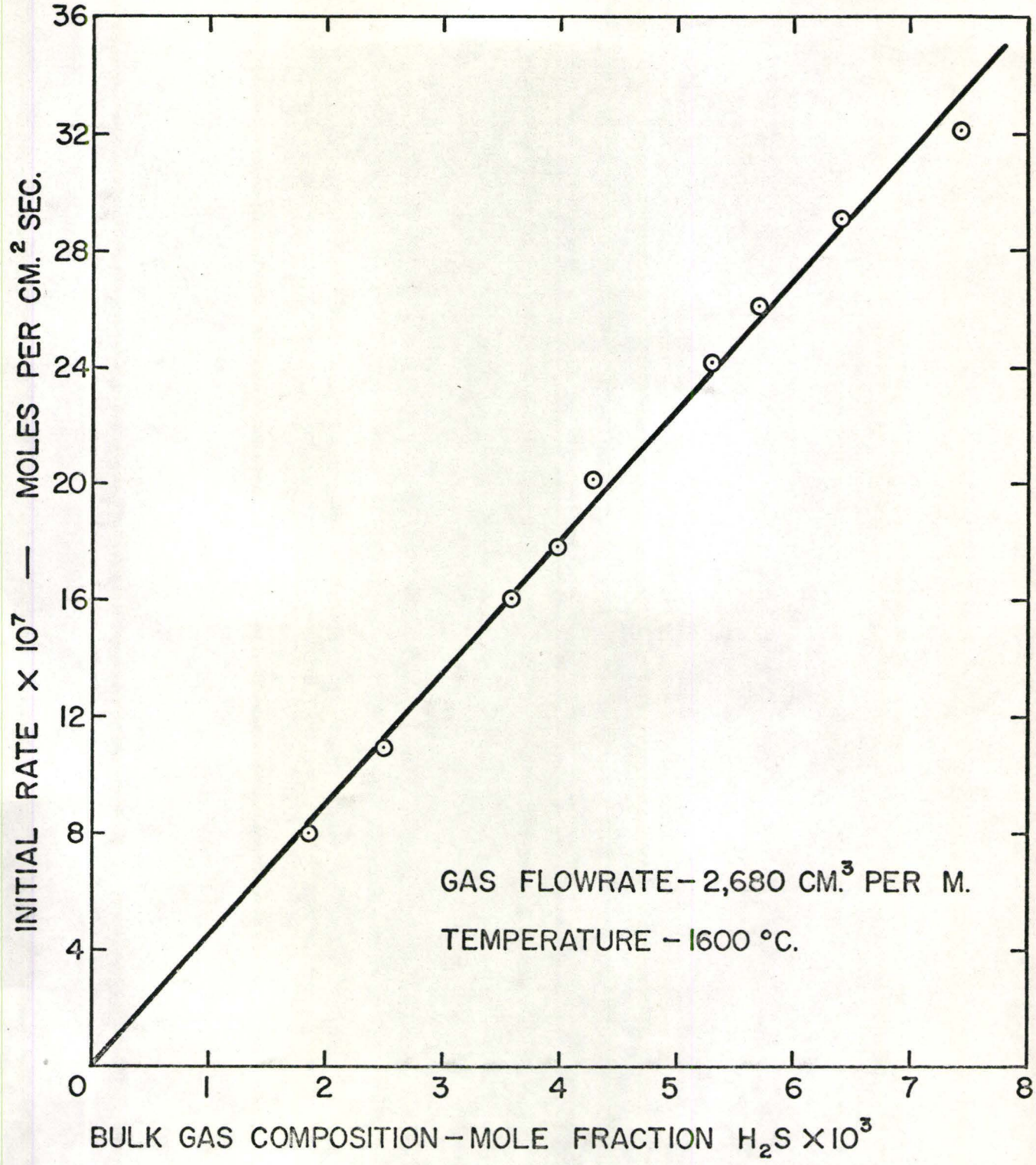

FIGURE 8 Initial Rates of Sulphurisation of Drops Levitated in Various H_2-H_2S Gas Ratios

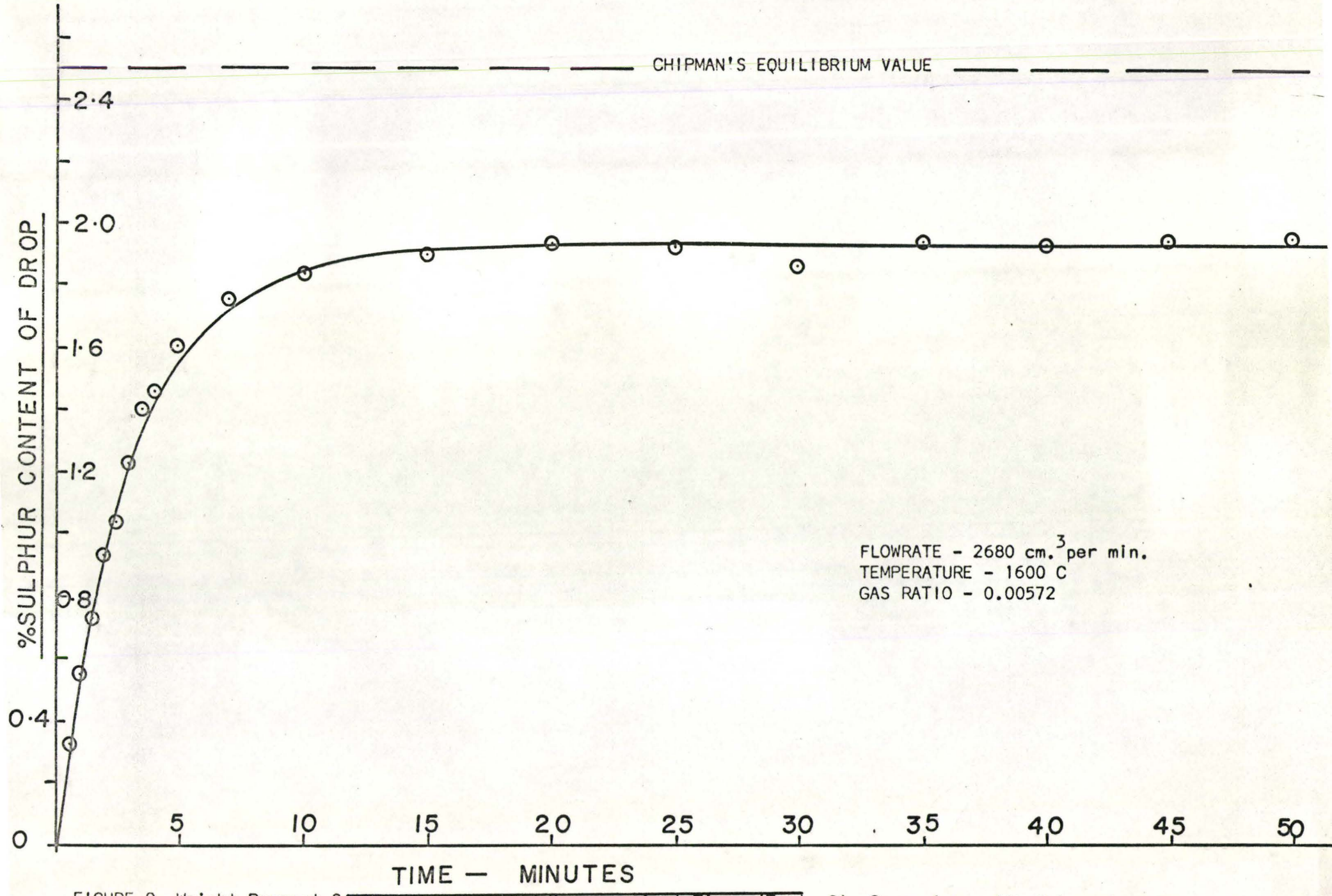

FIGURE 9 Weight Percent Sulphur in Levitated Drops against Time, (Table 8). Comparison with Chipman's Value

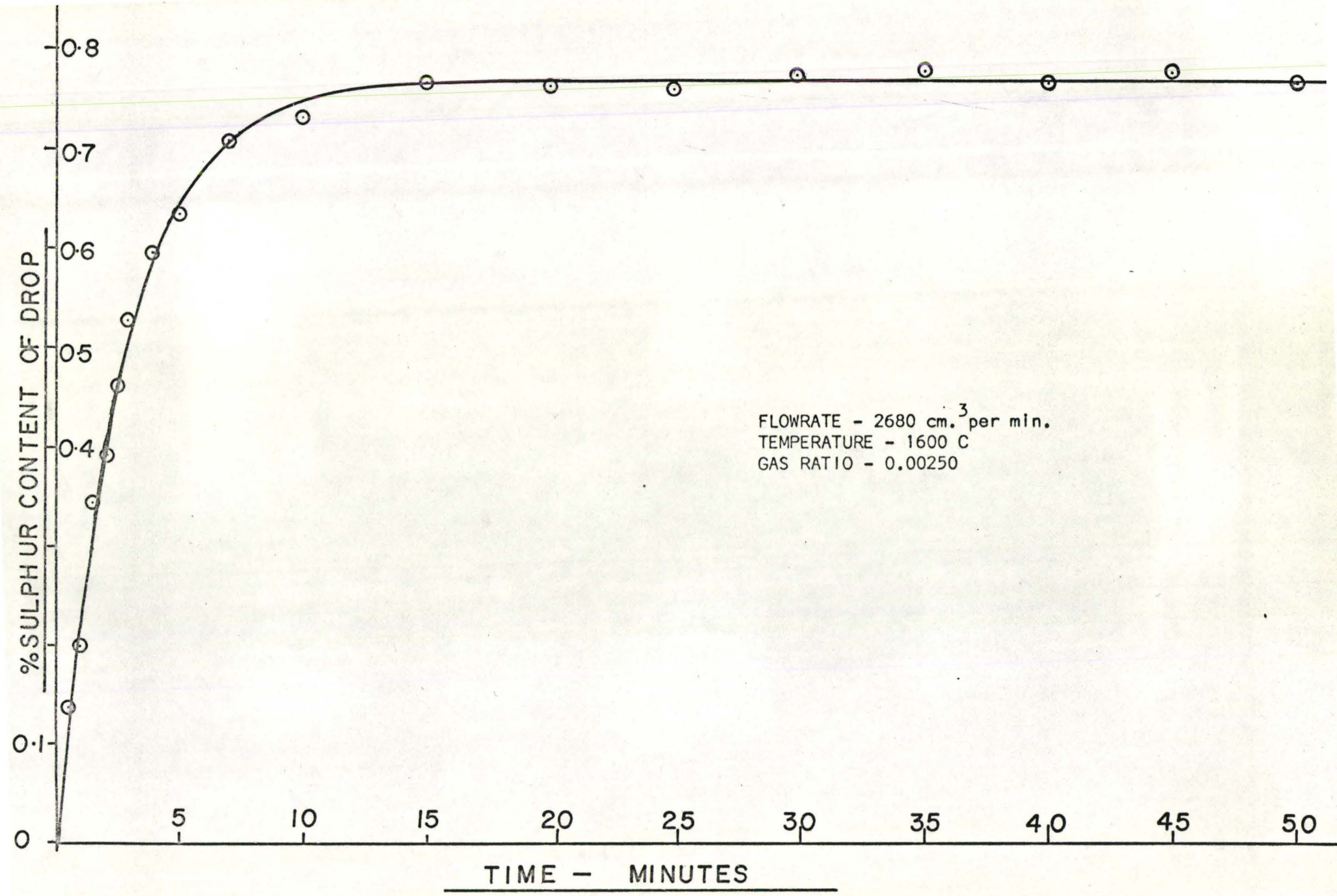

FIGURE 10 Weight Percent Sulphur in Levitated Drops against Time, (Table 3)

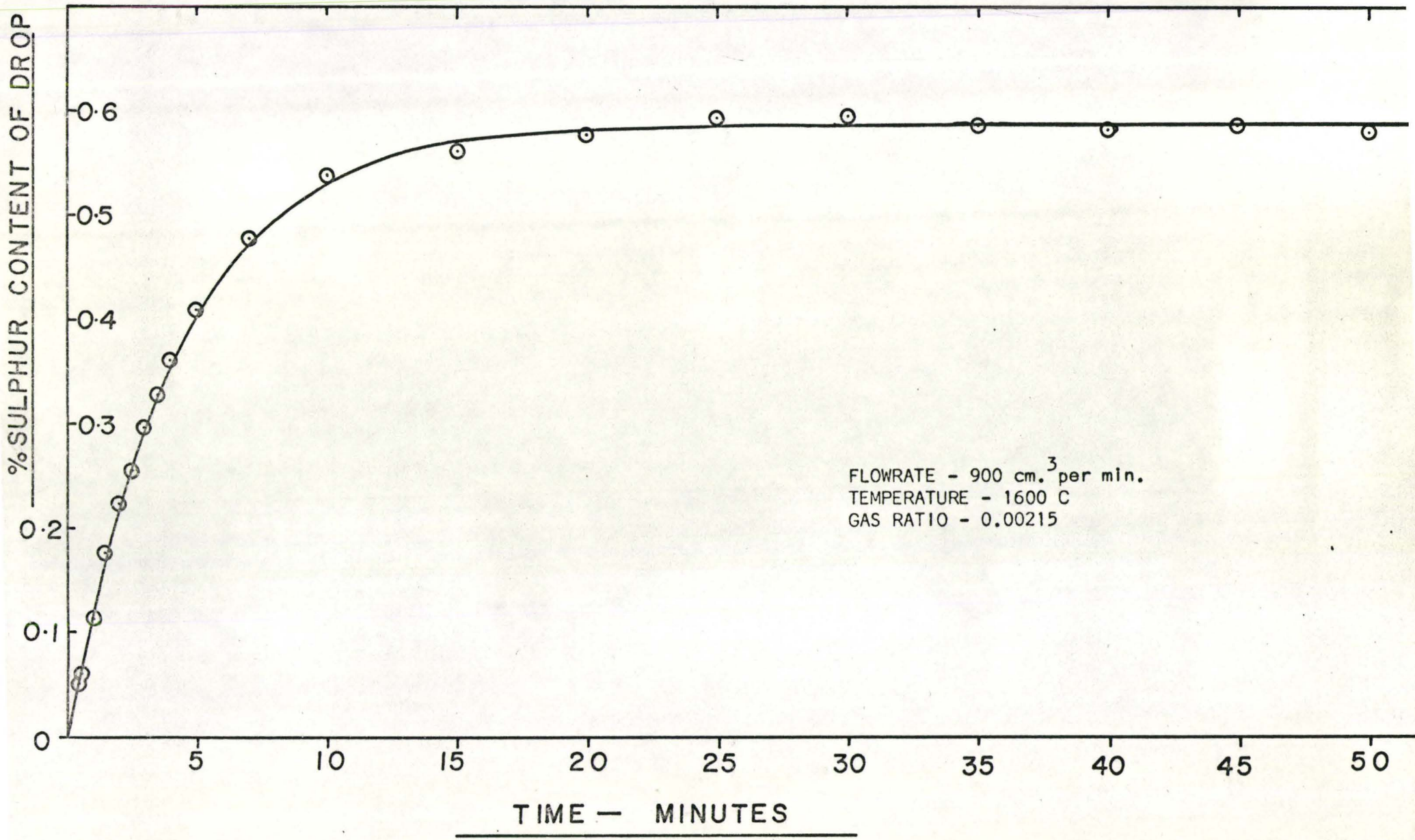

FIGURE 11 Weight Percent Sulphur in Levitated Drops against Time, (Table 12)

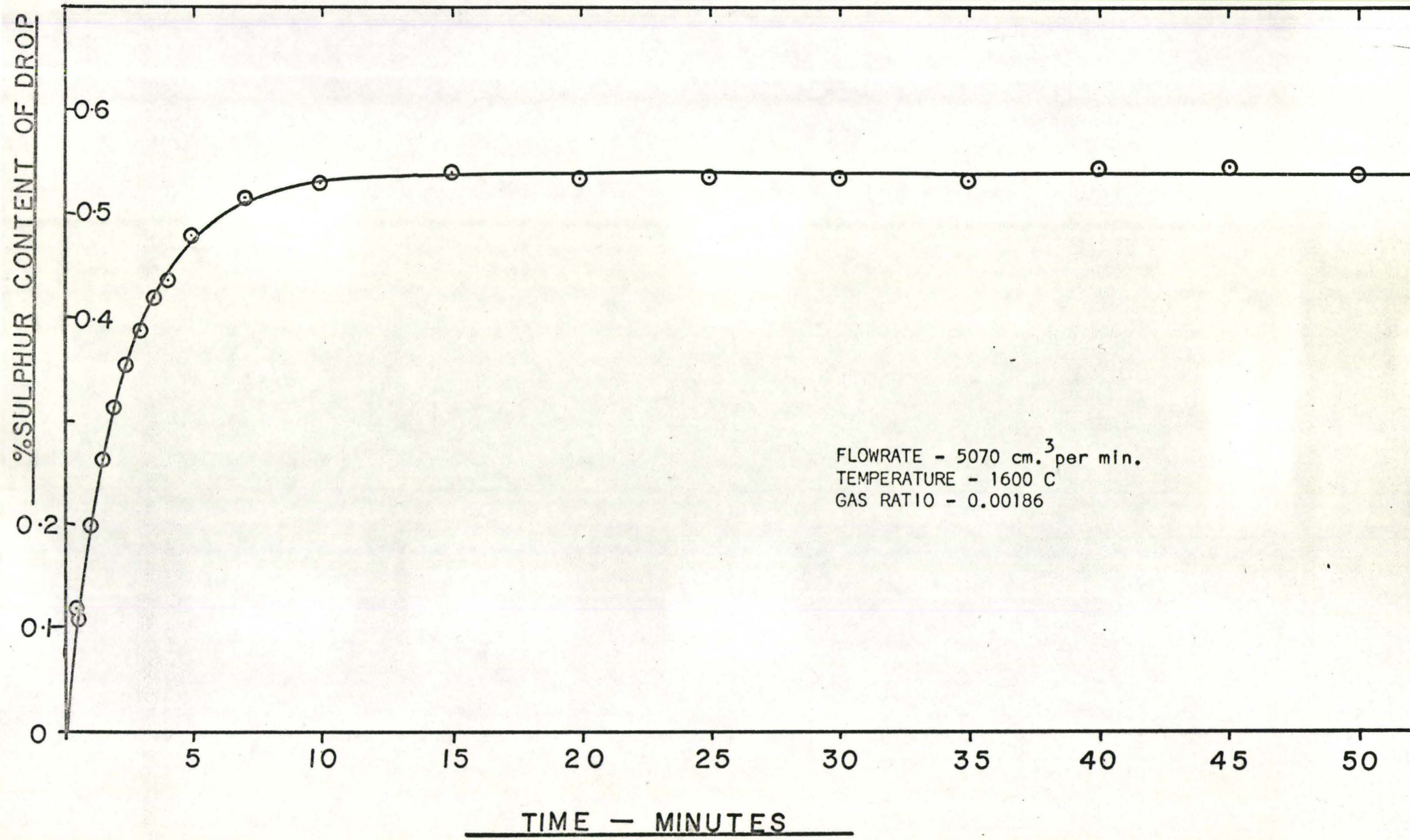

FIGURE 12 Weight Percent Sulphur in Levitated Drops against Time, (Table 14)

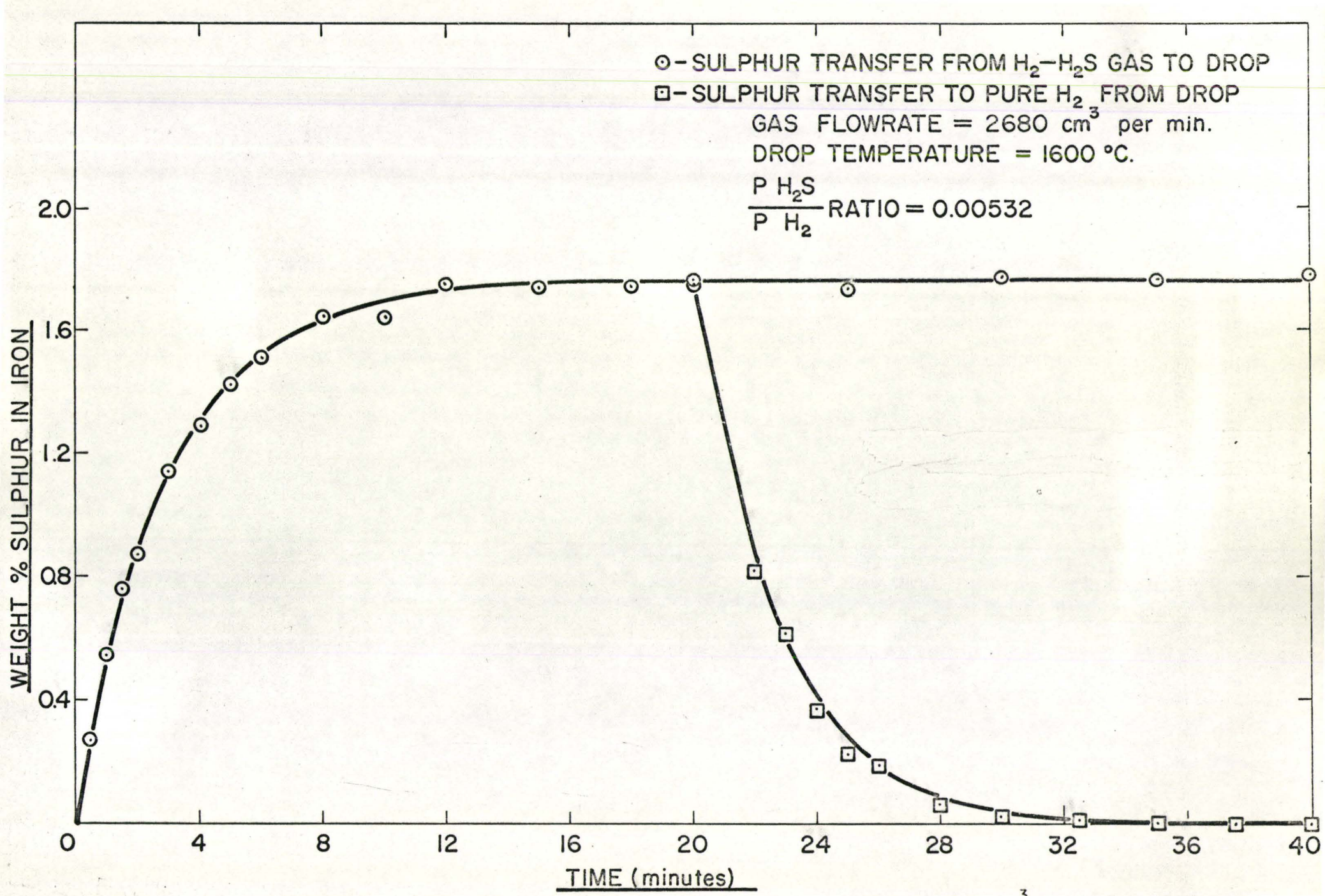

FIGURE 13 Desulphurisation of Iron Drops with Pure Hydrogen Flowing at 2680 cm.^{3} per min.

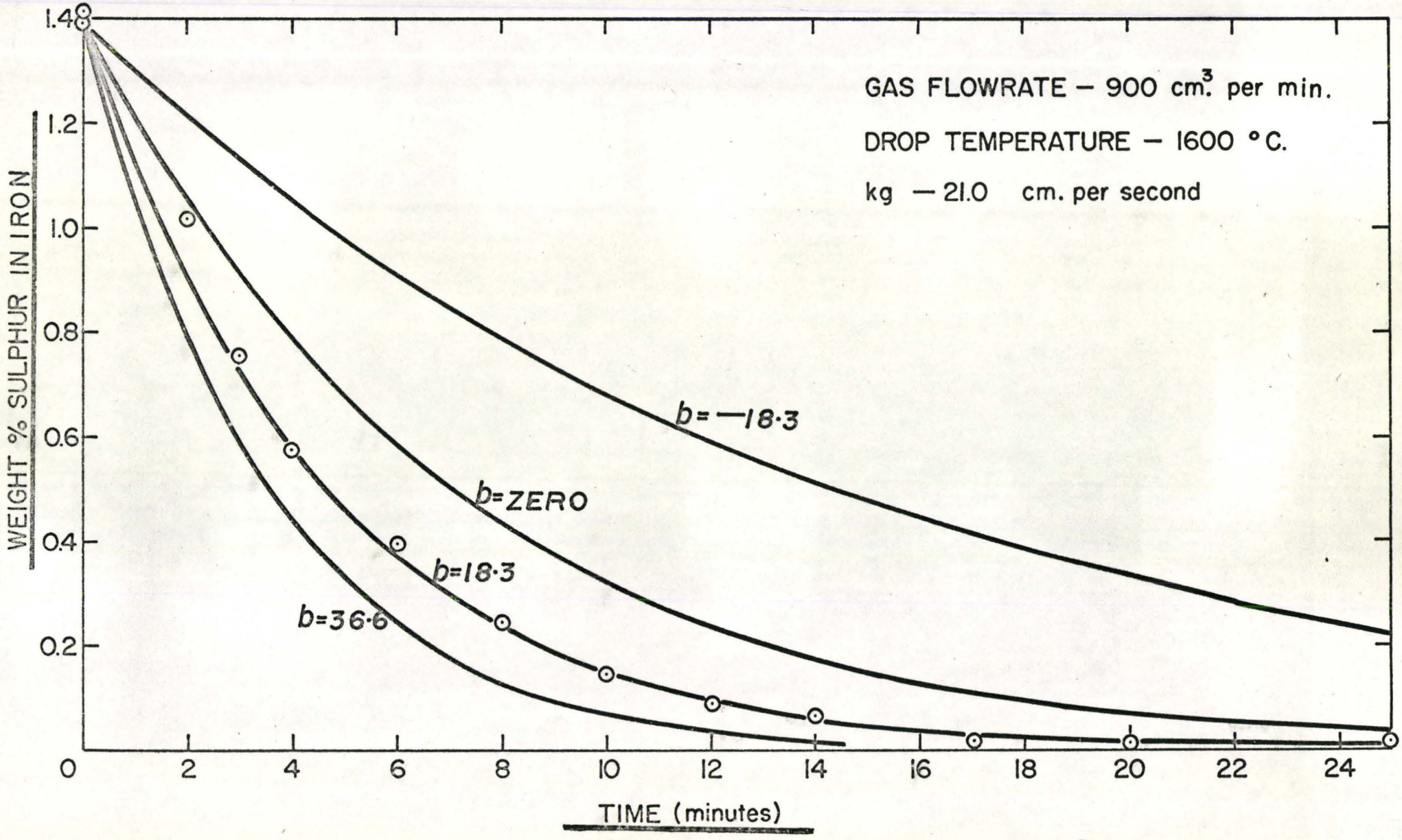

FIGURE 14 Desulphurisation of Iron Drops with Pure Hydrogen Flowing at 900 cm.^{3} per min.

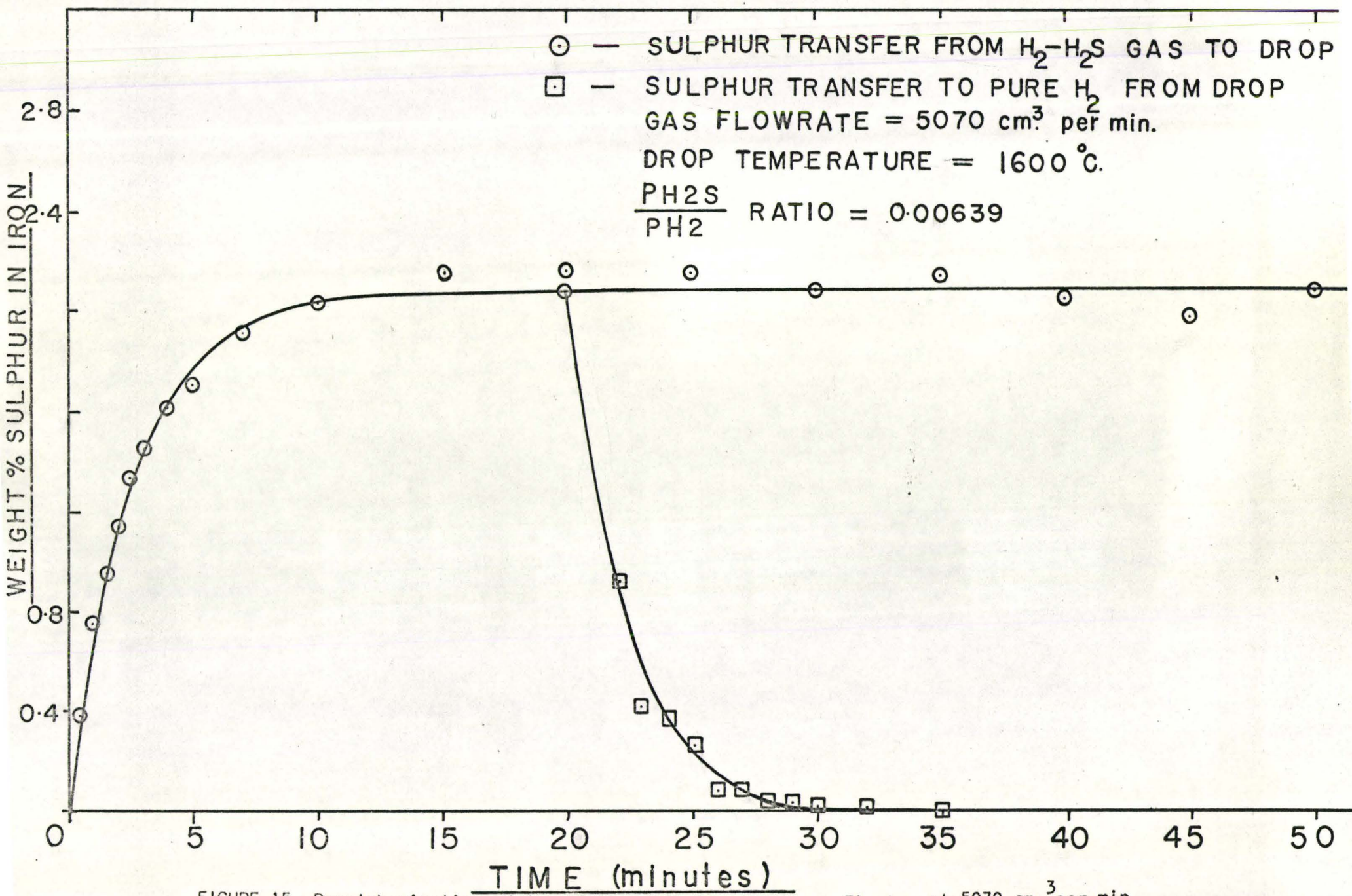

FIGURE 15 Desulphurisation of Iron Drops with Pure Hydrogen Flowing at 5070 $cm.^3$ per min.

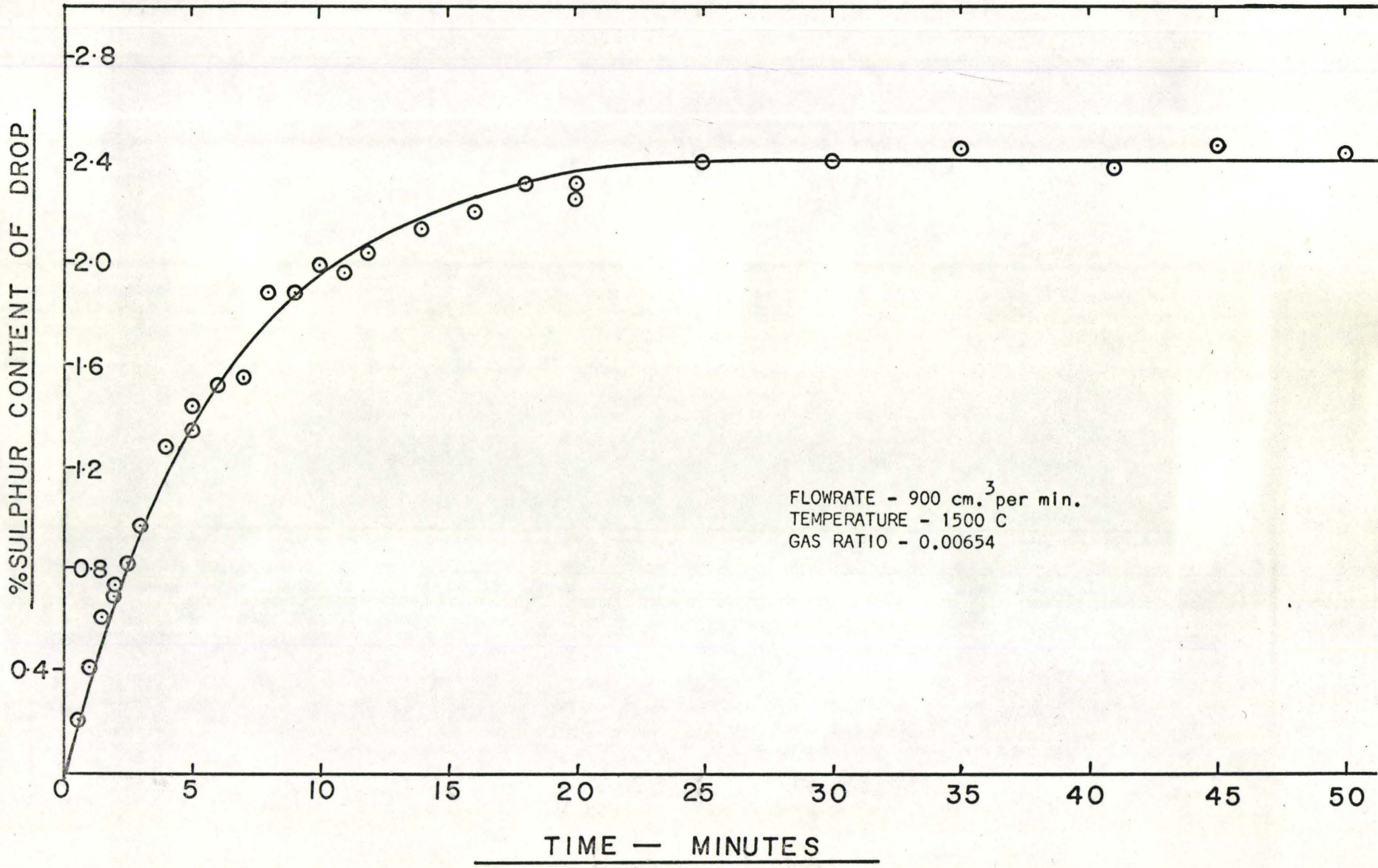

FIGURE 16 Weight Percent Sulphur in Levitated Drops against Time, (Table 18)

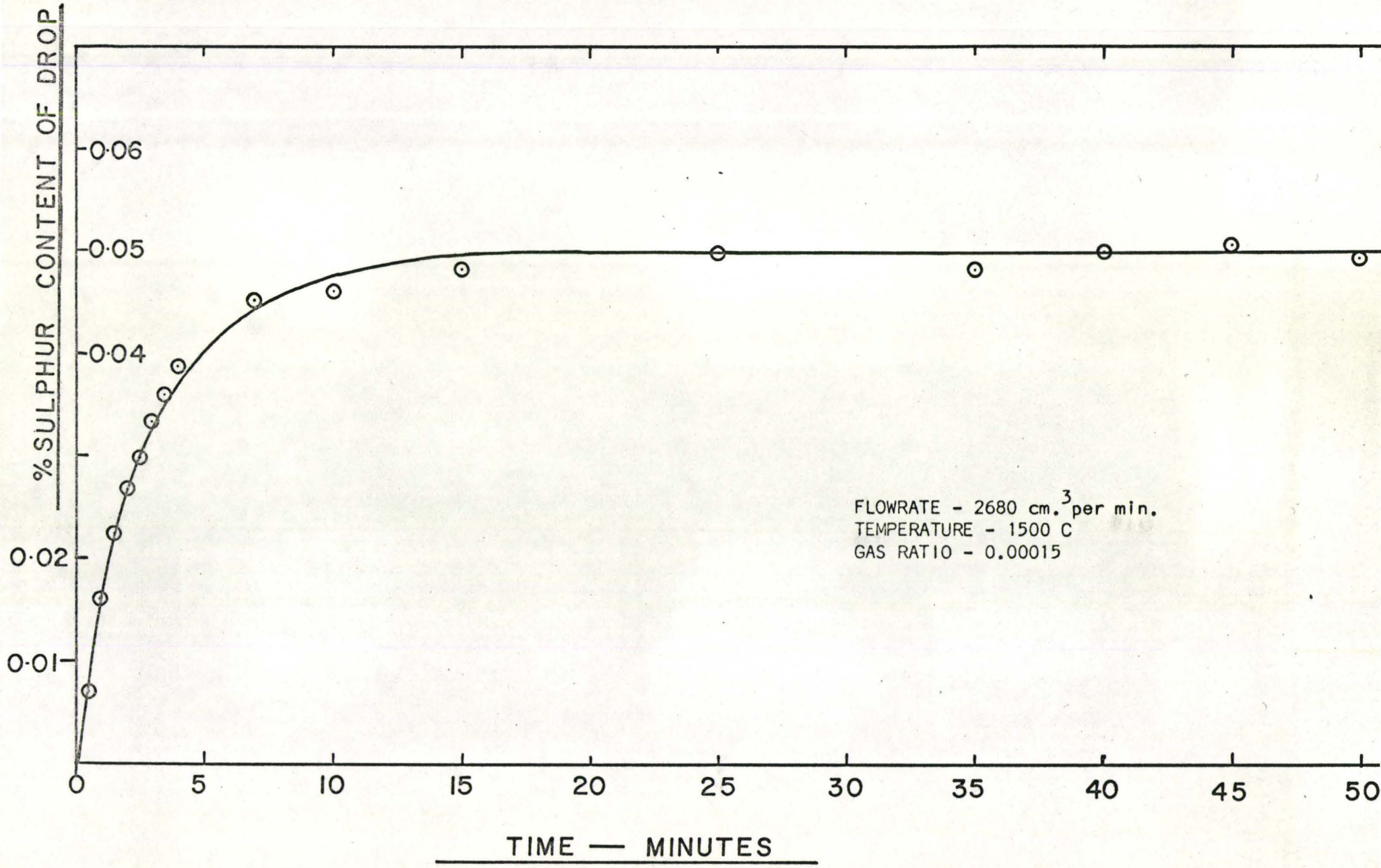

FIGURE 17 Weight Percent Sulphur in Levitated Drops against Time, (Table 19)

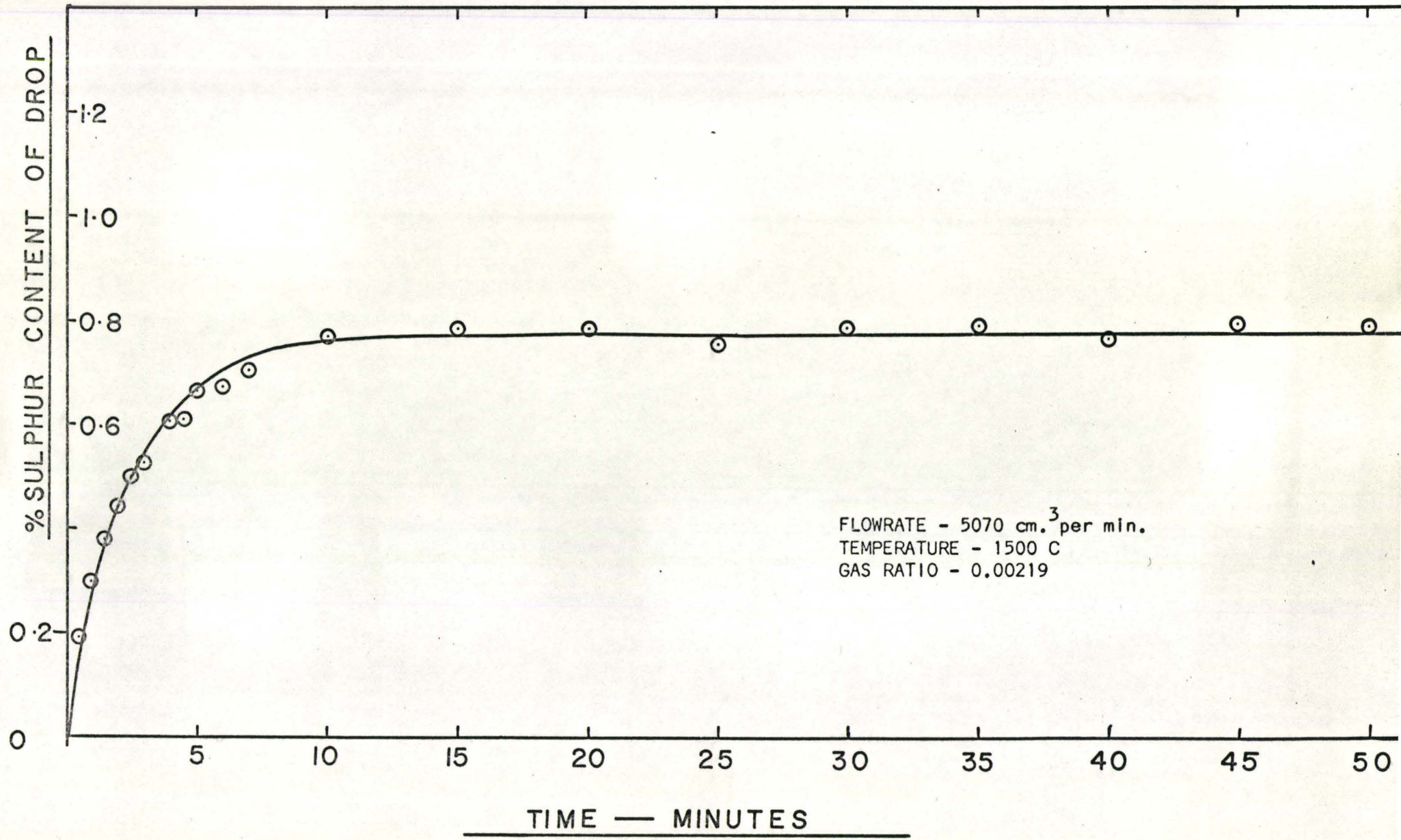

FIGURE 18 Weight Percent Sulphur in Levitated Drops against Time, (Table 21)

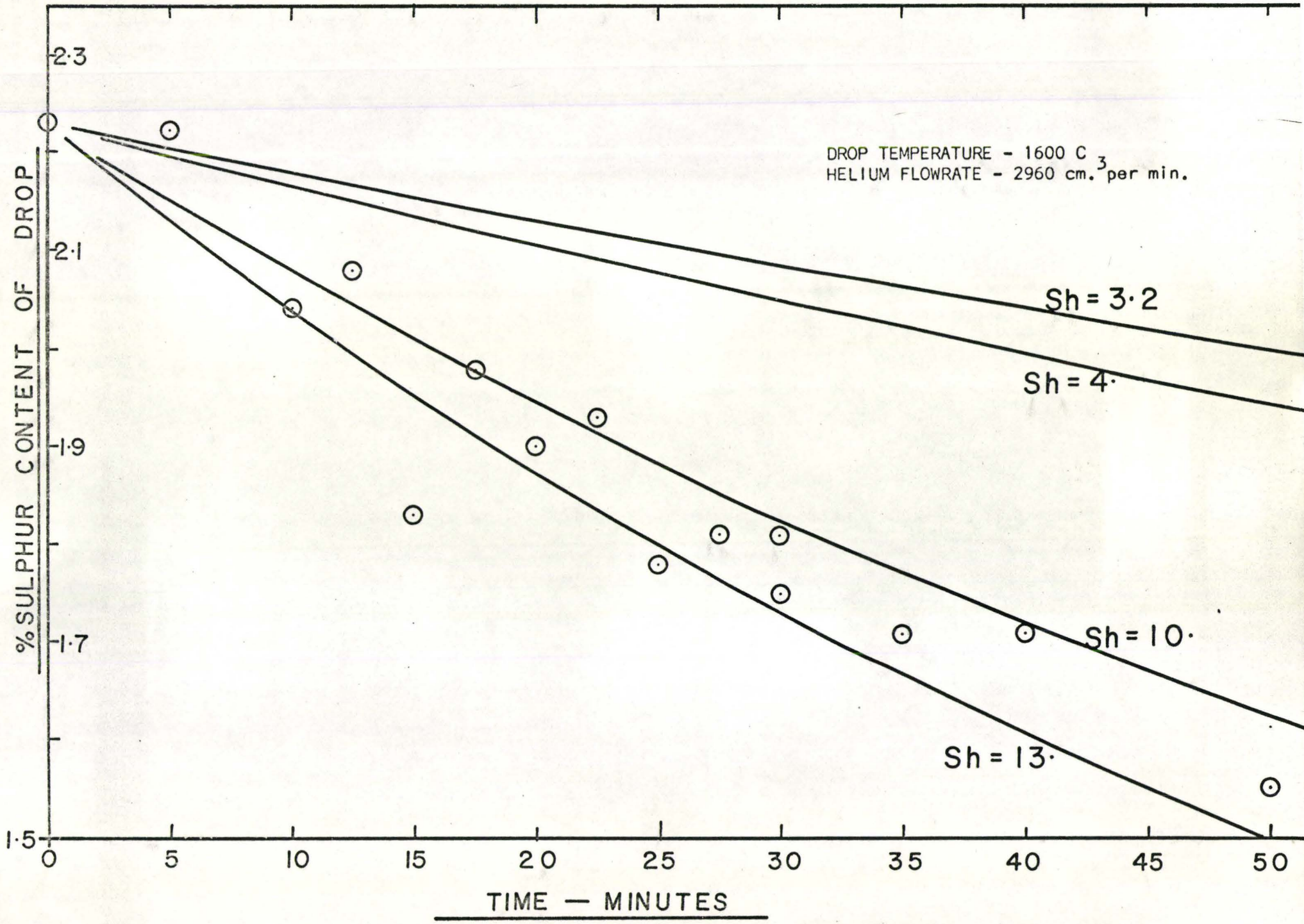

FIGURE 19 Desulphurisation of Iron Drops with Pure Helium

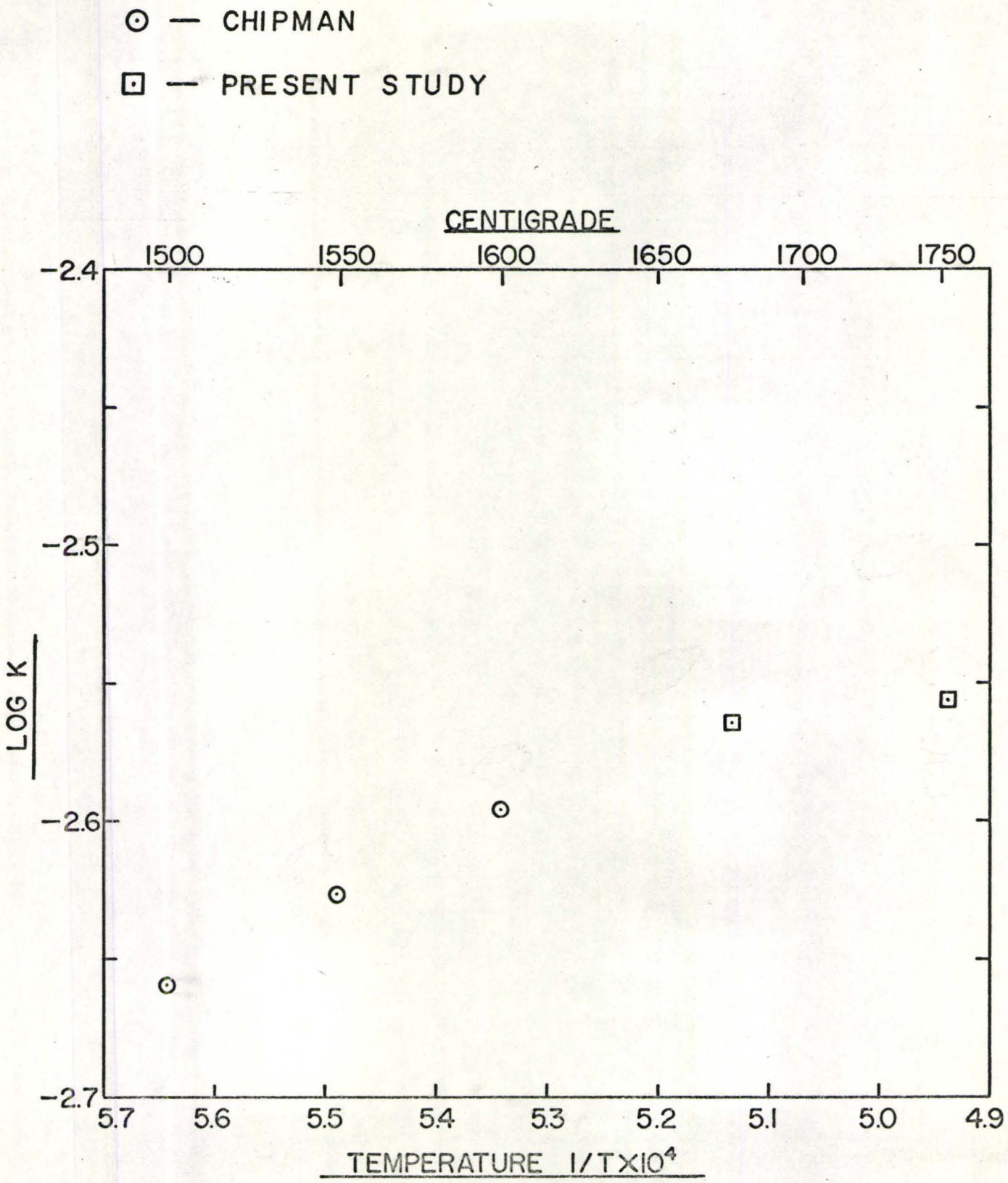

FIGURE 20 Equilibrium Constants at 1750 and 1675^{0}C found by Experimental Rate Curves at Different H_2-H_2S Gas Flowrates

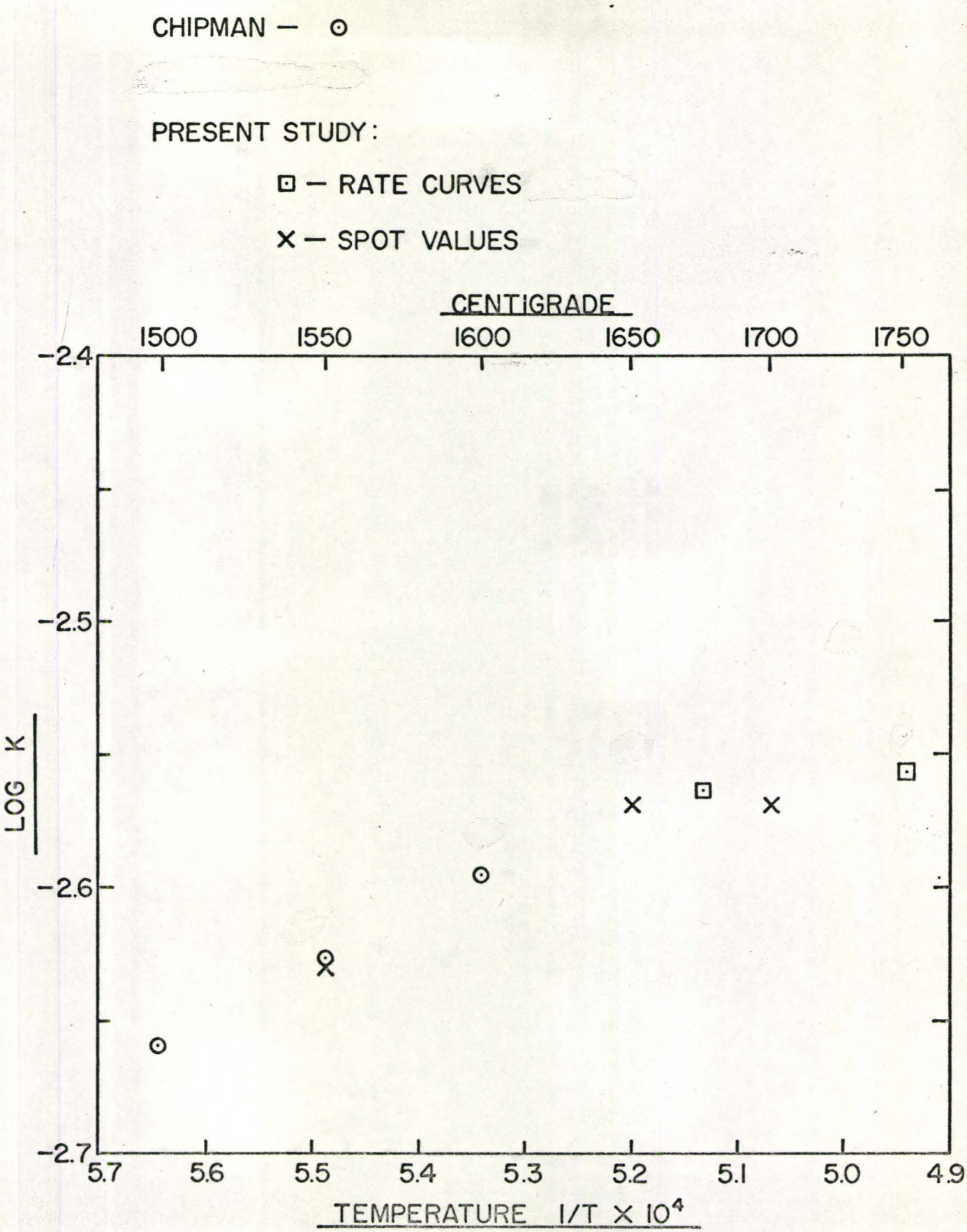

FIGURE 21 Equilibrium Constants by Rate Curves and by "Spot" Measurements in H_2-H_2S Gas Mixtures

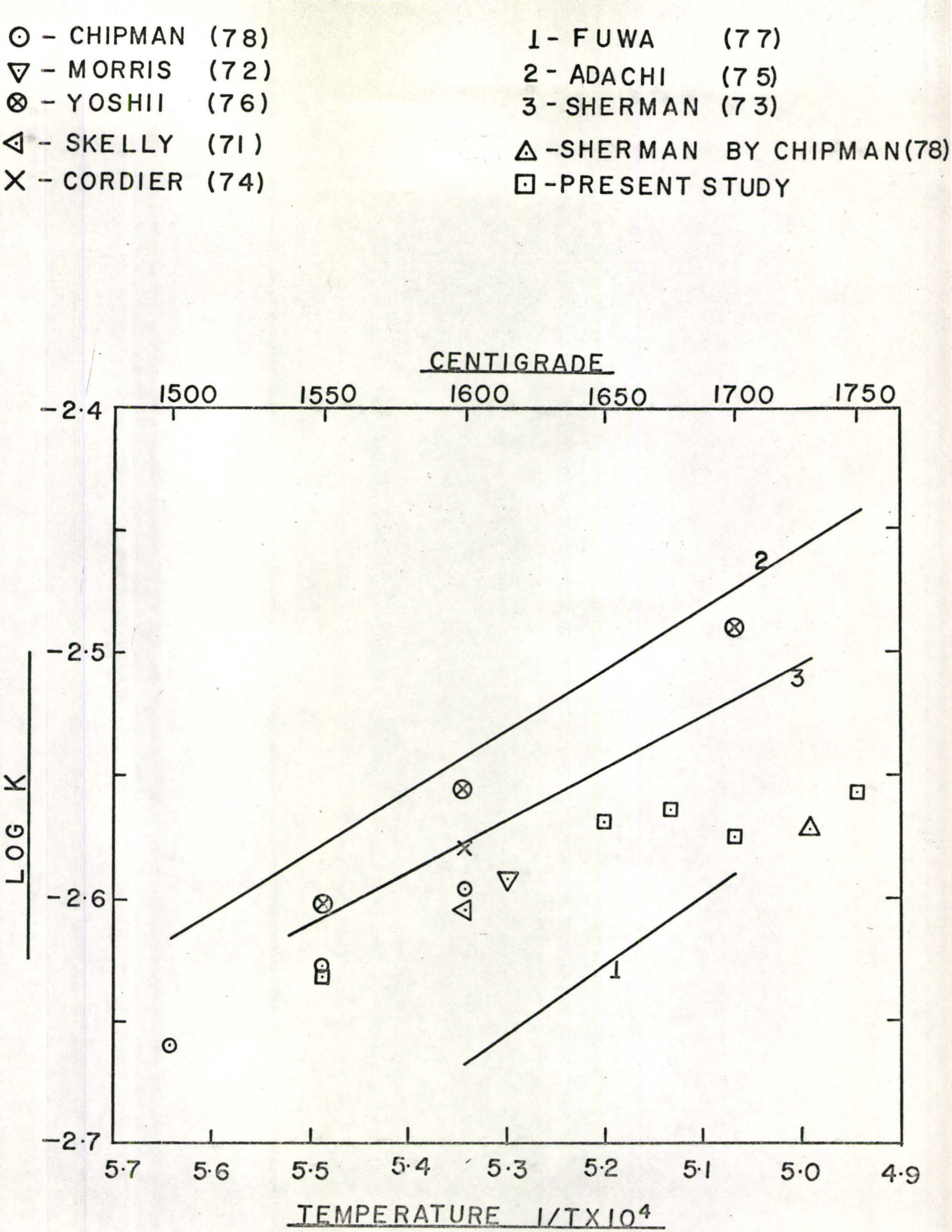

FIGURE 22 Comparison of Equilibrium Constants found in the Present Study with those of Other Workers over the Temperature Range 1500 to 1750 C in H_2-H_2S Gas Mixtures

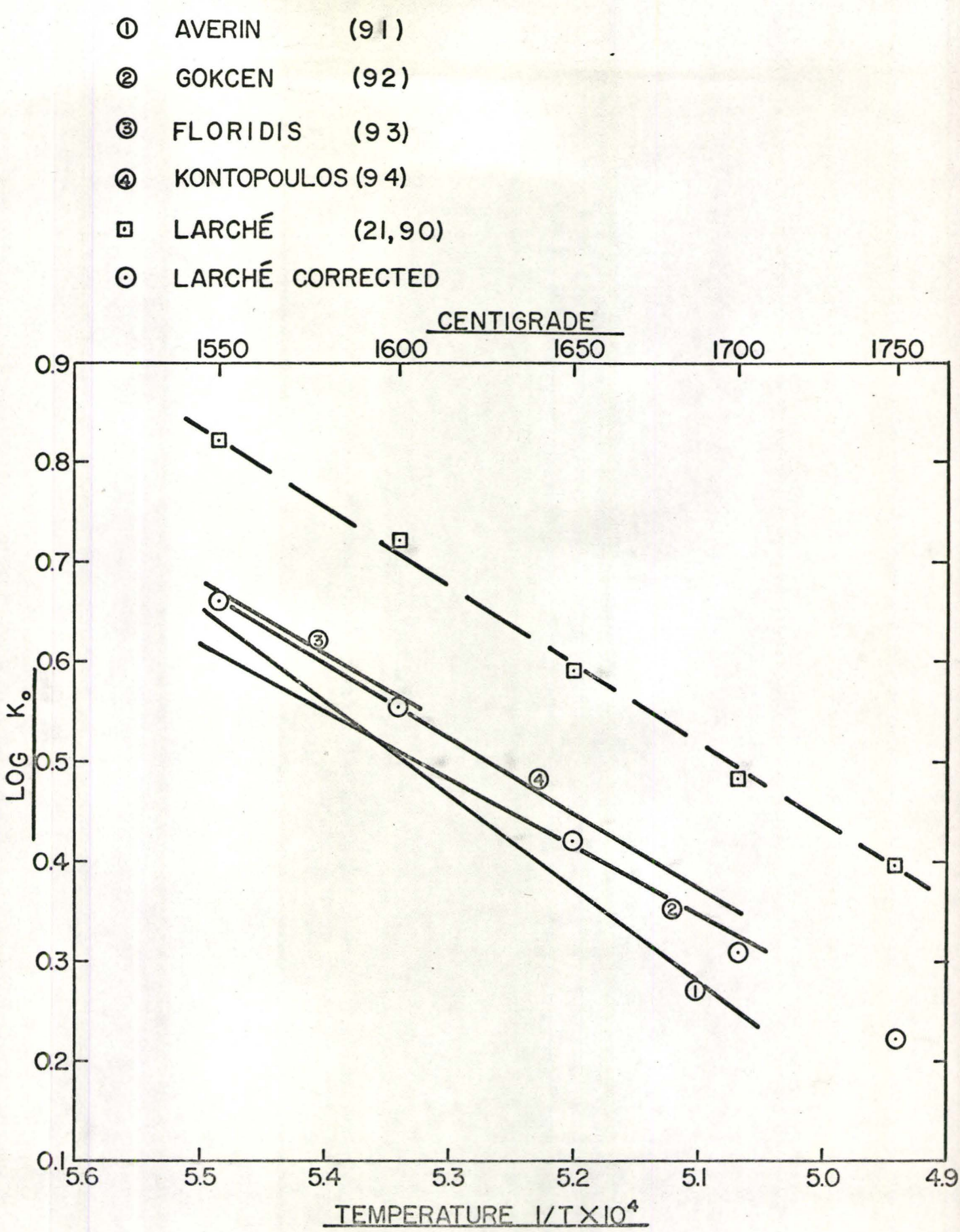

FIGURE 23 Correction of Larche's Measurements of the Equilibrium Constant for Hydrogen-Water Vapour Mixtures over Liquid Iron

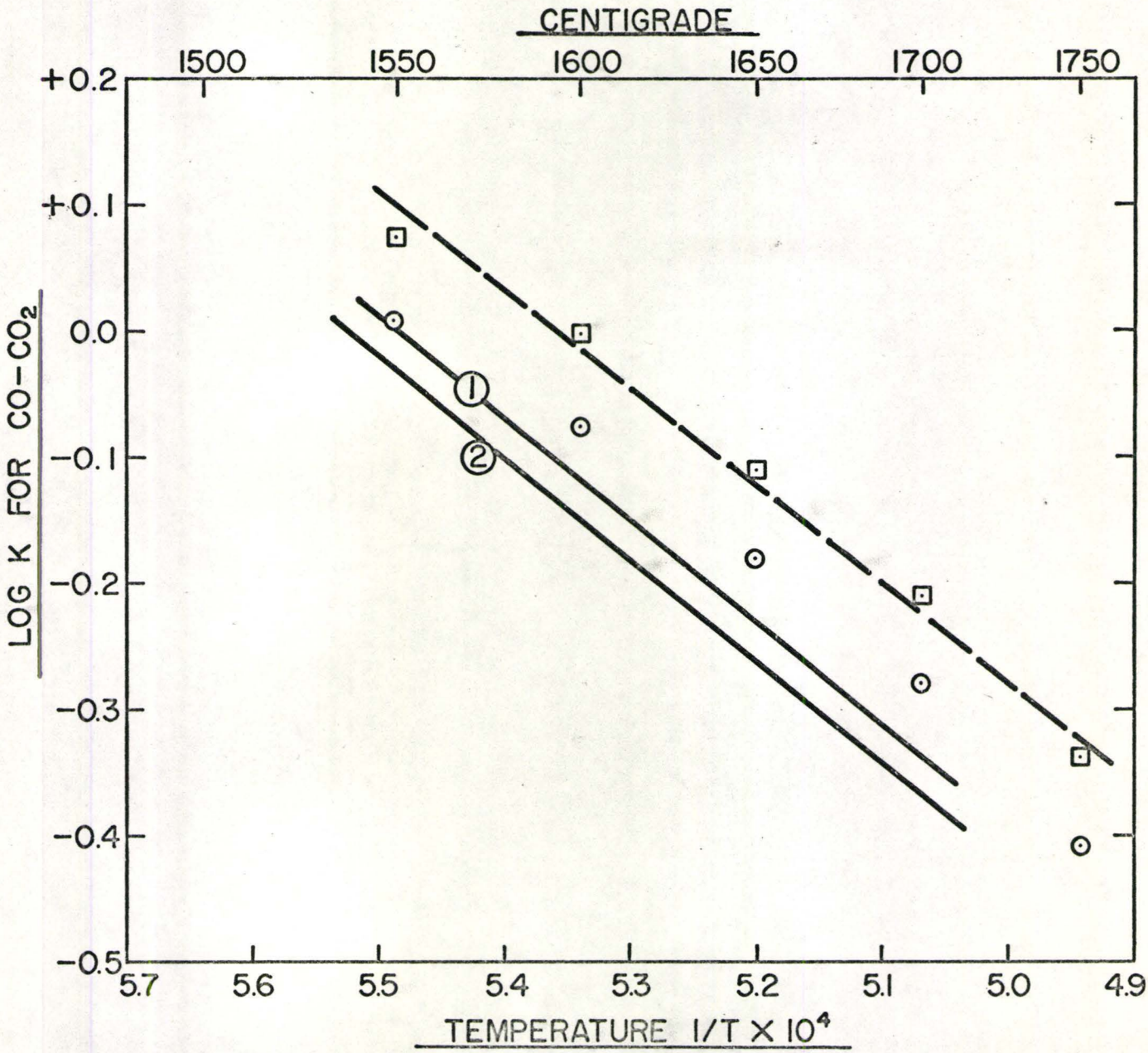

FIGURE 24 Correction of Larche's Measurements of the Equilibrium Constant for $CO-CO_2$ Mixtures over Liquid Iron

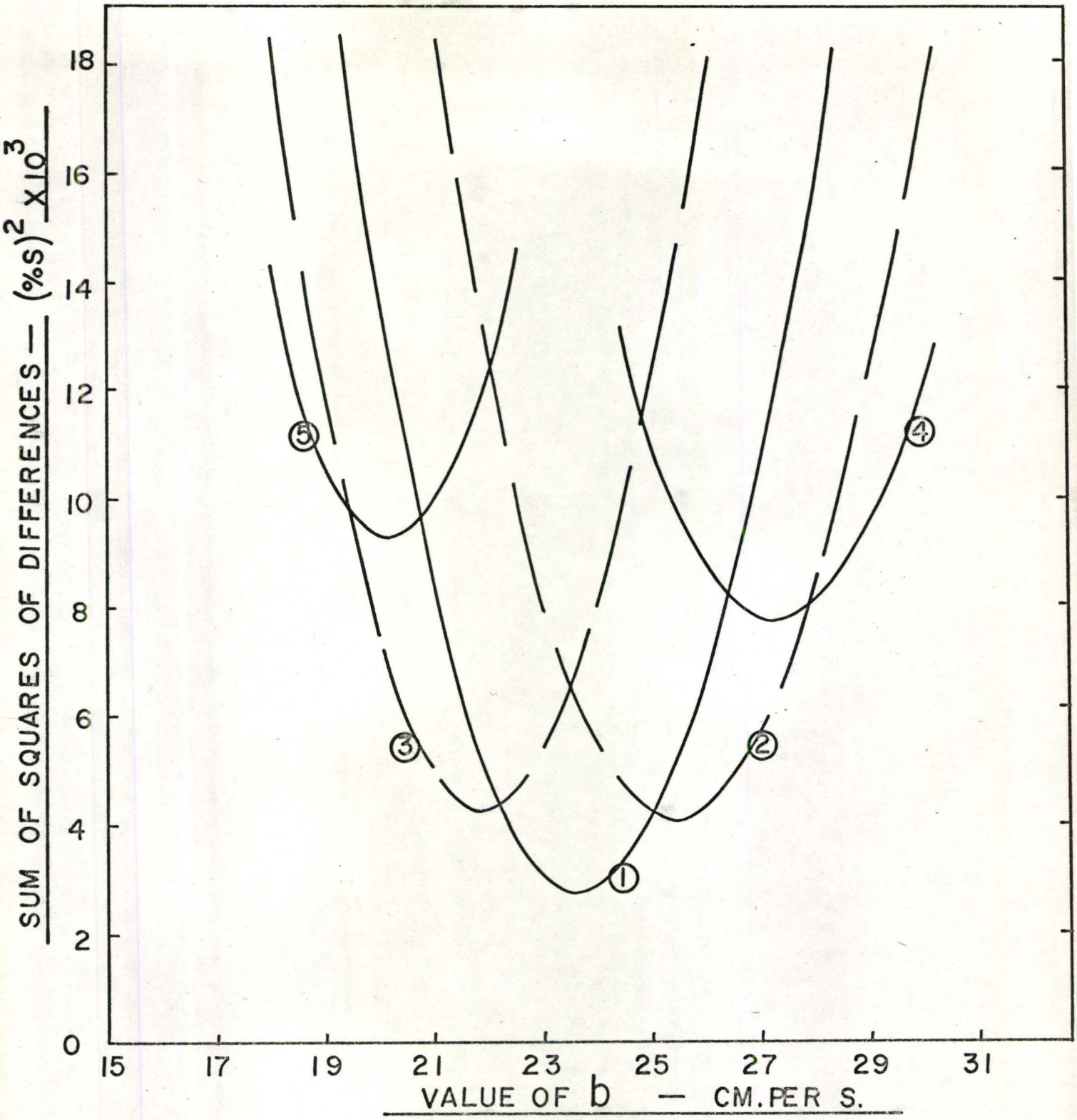

FIGURE 25 Comparison of Experimental Data for Sulphurisation at 1600 C and Flowrate of 2680 cm^3 per min. (Table 3), with Various Solutions of the Flux Equation.

Values of kg and b were perturbed and the resulting solutions compared with the experimental points by a least squares criterion.

Closest fit was given by kg=39.60 and b=23.64 cm. per s.

Curve 1 corresponds to kg = 39.60 cm. per s.
Curve 2 corresponds to kg = 41.85 cm. per s. ($+2\sigma$)
Curve 3 corresponds to kg = 37.34 cm. per s. (-2σ)
Curve 4 corresponds to kg = 44.10 cm. per s. ($+4\sigma$)
Curve 5 corresponds to kg = 35.09 cm. per s. (-4σ)

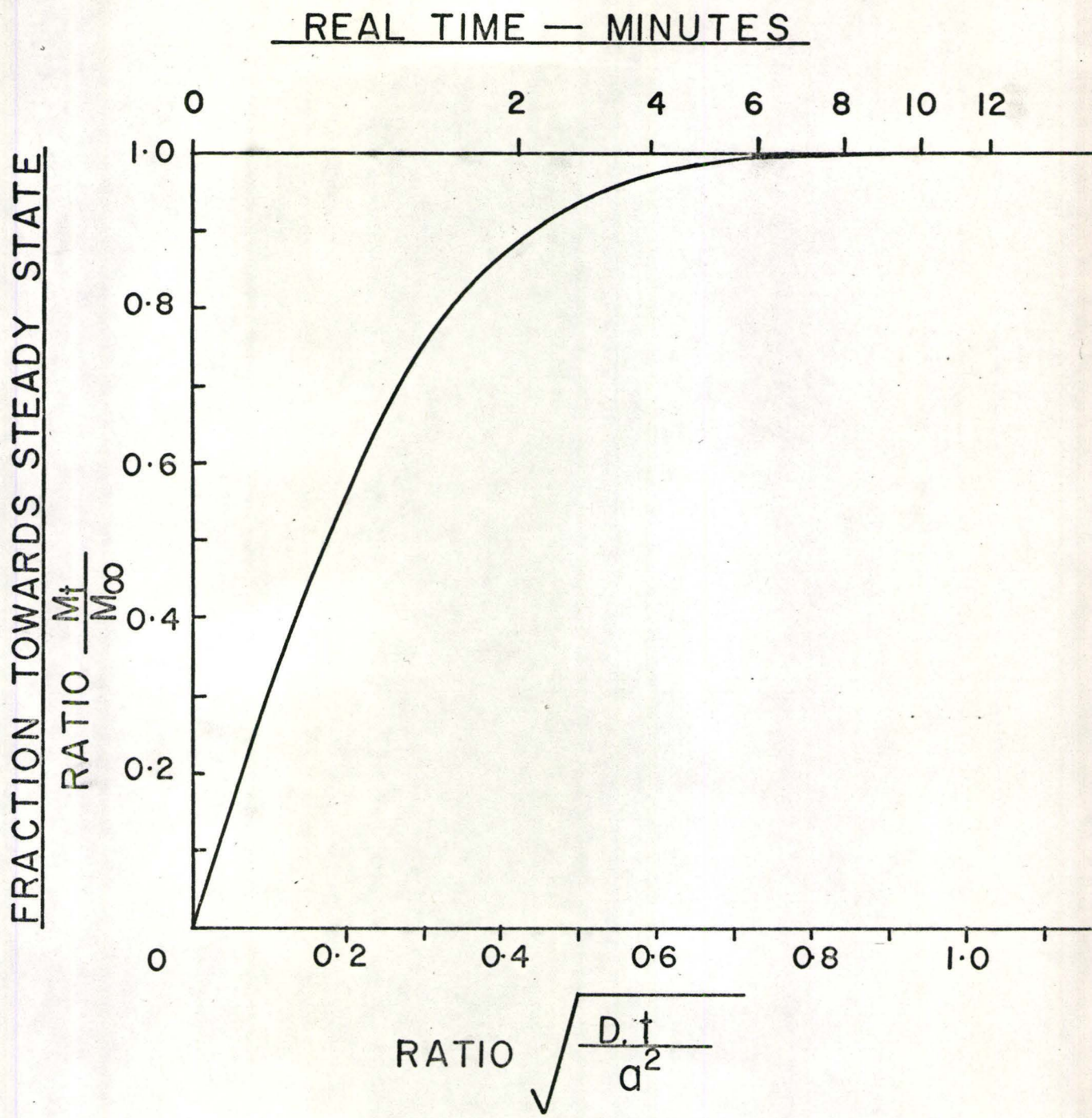

FIGURE 26 General Curve for Attainment of Steady State for Sulphur Transfer into a Stagnant Drop of Iron, where all Resistance to Transfer is in the Drop Alone, (Appendix 1)